Physics – Uspekhi **38** (8) 803 – 845 (1995)
©1995 Jointly Uspekhi Fizicheskikh Nauk and Turpion Ltd

REVIEWS OF TOPICAL PROBLEMS

PACS numbers: 25.10.+s; 24.30.Gd; 29.90.+r

Δ isobar in nuclei (review of experimental data)

K N Mukhin, O O Patarakin

Contents

Abstract. Experimental and elementary theoretical work relevant to the electromagnetic and hadron excitation of the Δ isobar in nuclei is reviewed. The historical development of the notion of non-nucleon degrees of freedom, from the quasinucleon and the pion to quarks and gluons, is described, and the role of Δ excitations is discussed. Gamma, electron, proton, pion and ion beam methodologies and detector and target designs are discussed. Preliminary suggestions about γ, e, p, π excitation mechanisms are made. Problem areas that need more research are highlighted, and trends for the future and prospective experiments are discussed.

1. Introduction

One of the most important problems in modern nuclear physics is the study of non-nucleon degrees of freedom in the nucleus. Historically, the subject has gone a long way from the quasinucleon and the pion, to pion and baryon resonances, partons, quarks, and gluons. Nearly every successive step on this route was in its time covered in detail in both original and (sometimes popular-level) review articles. The only exceptions perhaps are the baryon resonances, particularly the problem of the excitation of the Δ(1232) isobar inside nuclear matter (for brevity, the term nuclear Δ isobar will be used in the following). Reviews of this particular subject are relatively few, tend to be limited in scope, and are aimed at narrow specialists (see, e.g., Refs [1 – 3]). The fact is, however, the nuclear Δ isobar is receiving increasing attention from both experimentalists and theorists. From the former, because it may be excited in a wide variety of strong and electromagnetic nuclear processes involving pions, nucleons, nuclei, photons, and electrons. The latter are intrigued by the nontriviality of the data and by the diversity of interpretations they as yet unfortunately admit.

The present review is an attempt at a semipopular — intended for a physicist of any narrow specialisation — account of the up-to-date experimental data on the nuclear Δ isobar degree of freedom. The material is organised as follows. Section 2 provides a brief historical account of why particular non-nucleon degrees of freedom had to be introduced to describe nuclear structure, the properties of the nuclear forces, and some aspects of nuclear reaction processes. The basic parameters of the corresponding particles (quasinucleons, π, σ, ρ, ω and φ mesons, Δ isobar, partons, quarks, and gluons) are presented; the extent of the reality of their nuclear manifestation is characterised; a

K N Mukhin, **O O Patarakin** Russian Research Centre ‘Kurchatov Institute’, Institute of General and Nuclear Physics, pl. Kurchatova 1, 123182 Moscow
Tel. (7-095) 196-76-63; Fax (7-095) 196-91-33
E-mail: patarak@nuc53.kiae.su

Received 15 August 1994, revised 9 March 1995
Uspekhi Fizicheskikh Nauk **165** (8) 841 – 886 (1995)
Translated by E Strel'chenko; edited by H Milligan

brief comparative account of current nuclear models and nuclear force theories is given.

The section does not actually contain any new information because its material may be found in many fairly well-known sources. When brought together, however, this information may prove useful as a kind of introduction to the subject and as a brief reminder of some ideas, models, theories, etc., used or just mentioned in the sections that follow. The section concludes by emphasising the special importance the Δ degree of freedom assumes in connection with the now very topical research on spin–isospin excitations and the collective nuclear states.

It is hoped that having read through the second section the nonspecialist will have no difficulty in reading the remaining sections, and that the review as a whole will stimulate a desire for more investigation in more specialised literature. Of the Russian sources, perhaps the best choice is Ref. [3], a review article with a special emphasis on the $(^3\mathrm{He}, \mathrm{t})$ charge exchange reaction, which gives a clear-cut definition of the concept of a collective nuclear Δ excitation, and presents a detailed survey of theoretical work.

The logic behind the remaining sections of the present work is as follows: The third section is concerned with the processes of photoexcitation and electroexcitation of the nuclear Δ isobar. The topics discussed here are mechanisms of photonuclear reactions at intermediate γ energies; the sources of real and virtual γ quanta; work with bremsstrahlung spectra and with labelled-photon and electron beams; experimental data on the total photoabsorption cross section and on partial hadron photogeneration reactions; and, finally, the problem — and possible causes — of the change in nuclear relative to nucleon Δ maximum parameters. Based on indirect considerations, it is suggested that, apart from the quasifree Δ excitation mechanism, a competing collective mechanism may exist.

The fourth section discusses Δ excitation processes in hadron–nuclear interactions such as ion, nucleon, or pion charge exchange; experimental aspects (beams, facilities, targets); the change in the parameters of the nuclear Δ maximum with respect to the free and quasifree Δ excitation; the experimental proof of existence of collective effects.

The topics covered in this section are nuclear Δ formation mechanisms for various types and energies of the incident particles; the role of Fermi motion and of the nucleon binding energy; the role of the interaction in the final state; Δ formation at the surface and in the bulk; the relationship between the meson and mesonless de-excitation channels.

The simplest present-day theoretical concepts based on the Δ-hole (Δ-h) model are introduced in the most elementary fashion in the fifth section. The coverage includes the quasifree and collective mechanisms of Δ excitation; the basic features of the Δ-h model and its application to various primary particles; spin-longitudinal and spin-transverse nuclear responses; Δ maximum shift in the Δ-h model with π-exchange; optical theorem aspects. Also, Δ isobar binding energy, $\Delta-\mathrm{N}$ interaction, Δ nuclear potential, the hypothesis of 2Δ states and Δ balls, and some other questions are considered. A number of the theoretical studies of the past decade are discussed in detail, some of which rely on modern inclusive and exclusive experiments, and some on pure calculations. These very recent results have not yet received experimental support, but enable a very interesting and promising programme of future research to be marked out. Relativistic and related chiral models are not covered in the review.

The closing sixth section discusses the results already obtained and experiments for the near future.

The review covers the papers and international conference proceedings as of 1993 inclusive, with additional 1994 papers the authors became aware of at the very latest stage of their manuscript work.

2. Non-nucleon degrees of freedom in historical perspective

2.1 Difficulties of nuclear models with nucleon degrees of freedom

After the discovery of the neutron in 1932 nuclear physics came to be completely dominated by the proton–neutron model of the atomic nucleus — a concept which did away spectacularly with the then seemingly insurmountable difficulties of its proton–electron predecessor and was at first quite satisfactory in explaining the basic properties of the nucleus and the general features of nuclear reactions. At the heart of all particular implementations of the model was the notion of nucleon degrees of freedom, i.e., one considered in this model the behaviour of protons and nuclei which under the action of certain forces (such as nuclear, electromagnetic, or weak) may combine into nuclei, scatter one another, stimulate nuclear reactions, etc. The nuclear forces were treated purely phenomenologically. As the euphoria of the early successes faded away, however, the recognition came that, taken alone, the nucleon degrees of freedom were insufficient to describe nuclear phenomena. First evidence for this was that some specific versions of the purely nucleon models were found to contradict one another in their basic features.

This is most clearly demonstrated by comparing two early concepts, the drop model (N Bohr, Wheeler, Frenkel, 1939) and the shell model (Heppert-Meyer, Jensen, 1949–1950). Whereas the former involves the notion of a strong nucleon–nucleon interaction, in the latter noninteracting nucleons move independently in a certain self-consistent potential field. Nevertheless, either accounts for a very wide range of nuclear phenomena in its respective region. Suffice it to mention fission physics in the former model, and the magic and near-magic nuclei and isomery islands in the latter. A similar situation arose in the description of nuclear reactions. Here too some models assume a strong nucleon–nucleon interaction (composite Bohr nucleus, 1936), and some consider the motion of noninteracting nucleons in a self-consistent potential (optical model of nuclear reactions, 1954). Based on the shell concept, the optical model involves a complex potential whose real part describes elastic scattering, and the imaginary accounts for absorption and for elastic diffraction scattering.

The above disagreements between different models were at first reconciled by compromise. The drop-shell conflict was smoothed to some extent in the generalised nucleus model (1950–1953) in which the achievements of both models were used. Basically, the generalised model involves an inner core consisting of strongly interacting closed-shell nucleons (drop contribution), and outer nucleons moving in the field of the core (shell contribution). The mutual influence of the core and the outer nucleons — and this is the crucial point — leads to the deformation of the nucleus, changes the nature of the one-particle levels and gives rise to new — collective (though again nucleon) — degrees of freedom associated with the rotation and vibration of the core. The most pronounced manifestations of the collective excitation of the nucleus are giant resonances — collective vibrations of all the constituent nucleons.

The nuclear deformation idea was suggested by Rainwater, O Bohr and Mottelson in 1950. However, the concept of collective nucleon motion goes back to Niels - Bohr, who in particular put forward the idea of rotational motion of the nucleus and discussed the nature of the dipole giant resonance as far back as 1937 [4]†. The key role of Bohr's ideas in the genesis of nuclear physics and in its subsequent development both in the past and today is most completely described in Ref. [6], devoted to the great physicist's birthday centenary.

Later improvements in the nuclear models involved the separation of the residual interaction between the outer nucleons from the self-consistent potential effect, with a resulting correlation between nucleon motions. The common descriptive term for these models is 'pair correlation models' [7].

One of these, which separates a particular type of residual interaction — the short-range pair attraction of nucleons of the same energies and moments (with sign opposite projections) — is called a superfluid model. Here nucleon correlation has a specific nature reminiscent of the electron Cooper pairs in metals. The mathematical framework of the theory of superfluid type pair correlations is due to Belyaev and Solov'ev [8, 9]. The superfluid model accounts for the wide energy gap near the nonrotational ground state of even – even nuclei, the anomalously small inertia moment of these nuclei, etc.

Not only nuclear models but also models of nuclear reactions have been improved. In describing the interaction of fast particles, for example, the optical model becomes more accurate if one uses the expression of the total scattering amplitude in terms of the scattering amplitudes on individual nucleons (Glauber's multiple scattering theory [10, 11, 12]).

2.2 Unified microscopic theory and quasinucleons

The improved nucleon models of the nucleus and of nuclear reactions have been quite successful and are being used even now in interpreting nuclear processes (see, e. g., Sections 4 and 5, in which Glauber's theory is discussed). Physicists, however, have long been puzzled by the disagreement between the assumptions used in the models. It seemed unnatural to have models of equal predicting power based on entirely different and indeed conflicting assumptions. Thus came the idea of a unified microscopic theory of the nucleus, with the most general nucleon interaction concept as the starting point, whose different versions would be able to generate different — and mutually consistent — models.

A suitable tool for translating this fundamentally new idea into reality was provided by the theory of the Fermi liquid developed by Landau in 1956 – 1957 [13]. In this theory, the picture of the ideal Fermi gas of noninteracting particles was modified by adding an interaction term which, Landau believed, would have little effect on the momentum distribution properties of ideal Fermi particles (all the states up to the Fermi level being filled). The validity of this assumption, seemingly questionable for a strong particle interaction, was proved by Migdal and Galitskii who developed a rigorous Fermi-liquid theory [14] and extended it to include finite Fermi systems, in particular atomic nuclei [15]. The inclusion of the internucleon interaction required — because of the Pauli principle — allowance for (both real and virtual) transitions of nucleons beyond the Fermi level, with a simultaneous formation of holes in the lower filled states of the potential well.

Thus the simplest non-nucleon, or more precisely nucleon – hole degree of freedom came into being. Because the nucleon – nucleon interaction is strong, the chance for virtual nucleon hole pairs to form and subsequently annihilate is quite good, with a consequence that the motion now involves many nucleons and so the nucleon becomes a quasiparticle (quasinucleon). The lifetime of the quasinucleon depends on its energy ε as measured from the Fermi level ε_F. However, like the nucleon proper, the quasinucleon carries a half-integer spin, obeys the Pauli principle and hence, like nucleons in a noninteracting scheme, may under certain conditions (if long-lived enough at low energy) participate in the independent one-quasiparticle motion (gas of quasiparticles).

Thus the introduction of a strong nucleon – nucleon interaction, necessitating the replacement of the nucleon by the quasinucleon, does not invalidate the nuclear shell model. In the new shell model, instead of a nucleon we have a sufficiently long-lived quasinucleon moving in the self-consistent potential field. This approach conserves both the quantum numbers and filling order of the levels, i.e., the new model is adequate as before to explain the properties of the magic and near-magic nuclei. On the other hand, there is no longer any disagreement with the liquid drop model, which includes the strong interaction which the nucleons (not quasinucleons!) retain.

The quasinucleon and quasihole concepts can also be shown to reconcile other nuclear and nuclear reaction models. The optical model of nuclear reactions, previously based on the old (nucleon, complex potential) shell model now derives from the new (quasinucleon, complex potential) shell model. The same is true for collective giant-resonance processes occurring in the generalised model, which are described in a natural way in terms of interacting quasinucleons: a quasinucleon hole pair initially produced by an external influence annihilates and transforms into another pair; this, in its turn, transforms into a third, and so on — resulting in a high probability of nuclear excitement. One example of the successful application of the theory of finite Fermi systems is the prediction of the correct positions and of some properties of the Gamow – Teller resonance in spherical nuclei [16 – 18].

Similarly, the microscopic pair-correlation model exploits the characteristic features of the interaction of two super-Fermi quasinucleons as a function of the momentum, spin, and isospin of the pair. In particular, the superfluid model makes use of the mutual attraction of two quasinucleons with their total momentum and total spin both zero.

It is to be emphasised that the quasinucleon theory of finite Fermi systems yields many nuclear properties within a single framework and using identical parameters for all the nuclei involved. Among these are binding energy, the spectra

†The actual prediction of the existence and position of the giant dipole resonance was made by Migdal in 1944 [5].

of the low-lying excited states, magnetic moments, the probabilities of β decay and of electromagnetic transitions, electron scattering cross sections, and more.

2.3 Nuclear interaction quanta and meson theories

Whereas the quasinucleon concept came into nuclear physics as a result of the development of nuclear models, the other — non-nucleon — degrees of freedom are due to the better understanding of the nature of nuclear forces.

The meson degree of freedom was first predicted theoretically in 1935 by Yukawa [19] who assumed the existence of a boson of mass ≃100 in order to explain the nature of nuclear forces. As is known, in 1947 a particle of about this mass (140 MeV) was discovered experimentally and called a π meson. The π meson (or pion) has three charge states (π^+, π^-, π^0). This is an isovector ($T=1$) pseudoscalar ($J^\pi = 0^-$) with negative G parity and zero baryon charge ($B=0$). The π^0 meson has a positive charge parity. With reference to the manner in which it interacts with other particles, the π meson is classified as the lightest hadron. It interacts strongly with other hadrons (including itself) but, since its mass is the minimum among the hadrons, it decays by a weak or electromagnetic channel. The charge radius of the pion is $\langle r_\pi{}^2 \rangle^{1/2} = (0.66 \pm 0.01) \times 10^{-13}$ cm.

The basic properties of the π meson, such as its involvement in the strong interaction and the suitable value of its mass, permitted it to be treated as a quantum of strong interaction between nucleons in the nucleus. This is clearly seen from the fact that the π meson Compton wavelength $\lambda_\pi^{\text{compt}} = \hbar/m_\pi c = 1.4 \times 10^{-13}$ cm is just the range of the nuclear forces, r_{nucl}, as estimated from other considerations.

Meson theories of nuclear forces were constructed by analogy with quantum electrodynamics, but unlike this latter, in which the small dimensionless constant $\alpha = e^2/\hbar c = 1/137 \ll 1$ allows an extremely accurate perturbation evaluation of the virtual-photon interaction component (i.e., radiative corrections), the meson theories (where the corresponding constant $f^2 \approx 1$) do not offer such a possibility. The corrections due to the virtual π mesons are much too large to estimate perturbationally. Therefore, no exact meson theory of nuclear forces exists.

Still, there is a specific version of the meson theory (taking into account nucleon and π meson properties) which led to a (π–N) interaction constant $f^2 = 0.08 \ll 1$, thus allowing a first-order perturbation analysis for some phenomena. This is the 'one-pion exchange (OPE)' approximation. It has enabled, for example, calculation of (N–N) and (π–N) scattering in fair agreement with experiment; and even estimation of the (π–π) scattering cross section, which, because neither π meson targets nor colliding pion beams are available, cannot be obtained in direct experiments. The OPE approximation is still being used in present-day theories (see Section 5 of this review).

Whatever the accuracy of meson nuclear-force theories, it is clear that the role of the pion component is great and diverse. Suffice it to say that π mesons participate in nucleon charge exchange, in the formation of pion resonances in the nucleus, in the dipion exchange process, etc. The interaction of pions and nucleons with nucleons and nuclei gives rise to large cross-section multiple pion production, to pion charge exchange, etc. Further below certain particular manifestations of the π meson field in the nucleus will be discussed (such as participation in collective spin–isospin excitations, π condensate, baryon solitons). There is, however, another side to the question of the meson theory: π mesons alone prove to be insufficient to explain the properties of nuclear forces, either quantitatively or qualitatively.

It is known, for example, that at a distance equal to and somewhat smaller than $r_{\text{nucl}} = \lambda_\pi^{\text{compt}} = \hbar/m_\pi c$, nuclear forces are attractive, and at very small distances ($< 0.5\times 10^{-13}$ cm), repulsive. To explain this, other particles, vector mesons with a mass of about 800 MeV, are needed. The vector nature of the new mesons is clearly seen from the analogy between two nucleons of equal baryon charge and two like electric charges, the latter also repelling by means of a vector particle, the photon.

In addition to vector mesons, the meson model also requires a scalar ($J^\pi = 0^+$) σ meson with a mass of about 500 MeV to explain the repulsion at intermediate distances. Suitable vector mesons have indeed been discovered within the meson nonet 1^-. These are (i) a ρ resonance with a mass $m_\rho = 770$ MeV, $T^G = 1^+$, $\Gamma = 150$ MeV decaying to two pions; (ii) an ω resonance with a mass $m_\omega = 783$ MeV, $T^G = 0^-$, $\Gamma = 8.5$ MeV, decaying primarily by $\omega \to 3\pi$; and (iii) a φ resonance with a mass 1020 MeV $T^G = 0^-$, $\Gamma = 4.2$ MeV, decaying predominantly by $\varphi \to K\bar{K}$. As regards the σ meson, this is introduced into the theory in a formal way as a correlated pair of π mesons.

Introducing several nuclear quanta into the meson theory of nuclear forces is not inconsistent with the modern quantum field theory, in which any physical particle is surrounded by a cloud of the virtual quanta of the fields with which it interacts. The cloud is the denser the stronger the corresponding interaction. For the nucleon, which participates in all nuclear interactions, the densest cloud is the hadron one. Its periphery consists of virtual π mesons responsible for the longest-range part of the nuclear attraction force; next come σ mesons accounting for the attraction in the intermediate region, and still nearer to the centre are vector mesons responsible for the short-range repulsion forces. Although this form of phenomenological meson model is still being used in describing the hadron interaction, its predictive power is limited to the periphery. So by the meson degree of freedom of the nucleus one usually means its pion component.

2.3.1 Pion degrees of freedom in the nucleus. The problem of existence of π condensate and of superdense nuclei

Particularly intensive studies of the pion degree of freedom began in the 1970s in connection with the problem of π condensate introduced by Migdal [20–22]. Migdal considered the polarisation of nuclear matter by the π meson field existing inside it, a process which leads to the excitation from the Fermi sea of nucleon–hole and Δ-hole states with pion quantum number. He showed that, for nucleon density ρ above a certain critical value ($\rho > \rho_c$), the nuclear matter becomes unstable to the formation of π mesons. Since π mesons are bosons, they will accumulate in an energetically favourable state forming, in so doing, the so-called π condensate, whose interaction with the nucleon medium may lead to the modification of the nuclear matter state equation†.

†In studying such an exotic state as the π condensate (i.e., the ππ interaction in the nucleon medium) one can rely on the no longer exotic data on ππ scattering vacuum parameters (see, e.g., Refs [23, 24]).

According to Migdal, the π condensate modifies the properties of the nuclear matter ('softens' the short-distance repulsion) in such a way that the energy-density curve may develop a second minimum, one corresponding to a superdense state. In principle, both conditions $\rho_c > \rho_0$, and $\rho_c < \rho_0$ are possible. The critical density ρ_c depends on the value of the correlation parameter g' responsible for the short-range repulsion. For small values of the parameter ($g' \approx 0.3$), π condensation is possible for $\rho_c \leqslant \rho_0$. With increasing g', the ratio ρ_c/ρ_0 increases†.

Migdal's early estimates were that π condensation may even exist in real nuclei with $\rho_c = \rho_0$. However, the global data analysis in a 1981 review article [25] questioned this view and led to the conclusion that π condensate must be absent in normal nuclei, that is, the π exchange attraction is balanced by the g' repulsion. From this fact, together with some other experimental data, the realistic value of this parameter is $g' = 0.7$, so that $\rho_c \approx 3\rho_0$. Such nuclear density can be expected in experiments on nucleus–nucleus collisions at relativistic energies.

The absence of π condensate in normal nuclei does not rule out their being close to the π condensate instability point. In particular, it was shown in 1983 [26] that precritical nuclear medium phenomena may (for certain values of momentum transfer) enhance the $(\pi, 2\pi)$ cross section on nuclei, and an experiment to see this was in fact projected in the same year [27]. This prediction is presumably substantiated by the discovery, in 1991 [28], of the enhanced pion yield in the 250 MeV/c momentum transfer, low energy transfer $(\pi, 2\pi)$ reaction on Fe and Ti nuclei. The problem of the π condensate is still a subject of some interest, as is proved by the number of projects having the search of precriticality sensitive effects as one of their objectives (e. g., Refs [29, 30]).

2.3.2 Chiral models. Skyrme model

New, far-reaching and sometimes even quite unexpected applications of the meson degrees of freedom have emerged quite recently from systematic work on the chiral models, notably on the Skyrme model [31, 32] proposed back in the early 1960s (the original ideas dating indeed to the mid-50s [33]). The Skyrme scheme exemplifies the use of field-theoretical concepts for describing extended objects (baryons and nuclei) and their properties. Skyrme starts from a nonlinear, chiral meson Lagrangian, for which the Euler–Lagrange solutions come out in the form of topological solitons (skyrmions) and so represent localised finite-size objects, in particular baryons. Thus, the nonlinear nature of the interaction of light meson (i.e., boson) fields (baryon number zero) enables heavy particles (baryon number unity) with fermion properties to be obtained. In other words, the mass of a baryon is of pion origin. One of Skyrme's early ideas [33] is a nucleus consisting of an electrically neutral 'pion liquid' whose density fluctuations give rise to the nucleon mass. ππ scattering phase data imply a proton mass fairly close to the experimental value (0.85 GeV) [34]. Skyrme's model has been successful in the description of nuclear matter and in the analysis of many strong interaction problems (in particular, nucleon–nucleon forces, meson–nucleon scattering, meson exchange currents, static nucleon properties [35]). In quantum chromodynamics the model is being used in the low-energy region (chiral bag models, see, e.g., Ref. [36]).

†The parameter g' is often referred to as the Landau–Migdal correlation parameter. One considers g' parameters for the NN interaction (g'_{NN}) and for the $\mathrm{NN} \to \mathrm{N}\Delta$ and $\mathrm{N}\Delta \to \mathrm{N}\Delta$ processes ($g'_{\mathrm{N}\Delta}$ and $g'_{\Delta\Delta}$, respectively). We will encounter these parameters in Section 5.

2.3.3 Nucleon form factors and the parton model

As far as the description of the strong nuclear interaction at $\geqslant 1$ GeV is concerned, the nucleon (quasinucleon), pion, and other meson (resonance) degrees of freedom of the nucleus are not sufficient because in this energy range the internal structure of these particles must be important. The internal structure of the nucleons was first suggested by Fermi, who introduced the concept of a π meson cloud of nucleons of radius $\lambda_\pi^{\mathrm{comp}}$ to account for the anomalous part of nucleon magnetic moments. This simple model yielded nucleon magnetic moments and electric charge distribution consistent both with one another and with the concept of a nucleon as an isodoublet member.

Although the first attempts to discover distributed charge in the neutron date again to Fermi (1947), it was in a series of experiments by Hofstadter [37] where more convincing data on the internal nucleon structure were obtained. It was demonstrated quite reliably that the electric charge and magnetic moment are distributed spatially in nucleons, which necessitated introduction of form factors and hence eliminated the pointlike nucleon concept. Although remaining elementary, the nucleon became extended. The behaviour of nucleon form factors implies 0.86×10^{-13} cm as the nucleon radius.

The next step towards understanding nucleon structure was made in 1969 by Feynman, who, based on the behaviour of the form factor for deep-inelastic electron scattering on the proton, suggested the existence, within nucleons, of virtual, pointlike, weakly interacting subelementary particles — partons [38]. Thus, according to the parton model the nucleon is not an elementary but a composite particle. This conclusion is supported by the linear energy dependence of the inelastic neutrino scattering cross section on a nucleon, and by the energy independence of the ratio of the cross sections for e^+e^- annihilation into hadrons and muons. In later work the partons were identified with other subparticles, quarks, proposed as far back as 1964 by Gell-Mann [39] and Zweig [40].

2.4 Quark model and QCD

Recall that quarks are semi-hypothetical (as they have not been found free), semi-experimental (their existence was proved in indirect experiments) particles with fractional baryon ($B = +1/3$) and electric [$q = (+2/3)\,e$ and $q = (-1/3)\,e$] charges and with a half-integer spin. In all, we know of six types (or flavours) of quarks, of which five (u, d, s, c, b) have been convincingly demonstrated in experiment, and the sixth (t) is predicted theoretically‡. The first two quarks [u quark with $q = (+2/3)\,e$, $T = 1/2$,

‡Two 1994 studies [41, 42] were devoted to the search for the t quark using the 1.8 TeV Fermilab Tevatron $\mathrm{p\bar{p}}$ collider. The former study was the search for the t quark decaying to a charged Higgs boson H^+ (which, incidentally, also has not yet been discovered); the latter, for the decay of the $\mathrm{t\bar{t}}$ pair to lepton modes. From the properties of several t candidates, the lower bound for the t quark mass was estimated, at a 95% confidence level, to be $M_t > 131$ GeV/c^2. The theoretical values of the ('current') masses of the remaining quarks (u, d, s, c, b) are 4, 7, 150 MeV/c^2, 1.3 and 4.75 MeV/c^2, respectively.

$T_3 = +1/2$, and d quark with $q = (-1/3)e$, $T = 1/2$, $T_3 = -1/2$] form nonstrange hadrons, whereas the remaining, with corresponding additional quantum numbers, participate in the formation of strange (s), charmed (c), and beautiful (b) particles. Any baryon consists of three quarks (p = uud, n = udd, Δ^{++} = uuu, Ω^- = sss, etc.); any antibaryon consists of three antiquarks (with quantum numbers opposite to those of the corresponding quarks); and a meson, of a quark and antiquark tied by a very strong interaction (much stronger than the hadron one). The total number of quarks is conserved in all interactions whereas the number of quarks with a given flavour is only conserved in strong and electromagnetic interactions. Each quark type has three species dubbed as colours (red, blue, and green) [43–47]. The antiquark is characterised by three anticolours (antired, etc.). Colour has two meanings. First, as a new quantum number it secures wave function antisymmetrisation for three-quark baryons (fermions); second, it serves as an analogue of the electric charge in the electromagnetic interaction (colour charge). According to the modern theory of strong interaction (quantum chromodynamics, QCD), the quark–quark interaction proceeds via eight vector particles, gluons ($m = 0$, $q = 0$, $T = 0$, $J^{PC} = 1^{--}$), provided by the coloured quarks. In contrast to uncharged photons, and similarly to quarks, gluons are 'charged' with colour, that is, can generate other gluons and interact with one another.

The quark–gluon interaction is of such a nature that the effective colour charge of a quark is small in its neighbourhood but increases rapidly with distance away (antiscreening). Therefore the quark–quark interaction at very small separation is practically absent (cf. partons). This feature is termed asymptotic freedom [48, 49]. At large distances (of the order of the hadron radius) the interaction, in contrast, becomes so large that quarks find themselves confined in hadrons [50, 51]. It is therefore believed that quarks and gluons cannot exist free. In fact, in spite of very intensive searching, free quarks have not been found either in nature or in accelerators. The spectra of observed particles display only colourless hadrons, in which the quarks' colour charges cancel (quark and gluon hadronisation) and which interact only via conventional nuclear (meson) forces, much weaker than their colour counterparts.

Quantum chromodynamics at small distances is characterised by a small constant ($\simeq 0.16$), which enables fairly accurate perturbation calculations to be performed. With increasing distance the constant increases, perturbation calculations break down, and the QCD hadronisation and confinement problems remain unsolved. So to describe the quark–quark interaction at large distances one has to employ composite quark models of hadrons, the so-called bag models [36, 52, 53].

Essentially, the bag model involves the idea of quasi-independent relativistic particles, quarks and gluons, moving in a finite closed region of space. In this way, and using a particular confinement model, the masses, magnetic moments, radiation transition widths, and other static characteristics of low-energy hadron physics were obtained [54, 55].

In standard bag models the scale of confinement is specified by boundary conditions, i.e., is deduced from nonmodel considerations. In Refs [56, 57] the confinement is due to the quark–quark interaction (chiral, or hybrid bag model). The hybrid models have permitted a unified description of both the hadronisation and asymptotic-freedom regions [36].

An approach alternative to the bag method is to solve the QCD equations numerically by use of the lattice method, which does not involve perturbation theory and goes down to distances of the order of 3×10^{-13} cm [58, 59]. One can argue, however, that this distance is insufficient to justify the confinement approach [60].

Another independent theoretical approach, the QCD sum rule [61, 62], is one which relates chromodynamic quantities to hadron characteristics without considering the confinement problem. An attempt [63] at unifying the basic large-distance quark–hadron assumptions formulated above (i.e., the colour confinement, colourless hadronisation, and the phenomenology of low-energy hadron states) employed the model of confined relativistic quarks. The model reproduces the low-energy chiral-theoretical states and is consistent with the low-energy light-meson data. The confinement is accounted for phenomenologically.

We may summarise the situation concerning QCD and the quark model as follows. Although undiscovered free, the existence of quarks can hardly be questioned since the properties of quarks and gluons have been established in indirect experiments. The asymptotically free QCD is an exact theory, whereas in the low energy region quark model results are close to those of other models — the Skyrme model, for example [35, 36]. On the other hand, the confinement problem is not yet settled (even an incomplete colour confinement has been suggested [60]) and hence the nucleon — let alone the nucleus — is not yet amenable to a consistent QCD description.

If one still adheres to the view that QCD is an exact theory of strong interactions valid for all distances (and just having some temporary difficulties of technique at short quark spacings), then the optimum approach to the description of nucleons and nuclei will be apparently to take QCD as the basis on which to develop traditional microscopic theories involving the quasinucleonic, pion, and resonance degrees of freedom described above. In this connection, it is still important to keep gathering semi-empirical data on the carriers of non-nucleonic degrees of freedom, and to develop phenomenological methods for describing the properties of these carriers, their quark–gluon structure, departure from the corresponding free particles, etc. In concluding this section, Refs [64, 65] are to be recommended as good sourcebooks for the reader desiring to brush up his or her knowledge of the subject.

2.5 Δ-hole degree of freedom

2.5.1 Relation to spin–isospin excitations

The following sections review the state-of-the-art of experimental Δ isobar research, a fairly recent subject which was stimulated by the now topical studies on spin–isospin nuclear excitations and on the role of pion degrees of freedom in them. Let us explain what is so important about this subject. We have already mentioned the close relation between spin–isospin excitations and the problem of existence of π condensate and superdense nuclei. Some further examples from various areas of nuclear physics and elementary particle physics follow.

1. When comparing the masses and quantum numbers of the nucleon ($S = 1/2$, $T = 1/2$) and Δ resonance ($S = 3/2$, $T = 3/2$) it is seen that the simplest response of a nucleus to a spin–isospin excitation on a 300 MeV

energy transfer scale is when a nucleon in the nucleus makes an (N − Δ) transition to the Δ isobar. If the resulting Δ acquires in this process a low momentum (comparable to the Fermi momentum), this favours its subsequent interaction with the nucleons which, on account of the isobar decay properties, may result in the excitation of a peculiar pion-like wave collective state, a phenomenon which holds great promise of interesting physics (see Sections 3.1, 4.5.4, and 5.3.2 for more details).

2. A well-known problem is that of a large discrepancy between the strength of the Gamow – Teller resonance and the sum rule for nucleon degrees of freedom. Since the Gamow – Teller resonance is associated with collective spin – isospin $\Delta S = \Delta T = 1$ transitions, the discrepancy may be due to the Gamow – Teller transition strength leaking into the Δ isobar region, an effect which requires Δ-hole non-nucleon degrees of freedom to be accounted for. Microscopic schemes of the Gamow – Teller resonance, including the Δ-resonance and pionic branches and the breakdown of the Wigner SU(4) symmetry, are considered in the original paper [66] and in a review article [67].

3. The pion degrees of freedom have the potential to explain the so-called EMC effect discovered by the European Muon Collaboration. Basically, this is the departure from unity of the experimental nucleus/deuteron ratio, R, of the structural functions for the deep-inelastic muon (electron) scattering. The quantity R is defined as

$$R(X) = \frac{F_2^A(X)}{F_2^D(X)} = \frac{2\sigma^A}{\sigma^D} , \qquad (1)$$

where $X = Q^2/2M\nu$, $Q^2 = -t$ is the square of the four-momentum transfer, $\nu = E_\mu - E'_\mu$ is the energy transfer, M the nucleon mass, and $F_2^A(X)$ and $F_2^D(X)$ are the structural functions of the nucleon with mass number A and of the deuteron, respectively. If the nuclear wave function involves only nucleon degrees of freedom, then for all X we must have $R = 1$. Experimental data on ^{56}Fe [68, 69] suggest that $R = 1.17$ for $X = 0.05$, $R = 0.85$ for $X = 0.65$, and $R = 1.2$ for $X = 0.9$, necessitating inclusion of non-nucleon components in the nuclear wave function.

Analysis of the results of Refs [68, 69] has indicated [70] that the rise in R in the region of small X is due to 'long-range' meson fields, and at large X is associated with the dynamics of nucleon – nucleon interactions at small distances and, ultimately, with the mixture of multiquark states in nuclei†. According to Ref. [70], the introduction of π meson degrees of freedom (meson exchange currents) causes a rise in R for $0 \leqslant X \leqslant m_\pi/M \simeq 0.15$. This is a purely nuclear effect, its size increasing towards heavier nuclei.

4. Modern QCD considers the possibility for nuclear matter to make a phase transition to the hypothetical state of a quark – gluon plasma. A necessary condition for this is a very high temperature and/or a high baryon charge density. In nature the quark – gluon phase is achievable in neutron stars, and in the laboratory, in collisions of relativistic nuclei. Under such extremal conditions, it is natural to assume that transitions of ordinary nuclear matter to a quark – gluon plasma state and back will be accompanied by the excitation (de-excitation) of the internal degrees of freedom of the baryons and mesons (π, ρ, ω, etc.) that make up the nuclear matter.

†Experimental evidence for multiquark systems in nuclei and nuclear processes was obtained in Ref. [71].

If it is appropriate here to draw analogy with ordinary plasma, which is a 'gas' of electrically charged bare atomic nuclei and electrons, then quark – gluon plasma may be thought of as a 'gas' made up of 'colour-charged' quarks and gluons released from confinement captivity. The excitation spectrum of the nuclear matter at the phase transition line must be very complicated, but it seems certain that its lower states will be associated with the formation of the Δ isobar and other baryon resonances. Thus, knowledge of the properties of the Δ isobar inside nuclear matter is also essential to the development of one of the latest areas of research in physics — nucleus – nucleus collisions at superhigh energies [72].

2.5.2 Free versus nuclear Δ isobar

We assume throughout that, having been produced in the excitation of the nucleus, the Δ isobar exists for some time in it before decaying, in spite of the neighbouring nucleons interacting strongly both with one another and with the isobar itself. It is evident, however, that this neighbourhood cannot be of altogether no consequence for the Δ. The question is: What is the difference between the nuclear and the free isobars?

To begin, let us recall the familiar properties of the free Δ isobar, that is, of one resulting from the excitation of a free nucleon. The free (or nucleon, or vacuum) Δ is an isotopic quartet (Δ^{++}, Δ^+, Δ^0, Δ^-) of nonstrange particles of average mass $m_\Delta = 1232$ MeV that comprise the baryon decouplet $3/2^+$. The Δ isobar is a hadron, that is, a particle which has a large cross section for production in strong interactions but, unlike 'ordinary' long-lived hadrons such as the proton, neutron, and π meson, has a very short — nuclear — lifetime and hence belongs to the class of resonances — entities which are not only produced, but also decay by the strong interaction. The most probable decay channel for the Δ isobar is $\Delta \to N + \pi$, with a width $\Gamma = (115 + 5)$ MeV. Despite its extremely short lifetime, $\tau = \hbar/\Gamma \simeq 0.6 \times 10^{-23}$ s, the Δ resonance may, like ordinary long-lived particles, be characterised by a complete set of quantum numbers, may be given definite values of kinetic energy and momentum, etc., although it is of course impossible in principle to separate it in a single event.

We now proceed to a preliminary discussion of Δ isobar parameters. Note first that in the quark model the Δ resonance is 'organised' analogously to the nucleon, which is especially clear when one compares the quark compositions of the proton and the Δ^+ resonance. Either consists of the same set of quarks (uu and d), except that one of the quarks has its spin and isospin reversed, $S_p = T_p = 1/2$, $S_{\Delta^+} = T_{\Delta^+} = 3/2$. Often the Δ resonance is referred to as an excited state of the nucleon. In fact the nucleon's unique position of being stable to the strong interaction is simply due to the fact that it is the lightest baryon possible and hence, in contrast to the isobar, has nowhere to decay by the strong interaction. So the coexistence of the Δ isobar with nucleons in the nucleus appears quite natural, and in some nuclear models the Δ is simply treated as an extra baryon (see, e.g., Ref. [73]).

In this connection, much of what is known about the nucleon in a nucleus is presumably true — with due short lifetime corrections — for the nuclear Δ isobar as well. In particular, this is the possibility of collective effects, which are expected to produce a difference between the nuclear Δ and its nucleon counterpart.

The collective nuclear excitations associated with the appearance of the Δ isobar degree of freedom form a rather complicated subject. We note first that the Δ degree of freedom is closely related to the π meson one. The Δ isobar in the nucleus is excited as a result of very numerous and diverse processes triggered by primary π mesons (not by them alone, though); its formation within the nucleus is closely related to pion exchange currents, and the meson decay channel is accompanied by π meson emission. The Δ-hole type quasiparticle with pion quantum numbers is sometimes even called a 'quasipion'.

Because of its strong interaction with the nucleons and with the virtual pions in the nucleus, the nuclear Δ may and indeed must have different properties from the free. In appearance, there are only a few parameters which have changed, namely, the energy position of the Δ maximum, its width and height (per nucleon), and certain decay features (less correlation between the primary particle momentum and the total momentum of the Δ decay products, a new mesonless de-excitation channel for Δ). In actual fact, however, many more sources of difference exist. Among these one inevitably finds trivial effects which, although of nuclear origin, are obvious enough; as well as nontrivial collective effects, to be separated against the background of the obvious ones.

Among the nontrivial effects are the renormalisation of the Δ production vertex, the excitation of a virtual pion field, the collective nucleus excitation due to the motion of the Δ within the nuclear volume, etc. The difficulty in disentangling nontrivial collective effects lies in the fact that the other — obvious — effects are very large in number. First, there is the possibility of quasifree Δ excitation in a nucleon inside the nucleus, which makes it necessary to introduce Fermi motion and to consider the boundedness of the nucleons in the nucleus, with a resulting change in the Δ peak parameters (shift and broadening). Further, if the projectile particle is complex (nucleus), it can carry a Δ excitation itself. One also must take into consideration the details of its interaction with the target nucleus (surface or bulk interaction, form factor influence). The formation and decay of the Δ isobar in the nucleus must undoubtedly be influenced by the Pauli principle (phase volume decrease) and by the interaction in the final state (reduced correlation between the primary and the final momenta). Finally, the observed parameters of the Δ isobar in the nucleus may change because of background reactions. It is clear, for example, that the low-energy tail of the excitation of resonances heavier than Δ_{1232} must shift the Δ peak to higher invariant masses than for the case of the free Δ. Similarly, the quasideuteron mechanism (see Section 3.1.3) may shift it to smaller masses.

Although it seems that the above effects can in principle be accounted for individually — and we shall see later that this work is indeed underway — when acting in concert they may lead to unpredictable results. It is therefore desirable to begin by discussing processes for which some doubtful points associated with these effects may be discarded from the start, and those remaining may be cleared up more or less unambiguously. A suitable process is, in our view, the electromagnetic Δ excitation, which does not involve the excitation of the primary particle — the photon, and for which an exact theory of calculation exists. It is this process which is addressed in Section 3 of this review.

3. Electromagnetic excitation of the nuclear Δ isobar

3.1 Mechanisms of interaction of γ quanta with nucleons and nuclei in the intermediate energy region ($100 < E_\gamma < 500$ MeV). Basic diagrams

3.1.1 General remarks on the photoproduction of pions and Δ isobar on free and bound nucleons

The basic features of intermediate energy γ quanta are that their mean free path in nuclear matter is large compared with the size of the nucleus and that their wavelength is short compared to the nucleon spacing. It is these two characteristics which to a large extent determine the nature and mechanism of the photonuclear interaction. The former allows γ quanta to penetrate freely into the high density region of the nuclear matter, i.e., their interaction with the nucleus must be of a bulk (not surface) nature — a fact which may lead, in particular, to the proportionality between the total photoabsorption cross section and the mass number A (see Section 3.5); the latter feature implies that the γ quantum interaction is local, i.e., involves a particular individual nucleon inside the nucleus (or a pair of nucleons a small distance apart). One therefore expects that at intermediate energies the interaction of γ quanta with the nucleons in the nucleus will be similar to their interaction with free nucleons, although some differences due to the influence of neighbouring nucleons can of course be expected. In particular, a region of high nucleon density is expected to favour collective effects in the nucleus.

We will employ diagrammatic language to discuss the interaction of the γ quantum with a free nucleon and with a nucleon in the nucleus. Free nucleon processes are primarily pion photoproduction [one pion at $E_\gamma > 150$ MeV (Fig. 1a), two at $E_\gamma > 310$ MeV (Fig. 1b), etc.], and the excitation of Δ at $E_\gamma > 340$ MeV (Fig. 1c) and of other resonances at the higher energies. Therefore at least for the γ–nucleus interaction one would expect quasifree pion production and the excitation of Δ at one of the nucleons in the nucleus to occur.

In Fig. 1d the pion photoproduction diagram is shown. Here π is the resultant pion (π^+, π^-, π^0) and N′ is the (n, p) 'recoiling' nucleon, which usually leaves the nucleus together with the pion. The spectra of the π mesons produced and of the recoiling nucleons must be distorted with respect to the pion photoproduction on a free nucleon, the reason being the nucleon binding energy and Fermi motion effects and the interaction of the nucleons and π mesons in the final states caused, for example, by pion rescattering (Fig. 1e), or to pion absorption by a neighbouring nucleon (Fig. 1f) with a resulting excitation of the nucleus. The excitation can be released by one or more nucleon emissions. Because the nucleus is transparent for intermediate-energy γ, a nucleon interacting with a γ quantum may be at any point within the nucleus. The pion production and Δ photoexcitation thresholds on nuclei are somewhat below their free nucleon analogues (∼140 MeV for a single π meson, ∼280 MeV for two, and ∼300 MeV for the Δ).

3.1.2 Behaviour of the Δ isobar in the nucleus

For $E_\gamma > 300$ MeV, the photonuclear interaction cross section is characterised by a broad ($\Gamma \sim 150$ MeV) maximum associated with the Δ isobar excitation. The Δ isobar may be due to a quasifree mechanism, when all the

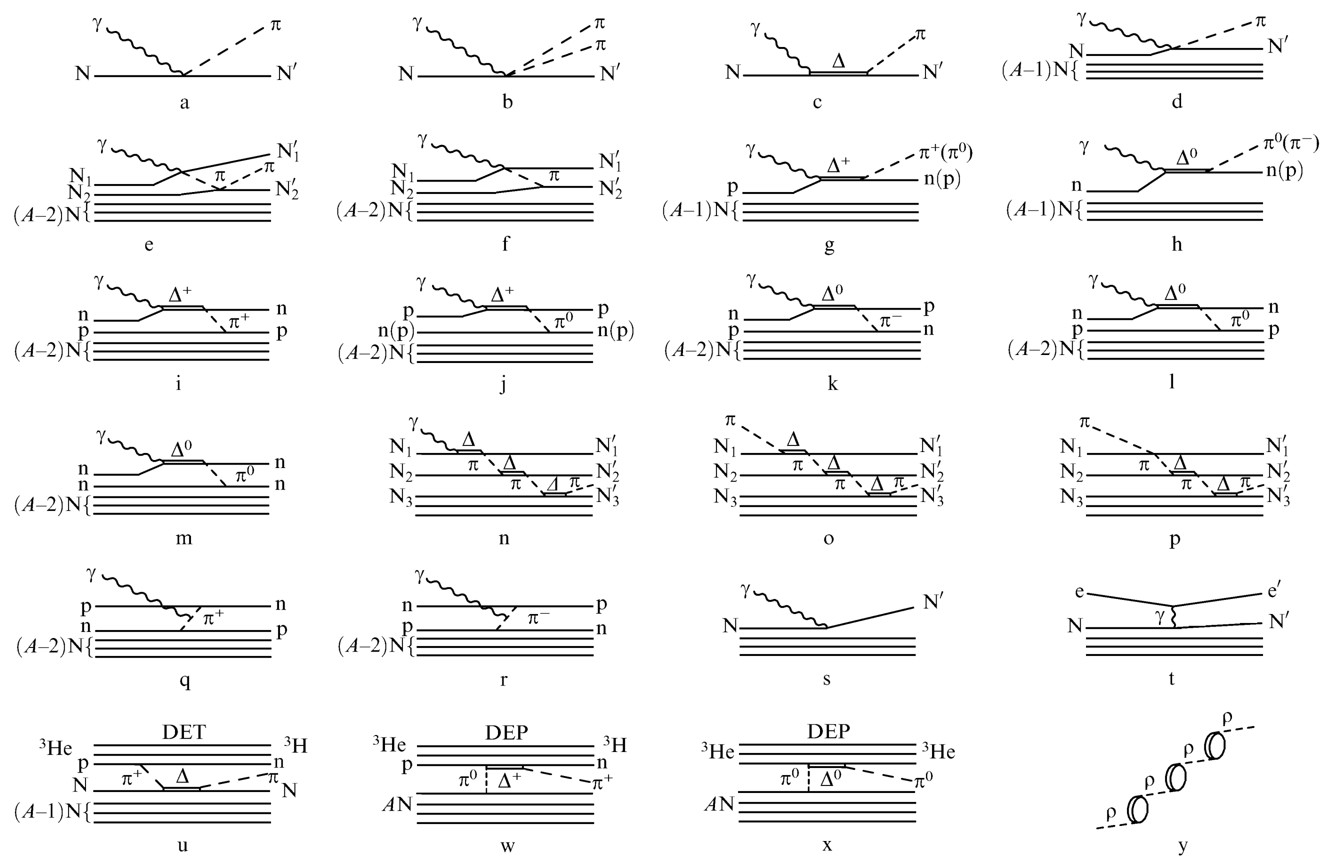

Figure 1.

required energy ($\sim$300 MeV) is transferred to one nucleon in the nucleus (Figs 1g, 1h). In another possibility, the Δ excitation of the nucleus results from the superposition of many Δ-hole states — a collective nuclear mechanism. Of course, in neither case must the excitation necessarily be electromagnetic, although for the sake of uniformity it is precisely this case which we show in the figures. For either mechanism, there are two alternatives for the resultant Δ isobar. One, the same as for the nucleon Δ isobar, is the decay by emitting a nucleon and a π meson (see Figs 1g, 1h). The other, specifically nuclear possibility is the interaction with a neighbouring nucleon, which yields two nucleons and no π meson (Figs 1i – 1m).

In principle, the collective Δ excitation mechanism may take an even more complex form of a superposition of Δ-hole and pion degrees of freedom (Fig. 1n). This is due to the large width and to the two-particle decay of the Δ, with the result that the π meson from the decay of the 'first' Δ isobar may conserve its resonance energy and form a 'second' one with another nucleon of the nucleus, etc. (pion-like wave [74]). Clearly this process is not sensitive to the manner of excitation of the first isobar, and this may be produced by any other primary particle (Fig. 1o)†.

Of course the transformation chain may break at any of its links, and the next π meson will either interact outside the resonance region or escape from the nucleus. In the latter case the decay product parameters of the 'last' Δ must correlate more weakly with the primary particle momentum than in the quasifree Δ production case. The above 'motion' of the Δ inside the nuclear matter may also be accompanied by changes in the width and location of the Δ excitation maximum, in the total charge of the decay products of the last relative to the first Δ, etc. In anticipation of the discussion below, note that all three mechanisms for the excitation of the nucleus in the Δ region have indeed been discovered experimentally.

†Indeed instead of the first isobar, a 'first' π meson of suitable energy — i.e., not necessarily a primary π meson but, say, a rescattering pion (Fig. 1p) — may be the first link of the chain.

3.1.3 Interaction of the photon with a meson exchange current. Quasideuteron mechanism

Apart from the processes illustrated in Figs 1l and 1m, a mesonless nucleon pair may be produced by another nuclear mechanism — the interaction of a γ quantum with a charged meson exchange current (Figs 1q and 1r).

The diagrams show that the above nuclear mechanisms for the formation of two nucleons in the final state both lead to the emission of primarily pn (not nn or pp) pairs, that is, the kinematics of these processes may be similar to the photosplitting of the deuteron.

The two-nucleon (quasideuteron) photonuclear interaction was first suggested in 1951 by Levinger to explain the formation of fast photoprotons at $E_\gamma > 150$ MeV [75, 76]. Considering the absorption of the γ quantum dipole component by an np pair (known to have an electrical dipole moment), Levinger showed that at short neutron – proton distances the two-nucleon wave function for positive energy (the quasideuteron has no binding energy!) is proportional to the deuteron wave function: $|\Psi_{\rm qd}|^2 \propto |\Psi_{\rm d}|^2$. The factor of proportionality depends on the density of the nuclear matter and the relative momentum of the neutron and the proton. A nucleus of radius $R = r_0 A^{1/3}$, where $r_0 = 1.2$ fm, behaves as if it contained $8NZ/A$ quasideuterons.

Accordingly, Levinger [77] proposed the following estimate for the cross section for the quasideuteron absorption of γ:

$$\sigma_{\gamma\,\mathrm{qd}} \simeq 8\,\frac{NZ}{A}\,\sigma_{\gamma\,\mathrm{d}}\ , \tag{2}$$

where N is the number of neutrons in the nucleus, Z the nuclear charge, A the mass number, and $\sigma_{\gamma\mathrm{d}}$ the total cross section for deuteron photosplitting.

In 1979, to match to the low-energy region Levinger [78] modified Eqn (2) to obtain

$$\sigma_{\gamma\,\mathrm{qd}} = L\,\frac{NZ}{A}\exp\left(-\frac{E_\gamma}{S}\right)\sigma_{\gamma\,\mathrm{d}}\ . \tag{3}$$

Here $L \sim 10$ is what is now known as the Levinger factor, E_γ is the energy of the γ quantum in MeV, and S is the fitting parameter ($S = 60$ MeV).

According to Ref. [77], the experimental dependence of the total deuteron photosplitting cross section $\sigma_{\gamma\mathrm{d}}$ on photon energy has two maxima, at $E_\gamma \approx 4$ MeV and $E_\gamma \approx 300$ MeV. Curiously, the maximum at $E_\gamma \approx 300$ MeV was interpreted as an isobar nucleon excitation as far back as 1955 [79, 80].

The small value of nucleon spacing in the quasideuteron is clearly seen from the analysis of the γ quantum – nucleon interaction [78]. A high-energy γ quantum cannot transfer its energy and momentum completely to a single nucleon, not even if this latter is bound in the nucleus (which cannot compensate for the excess nucleon momentum at high γ energies). It is readily shown, however, that this is possible for a pair of nucleons a small distance apart which do not interact with the remaining nucleons in the nucleus. In this connection, it is helpful to note that the above process may provide insight into the interaction of nucleons at very short distances (less than the average nucleon spacing in the nucleus).

3.1.4 Experiments necessary for the study of the photoproduction and electroproduction of the Δ isobar in nuclei

Thus, in studying the γ quantum – nucleus interactions for $100 < E_\gamma < 500$ MeV, some information on the excitation of the nuclear Δ isobar and on its properties may be hoped for. Global information on the Δ isobar, namely the confirmation of its existence and the principal parameters such as the location, width and height of the Δ maximum, is obtainable from measurements of the total photoabsorption cross section. Usually these data are obtained by detecting certain photonuclear reaction products (whose nature depends on the technique used) — i.e., the experimental arrangement is an inclusive one, and the contribution from undetected particles is accounted for either by calculation or by use of data from elsewhere.

More detailed investigation of the formation, decay, and absorption of the Δ — and in particular separating the decay products from the background of quasifree pions and nucleons from the excited nucleus, and the study of correlated nucleon pairs at short distances — requires more sophisticated experiments in a very nearly exclusive setup — those with coincident detection of πN and NN pairs. To get a feeling for the nuclear size effect, it is desirable that the target mass number range be as wide as possible (including hydrogen as a reference point). γ beams of high enough intensity and specified energy are preferred.

The experimental work on this programme is reviewed in Sections 3.3 – 3.5 following a brief description, in Section 3.2, of intermediate energy γ sources.

3.2 Intermediate energy γ sources

3.2.1 Real and virtual photons and their properties

The major sources of γ quanta of sufficiently high energy are bremsstrahlung and the reverse Compton scattering of laser photons on relativistic electrons. In-flight annihilation of accelerated positrons and the coherent emission of electrons in oriented crystals may also be used†.

All of the techniques we have listed above involve the formation of real photons, which are just another projectile to work with. Real photons can be collimated, target-directed, detected, etc. Their spectra may be measured and calculated and, needless to say, do not depend either on the nucleus or the reaction type. One further feature of real photons (except for annihilation-produced ones) is their longitudinal polarisation component (30% for bremsstrahlung and coherent photons and 100% for Compton photons).

Apart from real photons, electromagnetic interactions may also proceed via virtual photons, a concept which is used to interpret the interactions of charged leptons — electrons with nuclei, for example. From the experimental methodology viewpoint, these are not photonuclear but rather electronuclear reactions, and the virtual photons they involve only serve to transmit the interaction in question. The spectrum of the virtual photons cannot therefore be measured but can be calculated — although this is quite a challenge (in particular, because of the reaction and target dependences).

An interesting feature of virtual photons is the simultaneous presence of longitudinal and transverse polarisations. Because of this, virtual photons — unlike real ones — may transmit $L = 0$, thus exciting nuclear monopole transitions. Also, the spectrum of virtual photons shows an increase in the intensity of the multipole partial component with increasing L. Thus, using electronuclear reactions (by comparing them with photonuclear reactions) one can separate the quadrupole and higher contributions. Note, however, that electronuclear cross sections are about 10^2 times smaller than photonuclear ones, a point evident from a comparison of the nuclear photoexcitation (Fig. 1s) and electroexcitation (Fig. 1t) diagrams.

The analysis of electronuclear reactions is more complicated, because the theoretical spectra of virtual photons are rather poor in quality. For problems where such spectra are not needed, however, electronuclear reactions are quite informative. Among these is nuclear Δ electroproduction, a process which may be studied as a function of the square of the four-momentum transfer, Q^2 (see Section 3.5.2).

Of the real photon production methods we mentioned in the beginning of this section, only bremsstrahlung and inverse Compton scattering will be considered in some detail, as these two have a number of advantages which make them quite promising for the solution of nuclear physics problems.

†The reader is referred to monograph [81] to learn more on the subject matter of this section.

3.2.2 Bremsstrahlung and labelling technique

The bremsstrahlung energy spectrum is known to decrease as $1/E_\gamma$ to the maximum γ energy $E_\gamma^{\max} = T_e - m_e c^2$. Photons of different multiplicity weigh equally in the spectrum (starting from $L = 1$). Bremsstrahlung γ quanta are polarised linearly ($\sim 30\%$), and their propagation direction is that of the primary electron beam. The spread of the γ beam depends on multiple scattering in the bremsstrahlung target and the spread in angle of the primary beam electrons. With the high vacuum of modern electron accelerators, and using low-density jet targets, very low γ beam spreads may be achieved.

Naturally, the continuous energy spectrum of bremsstrahlung γ quanta makes them inconvenient to work with because in order to separate the effect due to a given energy one has either to use the difference method, which involves large intensity loss and introduces errors, or to extract the cross section from the reaction yield by solving an improper mathematical problem. For this reason modern photonuclear experiments usually employ labelling techniques, which act to pick out a certain γ energy from the continuous spectrum. The idea of labelling is that the energy of the reaction-producing bremsstrahlung γ quantum is determined from the energy of the scattered electron that had emitted the quantum. The schematic diagram of labelling is shown in Fig. 2a.

The energy of the scattered electrons is determined by a system of plastic counters in the focal plane of the analysing magnet (not shown in the figure). The size of the counters is determined by the required resolution and by the desire to separate about the same number of γ quanta into each energy interval.

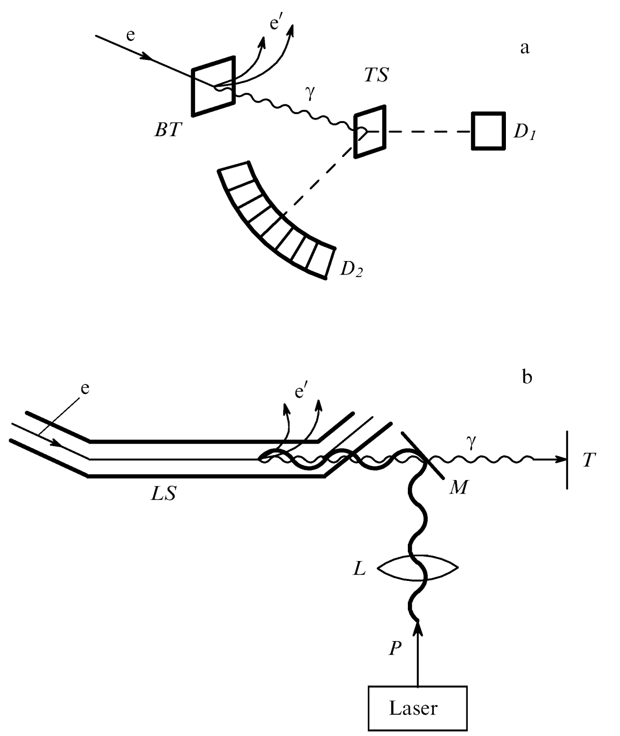

Figure 2. (a) Schematic diagram of a γ bremsstrahlung labelling facility: e — accelerator electron beam, BT — the bremsstrahlung target, e′ — scattered electrons that have emitted γ quanta; TS — target under study, D_1 and D_2 — reaction product detectors. (b) Schematic diagram of a Compton backscattering facility: LS — the linear segment of the accel-erator, e — accelerator electron beam, e′ — scattered electrons that form after the interaction of laser photons P with the electron beam, M — photon mirror, L — lens, γ — Compton γ quanta, T — target under study.

The idea of labelling implies working in coincidence with reaction product detectors. If the coincidence time resolution is taken to be 1 ns, then the total current N of labelled γ quanta may be as much as $10^8 \gamma\ s^{-1}$. Labelling facilities currently in operation yield $(1-5) \times 10^7 \gamma\ s^{-1}$ with energies 5 – 170 MeV [82, 83], $(10^5 - 10^6) \gamma\ s^{-1}$ with energies 100 – 500 MeV [84, 85], and up to $10^8 \gamma\ s^{-1}$ with energies 50 – 800 MeV [86].

State-of-the-art bremsstrahlung labelling systems now under development make use of the American CEBAF accelerator [87], with $E_\gamma = 30 - 4000$ MeV, $\Delta E_\gamma = 5$ MeV, $N = 10^7 \gamma\ s^{-1}$, and the Moscow 'Siberia-2' facility [88], $E_\gamma = 100 - 2500$ MeV, $\Delta E_\gamma = 5$ MeV, and $N = 10^7 \gamma\ s^{-1}$. The project of the first photonuclear experiment on the PLP (polarised labelled photons) channel of 'Siberia-2' is described in Ref. [89].

3.2.3 Laser photon Compton backscattering

In 1963 it was shown that the backscattering of laser photons of energy E_{ph} on colliding relativistic electrons gives rise to hard electromagnetic radiation whose energy E_γ may be comparable to the electron energy E_e [90]. The quantities E_{ph}, E_γ, E_e and the angle θ between the directions of the incident electron and the outgoing γ quantum are related by

$$E_\gamma = \frac{E_{ph}}{(m_e c^2/2E_e)^2 + E_{ph}/E_e + \theta^2/4}, \tag{4}$$

where m_e is the electron mass (θ in radians).

Equation (4) implies, for example, that ArF-laser photons of energy 6.42 eV, when scattered straight back ($\theta = 0°$) on electrons of energy $E_e = 2.5$ GeV, transform into hard γ radiation with $E_\gamma \sim 500$ MeV, i.e., the energy of the laser photons increases by a factor of almost 10^8.

The resultant γ quanta will have 100% linear (in the plane of the electron's orbit) or circular (above or below the plane) polarisation. For photon scattering angles $\theta \neq 0$, hard γ radiation of lower energy and of somewhat lower intensity can be obtained. The energy of the radiation may be varied (at fixed intensity) by changing the electron energy. There are other Compton backscattering features important to experiment: low bremsstrahlung background (because of the low gas pressure in the electron storage ring), low neutron background (few scattered electrons), and high (up to $10^7 \gamma\ s^{-1}$) intensity. The important advantage of backward Compton radiation is that its intensity is concentrated in a very narrow angle ($\theta \sim 1/E_\gamma$), which, for not very high radiation energies ($E_\gamma < 100$ MeV), enables good beam monochromatisation to be achieved by collimation alone. At higher energies, labelling techniques are employed.

The schematic diagram of a Compton backscattering facility is shown in Fig. 2b. An example of a facility for obtaining a Compton γ beam is the Novosibirsk ROKK machine in operation from 1984 [91]. Its basic components are the VEPP-4 accelerator ($E_e = 1.8 - 5.5$ GeV) and an argon laser ($E_{ph} = 2.4$ eV). The facility yielded a γ beam of intensity $2 \times 10^5 \gamma\ s^{-1}$ and monochromaticity $\Delta E_\gamma / E_\gamma = (3 - 10) \times 10^{-2}$. The beam intensity is concentrated within an angle of $\theta \sim 10^{-4}$ rad. The beam was monochromised by

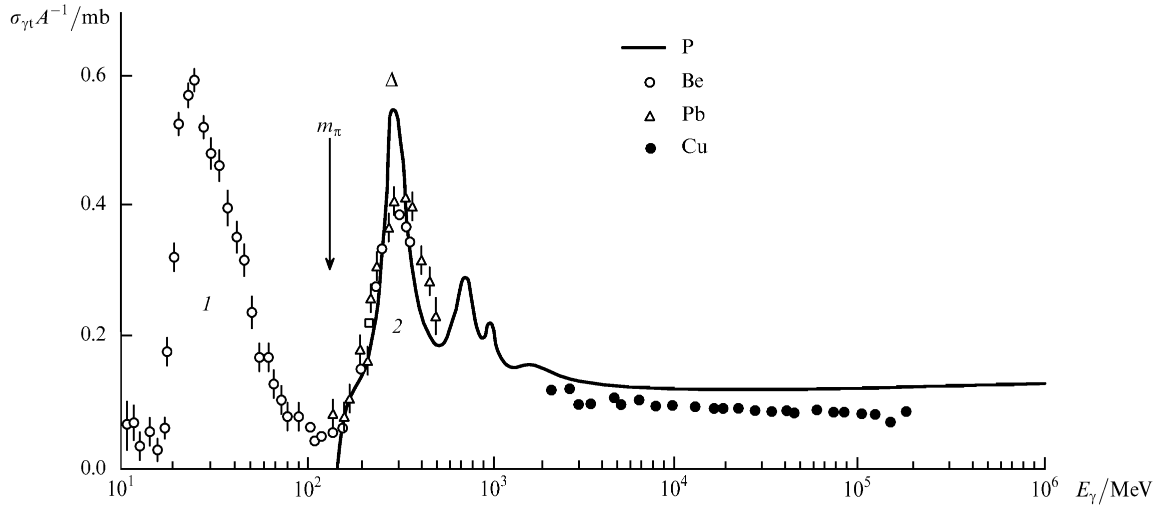

Figure 3.

means of a labelling technique with a high accuracy of detecting scattered electrons.

Of other Compton beam labelling facilities we shall mention the Novosibirsk machine [92] developed on the basis of the VEPP-3 accelerator [$E_\gamma = 60-140$ MeV, $\Delta E_\gamma \sim 2\%$, intensity of $10^6 \gamma$ s^{-1}], and the Brookhaven machine [93] based on the SLS (LEGS) accelerator ($E_\gamma = 100-300$ MeV, $\Delta E_\gamma = 5.5$ MeV, intensity $10^7 \gamma$ s^{-1}). The collimation principle is employed in the facility described in Ref. [94] which is based on the ADONE storage ring [$E_\gamma = 5-78$ MeV, $\Delta E_\gamma = 3-10\%$, intensity $5 \times 10^4 \gamma$ s^{-1}].

Good Compton beam parameters are expected from the facility now being developed in Moscow [88] based on the 'Siberia-2' facility [$E_\gamma = 100-500$ MeV, $\Delta E_\gamma = 5$ MeV, intensity $10^7 \gamma$ s^{-1}]. Still higher energy will be achieved in the labelled Compton beam facility now underway in Grenoble [95], using an argon laser and the storage ring ESRF (European Synchrotron Radiation Facility) [$E_e = 6$ GeV, $E_{ph} = 3.5$ eV, $E_\gamma = 1.5$ GeV, $\Delta E_\gamma = 15$ MeV, intensity $10^7 \gamma$ s^{-1}].

3.3 Total photoabsorption cross section at $10 < E_\gamma < 2 \times 10^5$ MeV

At the present time, the total photoabsorption data (of varying accuracy) cover a vast range of energies from the nuclear photoeffect threshold (1.8 MeV for Be and 2.22 MeV for ^{2}H) right up to $E_\gamma = 2 \times 10^5$ MeV [1]. The methods to obtain total photoabsorption cross sections are the summation of partial photoneutron cross sections ignoring reactions that produce charged particles only (and whose yield is low for $E_\gamma = 30-100$ MeV [96, 97]); or (for $E_\gamma > 200$ MeV) conversely, the summation of the cross sections for proton and π meson production, using the Monte Carlo simulation technique to account for the undetectable particles [85, 98]; or else the measurement of the cross section for photodetachment (this is very nearly complete for nuclei with $Z \geqslant 90$ and $E_\gamma > (20-30)$ MeV [99–101]); or, finally, a direct reduction of the beam intensity in the target [102–105) (mainly in the giant resonance neighbourhood, and making some calculations to account for the photoeffect and other non-nuclear processes).

The main results, obtained in various energy regions starting from $E_\gamma \sim 10$ MeV, may be summarised as follows†. In region *1* (Fig. 3) the increase in the cross section with energy is mainly determined by giant resonances, predominantly by the giant electric dipole resonance, with maxima at approximately $E_\gamma^{max} \simeq 80\ A^{-1/3}$ MeV, their width ranging from 3 to 10 MeV. The prediction [5], discovery [106], and subsequent study of this resonance (see, e. g., Ref. [107]) were instrumental in introducing collective particle–hole states into nuclear physics and in elucidating their effect in various reactions.

Along the right-hand branch of the curve that bounds region *1* in Fig. 3, the magnitude of the cross section is mainly determined by the quasideuteron mechanism. It decreases smoothly down to $\sigma_{\gamma t}/A \simeq 0.05$ mb at $E_\gamma \sim 100$ MeV.

In region *2* ($100 < E_\gamma < 500$ MeV) the cross section starts to increase rapidly due to the excitation of the nuclear Δ resonance and (for $E_\gamma > 140$ MeV) due to pion photoproduction. The maximum $\sigma_{\gamma t}/A \simeq 0.4$ mb occurs at the energy $E_\gamma \sim 300$ MeV, after which the cross section decreases to about 0.2 mb at $E_\gamma = 500$ MeV. This energy range has come under scrutiny due to the particular significance of the Δ degree of freedom of the nucleus. Specifically, the interest of the experimentalist lies with the observed difference in the properties of the nuclear and nucleon Δ resonances (solid curve in Fig. 3); in particular, the shift and broadening of the Δ maximum in the nucleus and the decrease of its excitation cross section attract attention. The important aspect of the problem is to separate out the trivial causes of the observed differences and to estimate the role of collective nuclear effects. Because photonuclear interactions are relatively simpler to interpret than the strong interaction, hope now lies in the photonuclear study of the Δ region.

Other resonances found on the free nucleon (see the solid curve in Fig. 3) have not yet been seen in the total nuclear photoabsorption cross section. The region of extremely high energies is little studied. It is known that $\sigma_{\gamma t}/A$ in the energy range $2 \times 10^3 - 2 \times 10^5$ MeV decreases

†We do not consider the nuclear photoeffect region $2 < E_\gamma < 10$ MeV.

smoothly from 0.12 to 0.07 mb. Among the specific studies in this range we should mention those concerned with the energy dependence of the photodetachment yield, a quantity which differs sharply from one nucleus to another. The maximum γ energy to be involved in photodetachment yield measurements is currently 16 GeV.

In concluding this brief survey of total photoabsorption cross section data, let us note that most of these come from no-labelling bremsstrahlung experiments, so that some results disagree not only quantitatively but also qualitatively with one another. Therefore remeasurements on monochromatic γ quanta are desirable. The first studies along these lines will be discussed in Section 3.5.3. The subsequent parts of Section 3 are devoted exclusively to the region of electromagnetic excitation of the Δ (region *2* in Fig. 3, of width 100 – 500 MeV), which for brevity we will call the region of intermediate energies, or Δ region.

3.4 Partial hadron photoproduction reactions

We consider first photonuclear reactions with $\pi, \mathrm{p}, \pi\mathrm{p}, \mathrm{pn}$ and pp emission in the Δ region. As already mentioned in Section 3.1.1, in this region a photon must preferentially interact with an individual nucleon, either producing a pion or exciting the Δ, which will subsequently decay as $\Delta \to \mathrm{N} + \pi$ or interact with a neighbouring nucleon according to the $\Delta + \mathrm{N} \to \mathrm{N} + \mathrm{N}$ scheme.

To the left of the Δ region ($E_\gamma \sim 50 - 100$ MeV) the quasideuteron mechanism is significant, and also leads to the two-nucleon emission. In both cases, a short-range correlation between the emitted nucleon pairs is observed. Thus, these processes not only provide information about the Δ photoproduction in a nucleus but also about the structure of the nuclear wave function at small nuclear spacings.

Early (1954 – 1967) experiments on two-nucleon photoemission employed the continuous bremsstrahlung spectrum [108 – 112]. The experiments yielded the angular correlations between p and n, which were interpreted (qualitatively) in terms of the quasideuteron model. The interpretation proved to be difficult because of the use of bremsstrahlung beams in experiments. Since the early 1980s labelled photon beams from the 500 MeV synchrotron in Bonn and the 1.3 GeV synchrotron at the Institute for Nuclear Study, University of Tokyo, have been available.

The Bonn experiments investigated the emission of protons [113] and of charged π mesons [114] at angles between 49° and 130° from the ^{12}C nucleus in an inclusive setup with 10 MeV resolution. Knowledge of the γ quantum energy and direction is important for determining the reaction kinematics. Further insight into photonuclear interactions requires pπ, pn and pp coincidence experiments.

The first experiments on coincidence of two nucleons from ^{12}C using labelled photons in the Δ region were made back in Ref. [113] mentioned above. An $A(\gamma, \mathrm{pp})$ cross section about an order of magnitude less than that for $A(\gamma, \mathrm{pn})$ is found, and angular pn correlations similar to those in older bremsstrahlung experiments were observed. However, detailed information on the reaction mechanism was again difficult to extract (because of poor momentum resolution this time). In the same years, studies on inclusive proton spectra were made with labelled photon beams from the Japanese synchrotron [115 – 117]. In particular, in Refs [115] and [116] two peaks for protons escaping

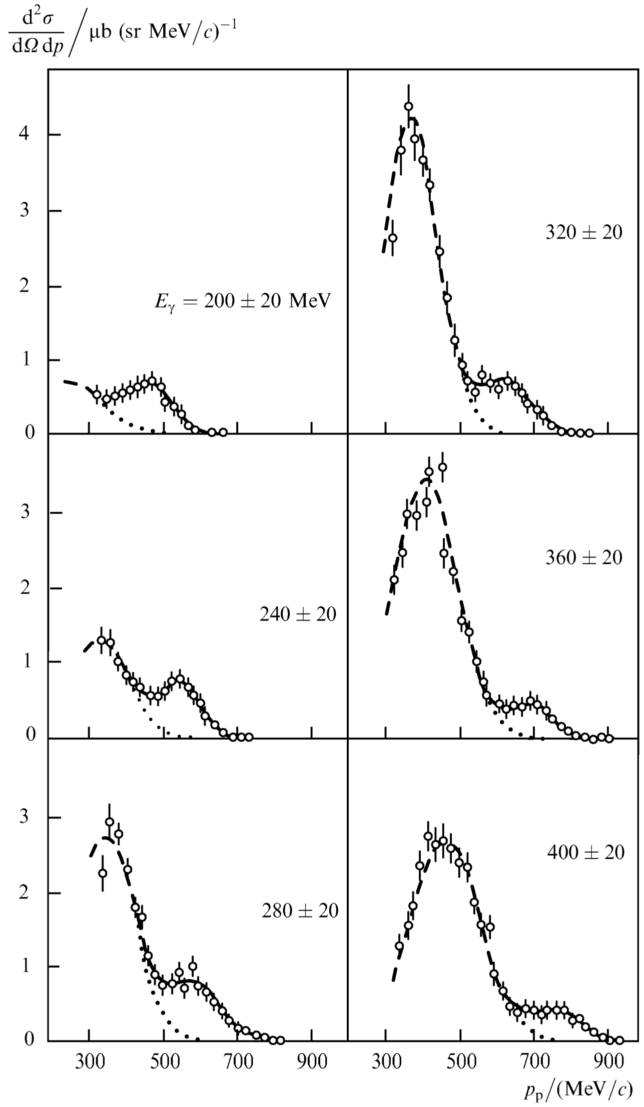

Figure 4.

from Be and C at a laboratory angle of 25° were detected and tentatively interpreted as arising from two quasifree reactions

$$\gamma + \text{"N"} \to \mathrm{p} + \pi\ , \tag{5}$$

$$\gamma + \text{"pN"} \to \mathrm{p} + \mathrm{N}\ , \tag{6}$$

where "N" designates a nucleon in the nucleus ("p" or "n"), and "pN" denotes a two-nucleon system ("pp" or "pn"). Fig. 4 shows the momentum spectrum of the protons from $^{9}\mathrm{Be}(\gamma, \mathrm{p})$ as measured in Ref. [115]. In the figure one indeed sees two maxima, whose locations in momentum correspond to the kinematics of the reactions (5) and (6). The absence of a second charged particle implies that reaction (6) should be identified as

$$\gamma + \text{"d"} \to \mathrm{p} + \mathrm{n}\ , \tag{7}$$

indicating the existence of neutron – proton correlations (quasideuterons) in nuclei. However, in order to obtain more definitive information on each of the (γ, pp) and (γ, pn) contributions, coincidence experiments in a close-to-exclusive setup are required (see a review of Ref. [117] below). In Ref. [118] the momentum spectrum of protons from ^{9}Be and ^{12}C was measured at 23°, 55° and 130° in the energy range $k = 360-600$ MeV. The structure of the forward angle spectrum was found to be attributable to quasifree pion production and quasideuteron decay reactions, whereas backscattered protons were the result primarily of internuclear multiple scattering.

More definitive results, in either series of experiments, are those from the bottomline studies on the Bonn and Tokyo synchrotrons (Refs [119] and [117], respectively). The studies are sufficiently important to warrant a more detailed discussion.

In Ref. [119], a labelled meson beam with $k = 220-450$ MeV was employed in a systematic study of proton and $\pi^{\pm}$ meson emission from Be, C, O, Ti, and Pb nuclei. The bremsstrahlung from electrons, with $E_0 = 450$ MeV and with an internal labelling system [120] was employed. Photon energy was variable within $k = (0.45-0.97)E_0$ with resolution of $\Delta k = 0.02E_0$. The synchrotron duty cycle was 3%, so the γ beam intensity was cut off at the level $N_\gamma = 10^5\ \mathrm{s}^{-1}$.

The hadron detector was made up of two parts; a reverse-field magnetic spectrometer for charged particles ($e^{\pm}$, $\pi^{\pm}$, p, d) in the momentum range 80–800 MeV, and 18 scintillation counters to detect the coincidence of charged or neutral particles. The magnetic spectrometer contains flat drift chambers in order to obtain 4 points on the particle trajectory. Charged and neutral particles were distinguished using thin scintillation counters. In the measurement of time of flight, paired-counter hodoscopes were used. The particles were identified by their momentum p and time of flight τ (Fig. 5). The key results of the study are the momentum distributions of $\pi^{\pm}$ mesons and protons detected by the spectrometer at $\theta_{\mathrm{lab}} = 52°$ and two photon energies, $k = 282\pm5$ MeV and $k = 227$ MeV. The spectra for the light nuclei (Be, C, O) display a distinct peak in the region of quasifree pion production, whereas for the higher nuclei (Ti, Pb), only a broad maximum is seen. In lead there is a definite distinction between π^+ and π^- meson production cross sections, which can be attributed to the difference in the number of neutrons and protons in this particular nucleus.

The data (especially those for low-energy photons) are in satisfactory agreement with a Monte Carlo intranuclear

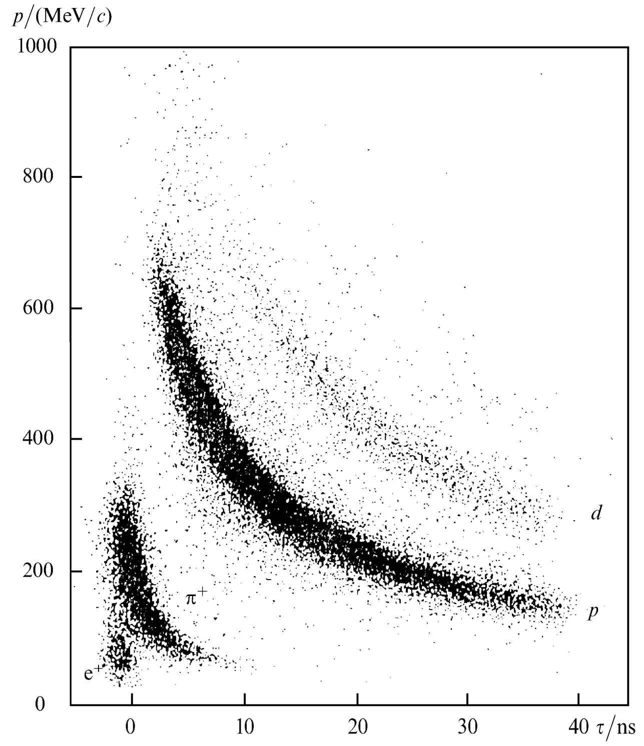

Figure 5.

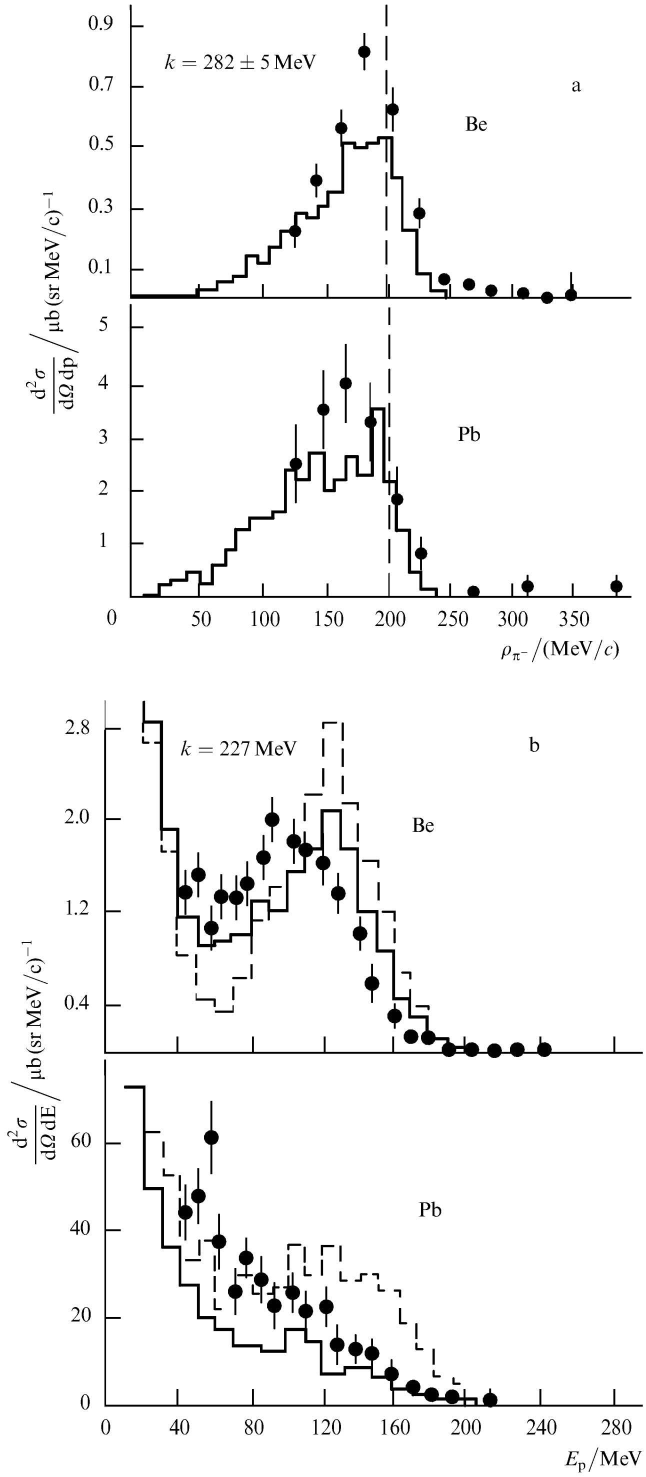

Figure 6.

cascade calculation taking into account such factors as the quasifree production of π mesons, their passage through the nucleus, πN scattering, πN charge exchange, absorption by nucleon pairs, and also the Pauli principle for the nucleons. The predicted cross section is very sensitive to the final state interaction, a fact which is evident, in particular, in the shift of the quasifree peak for lead. Fig. 6a shows the results for Be and Pb for $E_\gamma = 282 \pm 5$ MeV as an example. The intranuclear cascade calculations are shown by a histogram. The vertical dashed line shows the position of the pion momentum for the elementary process $\gamma N \to \pi N$.

The proton spectra had been expected to exhibit low-energy recoiling protons from π meson production processes, and high-energy ($T_p = k/2$) protons from two-nucleon emission. The latter were found in a peak for Be at low photon energies $k = 227$ MeV (Fig. 6b). As the size of the nucleus increases, the maximum gradually disappears. The two-nucleon emission cross section decreases with photon energy. The π meson production cross section, on the contrary, increases, but most of the protons from this process are below the 40 MeV spectrometer threshold. The experimental results were compared with the intranuclear cascade model (dashed histogram in Fig. 6b) and with a calculation in which the final state interaction is added (solid histogram). The comparison shows that including the final state interaction helps to explain the features of the proton spectra.

More information on reaction mechanisms was obtained from the observation, in oxygen, of the coincidence of the protons detected in the spectrometer with the protons, neutrons, and pions detected in the scintillation counters. Briefly, the results are as follows: the pπ coincidences display low-energy protons only; the pπ coincidences, on the contrary, are dominated by high-energy protons; the pp pairs have a lower cross section than the pn pairs and are dominated by low-energy protons. It is readily seen that these results are in satisfactory agreement with the photoreaction mechanisms discussed above, i.e., quasifree pion production (πp), quasideuteron decay (pn), and pion production followed by its absorption (pp).

Thus, Ref. [119] provided strong support to the picture of intermediate energy photonuclear reactions expected both on general grounds (see Section 3.1) and from theory (quasifree pion production, quasideuteron mechanism, bulk hadron production, hadron interaction in the final state, etc.), and even offered quantitative estimates for some processes.

The other fundamental work employed labelled beams from the Tokyo synchrotron [117]. The objective was to confirm the interpretation of two peaks in inclusive proton momentum spectra previously reported in Refs [115, 116], to measure the cross sections for the reactions

$$\gamma + \text{"pn"} \to p + n \,, \tag{8}$$

$$\gamma + \text{"pp"} \to p + p \tag{9}$$

[for each separately, see the comment on Eqns (5) and (6)], and also to measure the dependence of the cross section on E_γ and A to examine the mechanism of quasifree reactions in the Δ region.

The technique used was a semi-exclusive method [measuring E_γ, the momentum, and escape angles for both nucleons in Eqns (8) and (9)], which discriminated the quasifree reactions (6) against the large background from the quasifree generation of pions in Eqn (5).

The work was performed on labelled photon beams from the Institute for Nuclear Research electron synchrotron at Tokyo University in the energy range $187 < E_\gamma < 427$ MeV. The detector consisted of a magnetic spectrometer which detected the protons escaping from the reactions (γ, p), (γ, pn) and (γ, pp) at an angle of 30°, and a hodoscope made of 64 plastic scintillator counters measuring (in coincidences with a forward proton) the momenta of the protons and neutrons escaping at 90–170°. The targets used were distilled water (^{1}H and ^{16}O), liquid deuterium (^{2}H), and ^{9}Be and ^{12}C plates.

The magnetic spectrometer consisted of a bent magnet, trigger scintillation counters, and track chambers (multiwire proportional and drift types). The spectrometer was calibrated against electrons with momentum $p_e = 550$ MeV/c and the two-particle reaction $\gamma + d \to p + n$. p, e^+, π^+ and d were identified by measuring the time of flight between two triggering counters. In front of the hodoscope, 16 scintillation counters were located to discriminate charged particles from neutral ones. The proton and neutron momenta were determined from the time of flight from the counter near the target to the hodoscope. The same approach was used to distinguish between the photons from the decay of π^0 from $\gamma + \text{"p"} \to p + \pi^0$ and the neutrons from the $\gamma + \text{"pn"} \to p + n$ reaction.

The hodoscope-detected charged particles were distinguished by the flight time method combined with the signal amplitude measurement. The hodoscope was calibrated against neutrons from $\gamma + d \to p + n$ using the magnetic spectrometer. Both the trajectory of the proton and its momentum were reconstructed from the coordinates meas-

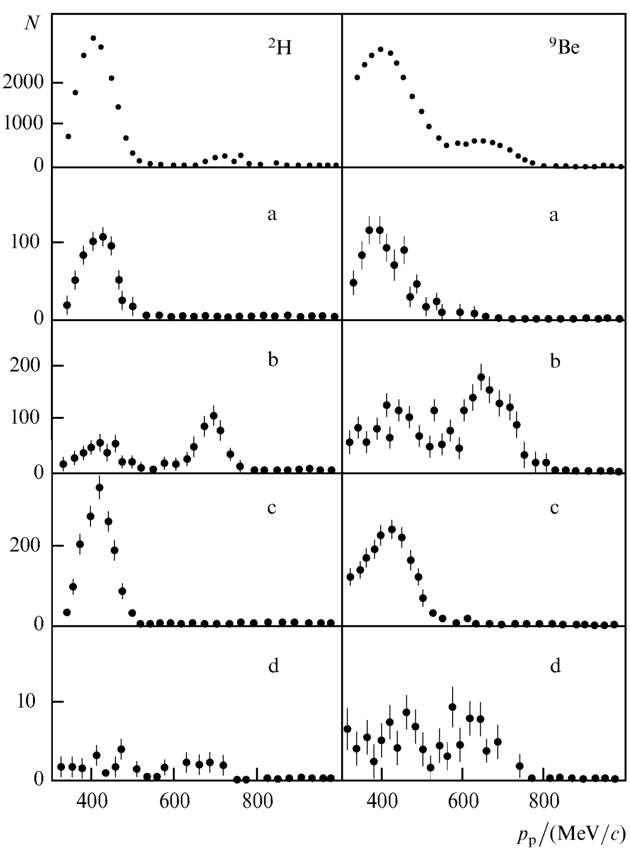

Figure 7.

ured in chambers in front of and behind the spectrometer magnet. In coincidence experiments, with each proton passing through the magnetic spectrometer was associated one of the hodoscope-identified particles (γ, n, π, p), i.e., the detector acted to separate the $(\gamma, p\gamma), (\gamma, pn), (\gamma, p\pi)$ and (γ, pp) reactions, respectively.

In Fig. 7, the spectra of the protons following the magnetic spectrometer are presented for deuterium and beryllium targets for the cases when the detected particles are (from top to bottom): proton in the spectrometer only; proton in the spectrometer coincident with a γ quantum in the hodoscope (A); proton coincident with a neutron (B); proton coincident with a π meson (C), and proton coincident with a proton (D). For deuterium, one can see (top of Fig. 7) two maxima, and calculations show that their locations in momentum correspond to the kinematics of the quasifree π pion production reactions

$$\gamma + p + (n) \to p + \pi^0 + (n) \,, \tag{10}$$

$$\gamma + n + (p) \to p + \pi^- + (p) \,, \tag{11}$$

(the left maximum; n and p are the nucleon spectators) and to that of the deuteron photodisintegration reaction

$$\gamma + d \to p + n \,, \tag{12}$$

(right maximum). As seen in the figure, in coincidence experiments the right-hand maximum remains only in the (γ, pn) channel, which obviously corresponds to the reaction (12). The high-energy products of this reaction are detected by the hodoscope (neutron) and by the magnetic spectroscope (proton). A few fast neutrons detected in the (γ, pp) channel are presumably caused by neutrons being incorrectly identified as protons. As to the left maximum, this exists for all reaction channels: in the (γ, pγ) channel the hodoscope detects a γ quantum from the decay of the π^0 meson from the reaction (10); in (γ, pn), the neutron-spectator from the same reaction; in (γ, pπ), the π^- meson from Eqn (11); and, finally, in (γ, pp), the proton-spectator from the same last reaction. In all these cases the proton detected by the magnetic spectrometer must obviously have its momentum in the neighbourhood of the first maximum.

The interpretation of the ^{9}Be results is different only for the (γ, pp) channel, which receives an additional high-energy proton contribution from the quasifree reaction

$$\gamma + \text{"pp"} \to p + p \,, \tag{13}$$

whereas for deuterium, fast neutrons appear only from the incorrect identification of the neutrons from

$$\gamma + \text{"np"} \to p + n \,. \tag{14}$$

It is from the above coincidence measurements that the reactions (13) and (14) have been identified.

The positions of the first and second maxima in the proton momentum spectrum are shown as a function of E_γ in the lower and upper parts of Fig. 8, respectively. The figure also shows the lines expected for the $\gamma + p \to p + \pi^0$ on a free proton (below) and for $\gamma + d \to p + n$ on a free deuteron (above). It is seen that in the case of nuclear targets the maxima are shifted to lower proton moments by 10–40 MeV$/c$ relative to the lines. The shift of the second maximum is about twice the first. The binding of one nucleon ("N") in reaction (5) and of two nucleons ("pN") in reaction (6) could account for the shifts.

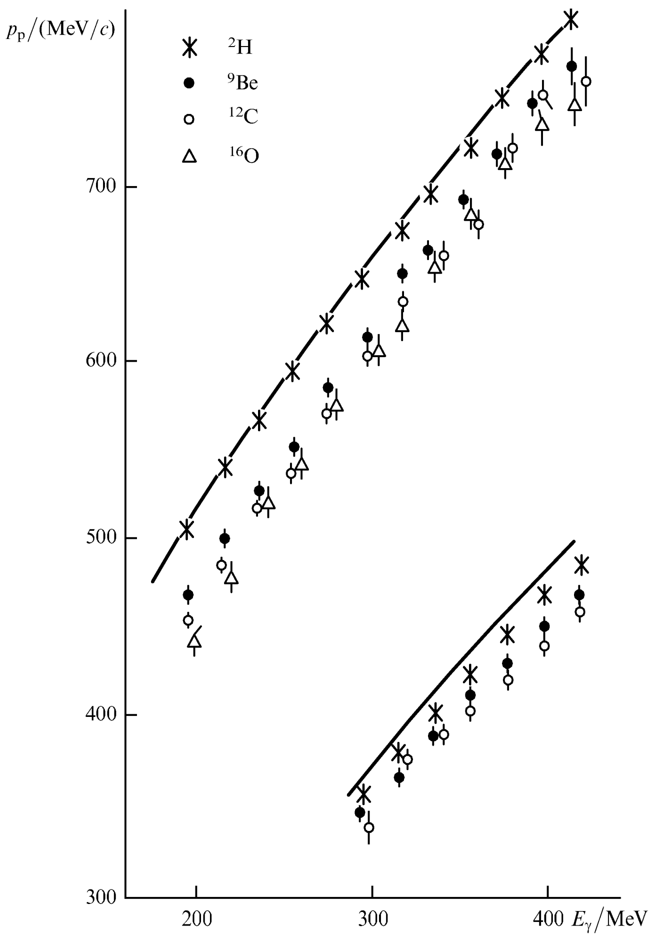

Figure 8.

3.5 Electromagnetic nuclear Δ excitation by virtual and real photons

In discussing nucleon and π meson photoproduction partial reactions, two underlying mechanisms have been recognised: quasifree pion production and the quasideuteron decay of pn pairs with the interaction of the resulting hadrons in the final state. Specially performed experiments showed that the resultant hadrons shifted down in energy with respect to those for elementary reactions (on the proton and deuteron, respectively) and also displayed flattening of the peak (broadening and decrease in height divided by mass number). The shifts are naturally accounted for by the influence of the binding energy of the quasifree nucleon or deuteron (some of the energy transfer goes to compensate the binding energy), and the flattening is attributed to the effect of the motion of nucleons in the nucleus.

From general considerations (see Section 3.1.2), it seems evident that the electromagnetically produced Δ may also differ from the nucleon isobar in the position, width, and height of the peak. If quasifree Δ production dominates, the Δ maximum must be observed at large energy transfers. Moreover, the nuclear medium can carry specifically background contributions which may lead to the deformation and shift of the Δ maximum.

Table 1.

Nucleus	ω_Δ/MeV	$\frac{1}{A}\frac{d^2\sigma}{d\Omega\,d\omega}\Big/$nb sr^{-1} MeV^{-1}	ω_{QF}/MeV	$\frac{1}{A}\frac{d^2\sigma(QF)}{d\Omega\,dQ}\Big/$nb sr^{-1} MeV^{-1}
H	380±10	1.03±0.08	100	
He	370±10	0.80±0.05	105±5	2.25±0.14
Be	375±10	0.84±0.04	115±5	1.91±0.08
C	360±10	0.80±0.04	115±5	1.83±0.08
O	375±10	0.77±0.06	120±5	1.76±0.12

3.5.1 Early experiments on Δ isobar electroproduction in light nuclei

The first experimental study of the shift and broadening of the nuclear Δ maximum in the electromagnetic process was associated with the investigation [121, 122] of virtual photons interacting with light He, Be, C, and O nuclei in the process of the scattering of 730 MeV electrons at an angle 37.19° [$Q^2 \sim 0.1$ (GeV/c)^2].

Table 1 presents the results of this study. Here the second column gives the values of energy transfer ω_Δ for the excitation of the Δ isobar; the third lists the cross sections per nucleon (at the maximum); the fourth, the positions of the quasielastic scattering peak, and the fifth, the cross sections in the quasielastic peak region.

The table shows that (i) the nuclear Δ peak has a slight tendency to shift to smaller ω from its free proton position (the amount of the shift is within errors, though); (ii) the peak of the quasielastic electron scattering shifts to larger ω compared to the scattering on the proton (as it should for the scattering on the bound nucleon); (iii) the shift of the nuclear Δ peak relative to the quasielastic scattering peak is more pronounced than for the proton. Although also moderate, this time the shift is beyond error limits, $\Delta\omega = (15-35) \pm 12$ MeV. Such a small value is of course difficult to interpret but seems to be associated with some effect other than quasifree Δ excitation. Very roughly (neglecting possible interference effects), it may be argued that the position of the nuclear Δ peak is determined not only by the quasifree mechanism, which shifts the peak to larger ω, but also by one (or more) other mechanism(s) than those listed in Section 2.5.2, which for some reason(s) act(s) to shift it to lower ω. As a result, the nuclear Δ peak shifts to slightly lower ω compared with the nucleon Δ peak.

One further work with the same $Q^2 = 0.1$ (GeV/c)^2 [123] also reports the Δ peak slightly shifting toward lower energy loss than for the production from the nucleon. Moreover, in all of the above studies nuclear medium effects caused a broadening of the Δ peak and a large increase of the cross section between the quasielastic and the Δ peaks ('dip region').

All the discussion above concerns the electroproduction of the Δ isobar at one and the same $Q^2 \sim 0.1$ (MeV/c)^2. The dependence of the Δ peak shift on Q^2 seems first to be noted in Ref. [124] which, for Q^2 at $Q^2 = 0.09$ (GeV/c)^2 reports the same shift as in Refs [121–123], and at $Q^2 = 0.16$ (GeV/c)^2, no shift at all. Finally, work on Ca and Fe at $Q^2 = 0.16$ (GeV/c)^2 [125] revealed a Δ peak shift to higher energy loss than for the free nucleon case.

3.5.2 Systematic study of the Δ isobar electroproduction in the range 0.2 < Q^2 < 0.52 (GeV/c)^2

The summary of results above shows that by the late 1980s a systematic study of Δ electroproduction was on the agenda, and in particular the problem of existence of the Δ maximum shift and of its dependence on nuclear properties (mass number, size, binding energy, etc.) and on Q^2 had to be cleared up. The start was made [126] with the nuclei of H, He, C, Fe, and W at four-momentum squared (Q^2) from 0.2 (GeV/c)^2 to 0.52 (GeV/c)^2.

The experiment was performed at the Stanford Linear Accelerator Centre (SLAC) using an electron beam with energies in the 0.96–1.5 GeV range. The 1.6 GeV/c spectrometer [127] and a new electron detector constructed for this experiment were used. The latter consisted of three multiwire drift chambers each with four planes of wires; an isobutane-filled Cherenkov detector; two planes of scintillator hodoscope; and a 35-segment lead-glass shower counter. An event trigger was a coincidence between the hodoscopes and either the 35-segment counter or the Cherenkov detector. A 15 cm long recirculating liquid-hydrogen target; a 25 cm long, high-pressure (25 atm), recirculating helium target; and thin solid plates of natural isotopic abundance were used. For all the targets, electron scattering at an angle of 37.5° was examined, which corresponds to $Q^2 = 0.2$ (GeV/c)^2 for $E_e = 0.96$ GeV and $Q^2 = 0.52$ (GeV/c)^2 for $E_e = 1.5$ GeV. The cross sections obtained were corrected for radiation, target thickness, detector efficiency, electronic dead time, spectrometer acceptance, etc. The cross sections for electron scattering from hydrogen were within 1% of the average over all the earlier results [128].

Measurements revealed that the mass number (A) averaged value of the invariant mass W for the Δ peak at $Q^2 = 0.2$ (MeV/c)^2 is approximately equal to the free nucleon value of $W_N = 1220$ MeV and increases with increasing Q^2. Fig. 9a shows the dependence of W on Q^2 as obtained in Ref. [126] and also represents data for light nuclei (He, Be, C, O) from Refs [121–124]. With the exception of only the tungsten point, the dependence is approximately linear within -30 to $+60$ MeV relative to $W_N = 1220$ MeV.

The occurrence of the Δ peak shift with variation of Q^2 may be due either to some special in-medium properties of the Δ resonance, or to background from competing reactions, or both. The discussion of this question was taken further in Ref. [129], which gives about 35 MeV for the real (as opposed to background) shift. However, the shift is there attributed not to the quasifree excitation of the Δ but to specifics of its interaction with the Δ nuclear potential (see Section 5.2.4).

Among other results of Ref. [126], we note the large width of the Δ peak, which for all nuclei except ^{4}H is $\Gamma_\Delta^{\text{nucl}} = 250$ MeV, twice Γ_Δ^{H} for hydrogen (118–127 MeV); and a weak A dependence of the cross section per nucleon in the dip region. The latter fact suggests a relatively small contribution of the specifically nuclear, for example qua-

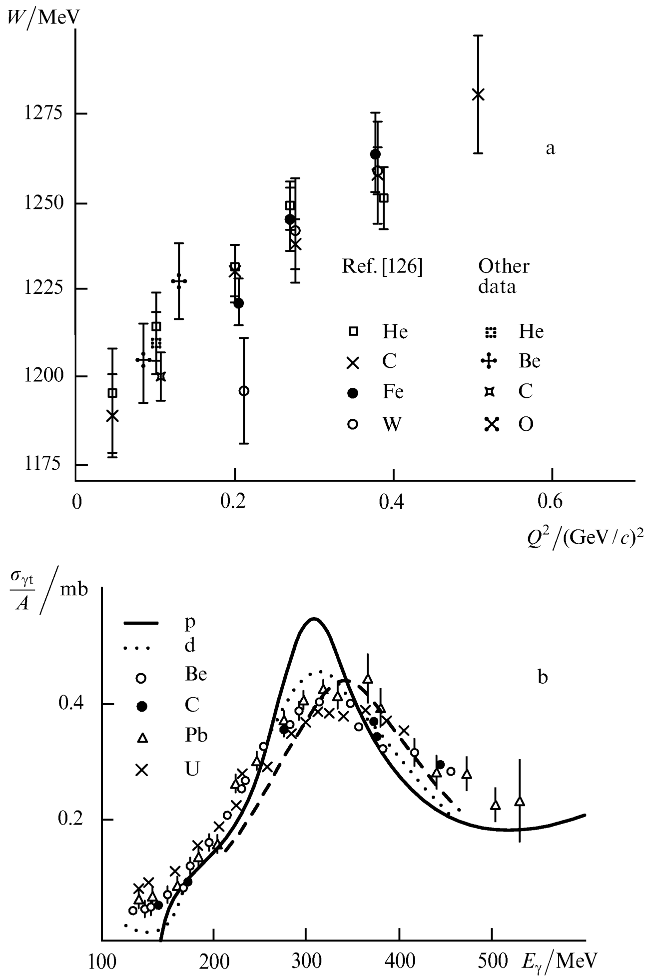

Figure 9.

sideuteron background at Q^2 in the range 0.2 – 0.52 $(\text{GeV}/c)^2$.

3.5.3 Photoabsorption in the Δ region

The total photoabsorption cross section $\sigma_{\gamma T}$ in the Δ region ($100 < E_\gamma < 500$ MeV) is discussed in a review of the exclusive work on real photons in Ref. [1] (see also Ref. [130]). The cross sections per nucleon for H, Be, C, Pb, and U nuclei are compared with that for the proton and it is noted that the Δ maximum is seen clearly for all the nuclei and that, within experimental error, $\sigma_{\gamma T}/A \simeq$ const, that is, the curves for all the nuclei are identical in shape, averaged energy, and scale ('universal curve'). These results are shown in Fig. 9b. Note that the data on the fissionable nuclei ^{235}U and ^{238}U were obtained [100] on the Bonn synchrotron labelled photon beam in the energy range $120 < E_\gamma < 460$ MeV. The major conclusion of Ref. [1] is that the Δ resonance does manifest itself in the nuclear medium, although the shape of the cross section curve is somewhat different from the corresponding proton curve in having a larger width and a lower Δ maximum height divided by mass number. The suggested reasons are Fermi motion, which adds about 50 MeV to the 115 MeV wide nucleon resonance, and the Pauli principle, which forbids some nucleon transitions thus decreasing σ/A. Moreover, the formation of NΔ systems in nuclei may be important, as it opens up the NN channel and gives rise to motion of the Δ in the nuclear matter — something uncharacteristic of the free isobar.

As regards the shift of the Δ maximum from its free nucleon position (solid curve in Fig. 9b), one can hardly attach any significance to the barely visible rightward shift of the ensemble of experimental points, which for the ^{12}C nucleus is (19 ± 5) MeV. A calculation [131] assuming quasifree Δ production (and including Fermi motion) yields a larger shift (dashed curve in Fig. 9b).

We note here that the lack of a Δ maximum shift in the electromagnetic process can be obtained from a model-independent dispersion relation analysis of nuclear Compton scattering [2]. The analysis suggests that the resonance energies for nuclei and free nucleons are within $\Delta E = 5$ MeV of each other.

Of more recent work, note the new measurements [132] of the total photofission cross sections of ^{235}U and ^{238}U using the labelled photon beam from the MAMI B microtron (Mainz, Germany). In this study a wideband mass spectrometer with a labelling system covering the photon energy range $50 < E_\gamma < 800$ MeV [86] is employed. The energy resolution of the machine is about 2 MeV. The total flux of labelled photons may be as high as $10^8 \gamma\ \text{s}^{-1}$. It is pointed out that the new Δ region results are identical for both of the uranium isotopes and agree with both the previous data [100] and the universal curve. Referring to their recent work [133] the authors of Ref. [132] note the absence of any observable feature near the D_{13} resonance ($E_\gamma \sim 710$ MeV).

The ^{238}U photofission results of Ref. [132] were confirmed by the Frascatti group (Italy) [134]. As to the D_{13} resonance, the preliminary data of the Italian group [135] also indicate its strong reduction for Be and C as compared to the proton.

It would seem that the experimental investigation of the mass dependence of this reduction of the D_{13} and higher resonances is an important direction in γ labelling photo-absorption studies.

4. Nuclear Δ excitation in nucleus – nucleus and hadron – nucleus interactions

In the preceding section, some indirect arguments based on the study of electromagnetic processes were presented to show that along with the quasifree excitation of the nuclear Δ a collective excitation mechanism may exist. However, the most convincing and direct evidence for its existence has come from the study of the hadron and nucleus charge exchange reactions. The present section describes inclusive charge exchange reactions on light and heavy ions, on protons, and pions. At the end of this section, a number of exclusive experiments are discussed, which give more detailed information about the nuclear Δ excitation.

4.1 (^{3}He, t) charge exchange reaction

First direct evidence for the collective Δ excitation mechanism was obtained in 1983 simultaneously in the Dubna LHE JINR [136] and Saclay Saturne [137] studies on (^{3}He, t) charge exchange reactions†. Both groups then followed up by continuously increasing the number of

†Still earlier (1977 – 1979), the collective nuclear Δ excitation had been detected in (p, n) charge exchange reactions (see Section 4.2). The proposed explanation was different, though.

nuclear species and enlarging the scope of the investigation. Below, some of the results obtained and the technique employed are discussed.

4.1.1 LHE JINR (^{3}He, t) charge exchange studies on hydrogen and nuclei. Δ peak shift and broadening observation The most convincing evidence for the collective Δ excitation was found in the series of Dubna studies [136, 138–144]. These were the first to reveal all the main features of the collective mechanism, namely, the shift of the Δ peak to lower excitation energies, its broadening, and the dramatic increase in the cross section in this region compared to the hydrogen case. Also, specially performed calculations showed that it is impossible for all these effects to be placed within the single quasifree Δ excitation framework. Let us consider this work in some detail.

The first study [136] was made on the ^{3}H nucleus beam of the LHE JINR synchrophasotron. The schematic diagram of the facility is shown in Fig. 10a.

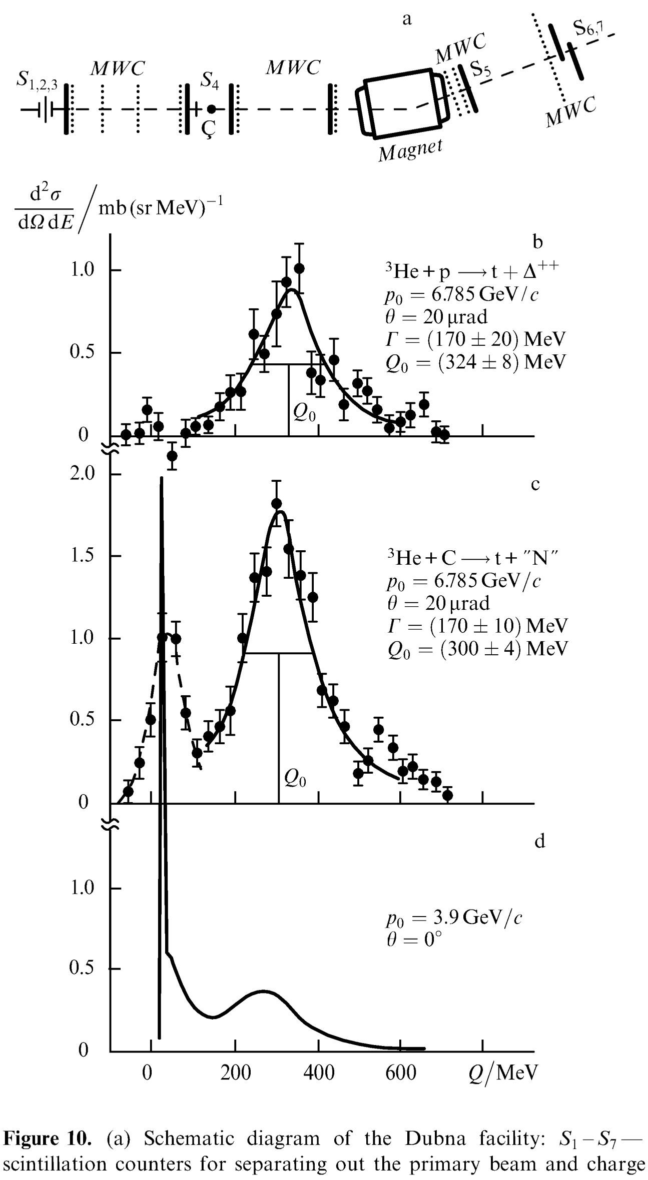

Figure 10. (a) Schematic diagram of the Dubna facility: $S_1 - S_7$ — scintillation counters for separating out the primary beam and charge exchange tritons, *MWC* — multiwire chambers for determining the parameters of the detected particles, T — target. (b) Charge exchange cross section on hydrogen. (c), (d) Charge cross sections on carbon.

The same Fig. 10 presents the charge exchange cross sections on hydrogen (Fig. 10b) and carbon (Fig. 10c) measured for the initial beam momentum $p_0 = 6.785$ GeV/c and $\theta_t = 0°$. The cross sections are shown as a function of the recoiling nucleus excitation energy Q,

$$Q = E_{^3\mathrm{He}} - E_{\mathrm{t}} \,, \tag{15}$$

where $E_{^3\mathrm{He}}$ is the energy of ^{3}He, and E_{t} the triton energy, in the notation of Ref. [136].

It is seen that the charge exchange cross section on carbon has two maxima, for low ($Q_0 < 100$ MeV) and high ($Q_0 = 300$ MeV) excitation energies. The former corresponds to spin–isospin excitations of the final nucleus, whose cross sections, as seen from comparison with the results for the $p_0 = 3.9$ GeV/c [137], exhibits little or no change with energy (Fig. 10d). The latter maximum is for the Δ excitation of the carbon nucleus. The cross section for this process increases sharply with energy (sevenfold in the initial momentum region mentioned) and becomes dominant as the energy increases still further.

The main result of Ref. [136] is the discovery of the shift of the Δ maximum for the carbon nucleus relative to its position for charge exchange on the proton. The excitation energy difference between the carbon and the proton is

$$\begin{aligned}\Delta Q_0 &= Q_0(\mathrm{C}) - Q_0(\mathrm{p}) \\ &= 300 \text{ MeV} - 324 \text{ MeV} = -24 \text{ MeV}\end{aligned} \tag{16}$$

toward lower excitation energies. As has already been said and will be elaborated somewhat later, this shift, the dramatic cross section enhancement in the Δ excitation region, and the later [138–140] established broadening of the carbon relative to the hydrogen Δ peak are the main indications of the collective nature of the Δ isobar nuclear excitations.

The experiments of Refs [138–140] were carried out on the LHE JINR synchrophasotron ^{3}He beam using the ALPHA facility [141], whose schematic diagram is shown in Fig. 11. The physical parameters of the ALPHA are as follows: the ^{3}He beam working intensity is 10^6 particles/cycle (the maximum value is 10^{11}), the accuracy of the triton momentum $\Delta p/p \leqslant 0.5\%$, the accuracy of energy transfer $\Delta Q = \pm 3$ MeV.

The production of the Δ by the collective mechanism is facilitated by its momentum being comparable with the Fermi one. Therefore the ^{12}C (^{3}He, t) reaction was studied for low transverse ($p_\perp \sim 0$) and small longitudinal ($p_\parallel = 0.35 - 0.40$ GeV/c) momentum transfer. The results of Refs [138–140] can be found summarised in conference proceedings [142] and in a dissertation [143] and are most clearly illustrated by Table 2 from Ref. [142]

Let us discuss Table 2. The most notable point here is the wide interval of momenta covered in the study (4.4–18.3 GeV/c), which enables one to examine the energy dependence of the effects observed. One such effect is (see the fifth row) the increased relative contribution to the cross section for ^{12}C(^{3}He, t) (with t escaping at 0°) from the Δ excitation region ($Q > 150$ MeV). The contribution from the other component ('quasielastic' charge exchange with the excitation of low-lying nuclear levels) continuously decreases with projectile energy and at $p_{^3\mathrm{He}} = 10.79$ GeV/c is only 8%. Further, a comparison of the second and third columns shows that the Δ maximum for ^{12}C (^{3}He, t) is shifted relative to p (^{3}He, t) by about

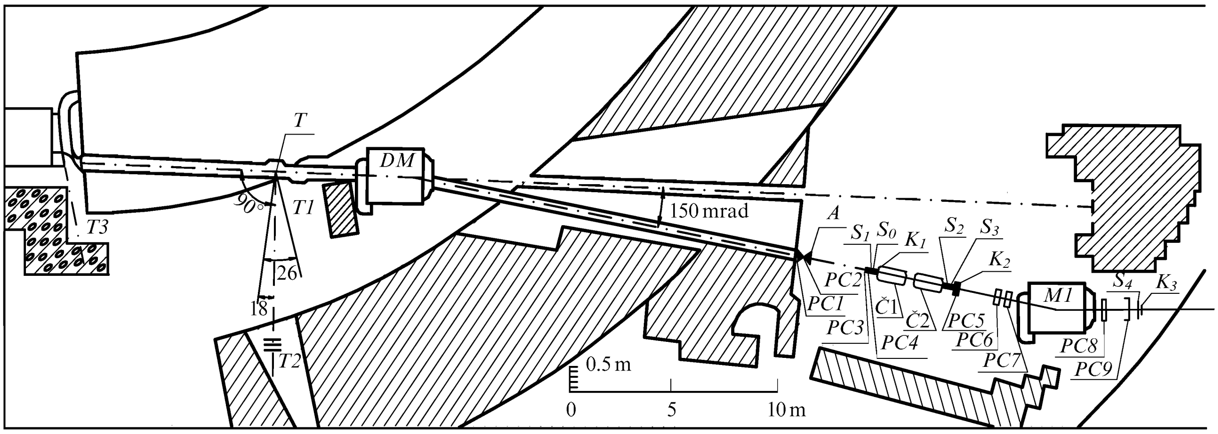

Figure 11. Schematic diagram of the 'ALPHA' facility: T — target; T_1 and T_2 — monitor telescopes consisting of scintillation counters, to determine the flux of target-hitting ^{3}He nuclei; A, K_i, S_i — scintillation counters; $\check{C}_1$, $\check{C}_2$ — threshold Cherenkov counters; PC_i — multiwire proportional chambers; DM — deflecting magnet; $M1$ — analysing magnet.

Table 2.

Momentum $p/(\mathrm{GeV}/c)$ and energy E/GeV per nucleon of the beam	Position of the maximum Q_0 and width Γ/MeV				
	$p(^3\mathrm{He}, \mathrm{t})$	$^{12}\mathrm{C}(^3\mathrm{He}, \mathrm{t})$	nonquasifree	$\dfrac{\Delta\sigma}{\sigma}$	R_{exp}
4.4 (0.8)	322±2.5 138±9	274±2.5 182±16	253±2 142±6	62%	1.82±0.05
6.81 (1.52)	327±1.5 109±5	295±1.5 204±9	275±1 142±4	82%	1.77±0.03
10.79 (2.77)	327±2 109±5	305±2 257±14	281±2 153±6	92%	1.95±0.03
18.3 (5.23)	—	—	—	—	214±0.17

Here $\Delta\sigma/\sigma$ is the relative contribution to the cross section for $^{12}\mathrm{C}(^3\mathrm{He}, \mathrm{t})$ in the range $Q > 150$ MeV, and $R_{\mathrm{exp}} = (\mathrm{d}\sigma/\mathrm{d}\Omega)(0°)_{\mathrm{C}}/(\mathrm{d}\sigma/\mathrm{d}\Omega)(0°)_{\mathrm{p}}$.

30 MeV to lower excitation energies, and that its width is markedly greater†. Calculations (see Section 5.1) show that this cannot be explained by quasifree Δ production. It turns out that the quasifree mechanism (with Fermi motion and the binding energy of the nucleons taken into account) must shift the Δ maximum to higher excitation energies. If one 'subtracts' the quasifree contribution to the $^{12}\mathrm{C}(^3\mathrm{He}, \mathrm{t})$ reaction, then the Δ peak shift due to the nonquasifree (collective) mechanism increases to about 50 MeV (see the fourth column in the table).

The existence of the collective mechanism for the nuclear Δ excitation in ^{12}C is also favoured by the values in the sixth column in the table, which are about twice the $R_{\mathrm{th}} \sim 0.8$, predicted [140, 143] by the Glauber–Sitenko model [145, 146]. The point is that the GS model assumes the quasifree excitation of nuclear isobars and, as seen from a comparison with experiment [139], describes well the $\mathrm{p}(^3\mathrm{He}, \mathrm{t})$ reaction. The twofold predominance of R_{exp} over R_{th} for ^{12}C, therefore, shows the model to be inapplicable to the $^{12}\mathrm{C}(^3\mathrm{He}, \mathrm{t})$ reaction thus implying a considerable nonquasifree contribution to the Δ excitation of the ^{12}C nucleus.

Thus, to summarise the sum total of the work discussed [136, 138–144], the $^{12}\mathrm{C}(^3\mathrm{He}, \mathrm{t})$ cross section features listed above cannot be explained in terms of only one Δ excitation mechanism, the quasifree production on nucleons in the target nucleus, and so imply the existence of, and a quite considerable contribution from, another — collective — mechanism.

†The Δ peak shift with ^{3}He energy in the third column is accounted for by the different influence of the form factor of this nucleus, $E \sim \exp(-27.74|t|)$, at different values of $|t| = Q^2 - \Delta p^2$ (where $\Delta p = p_{^3\mathrm{He}} - p_{\mathrm{t}}$) within the Δ peak (especially for low ^{3}He energies) [143].

4.1.2 Saturne $^{12}\mathrm{C}(^3\mathrm{He}, \mathrm{t})$ charge exchange study

The first study of the Saclay Saturne group [137] on the $(^3\mathrm{He}, \mathrm{t})$ charge exchange on nuclei was performed in 1983 simultaneously with the first Dubna study [136]. In this and subsequent Saturne work, triton detection was performed by the magnetic spectrometer SPES-4 [147] with a 35 m total separation between the target and the final focal plane. The mass of the analysed particle was determined from the time of flight between two sets of scintillators 16 m apart. The high (300 ps) resolution secured a fairly reliable particle identification. To select events in the target, two sets of focal-plane drift chambers with momentum resolution of 7×10^{-4} were used.

Ref. [137] presents (^{3}He, t) data at energies 0.6, 1.2, and 2 GeV on ^{12}C, ^{54}Fe and ^{89}Y. At 2 GeV ($p = 3.9$ GeV/c) all of the targets exhibit strong Δ resonance excitation in the form of a wide maximum at reaction energy $Q = -270$ MeV ($\Gamma = 150$ MeV). A proposed explanation is the quasifree Δ excitation, inside the nucleus, of a nucleon involved in the Fermi motion. Another suggestion is the excitation of Δ-hole states of different spin and parity. New results on nuclear Δ excitation in the (^{3}He, t) reaction were published by the Saturne group in 1986 [148]. In that work the SPES-4 facility described above was employed to investigate the H, ^{12}C, ^{48}Ca, ^{54}Fe, ^{89}Y, ^{159}Tb and ^{208}Pb nuclei at 2 GeV, and additionally ^{12}C nuclei at 1.5 and 2.3 GeV.

Comparison of triton spectra at $E = 2$ GeV for different targets showed that the position of the Δ peak is (to within 10 MeV) mass number independent† from ^{12}C to ^{208}Pb and corresponds to an energy transfer of $\omega = 255$ MeV. The width of the peaks is also the same and equals $\Gamma = 160$ MeV. Comparison with the Δ peak position for p(^{3}He, t)Δ previously found at $\omega = 325$ MeV [149] emphasises the large size of the shift (70 MeV), indicative of nuclear medium effects.

For the ^{12}C nucleus, the dependence of the Δ excitation on energy was examined. The results are presented in Fig. 12, which shows triton spectra at 0° for ^{12}C(^{3}He, t) as a function of the energy transfer $\omega = E_{^3\mathrm{He}} - E_{\mathrm{t}}$. For 2.0 and 2.3 GeV, the spectra display wide Δ maxima around $\omega \sim 250$ MeV. The cross section in this region increases with energy. For the sake of comparison, the dotted curve in the same figure shows the computed cross section (in arbitrary units) for the 2.3 GeV quasifree Δ. The curve is clearly seen to be shifted to large energy transfers, ω, relative to the experimental Δ maximum.

†It is argued [3] that this conclusion is incorrect because of the neglect of the form factor effect, which is particularly important at the near-threshold Saclay energies (see the footnote to Table 2). Analysis of the A dependence for the (p, n) and (^{3}He, t) reactions [3] showed the cross section roughly scales with A (see Section 4.2 for more details).

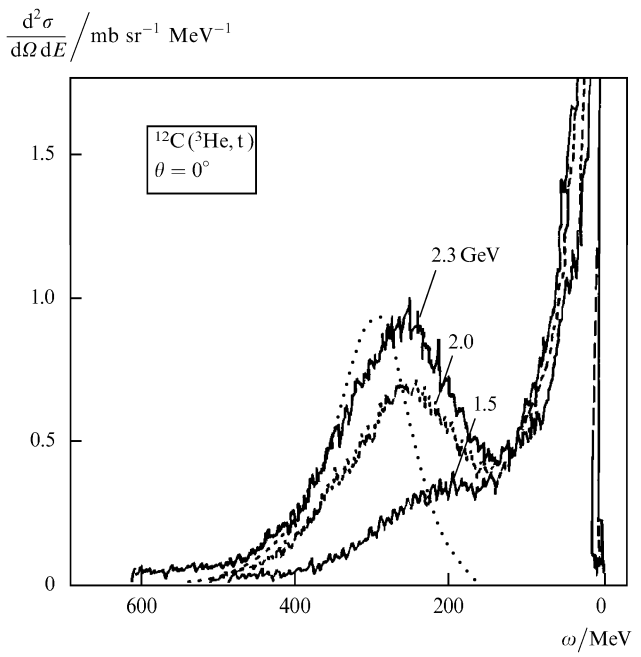

Figure 12.

Thus, in the same years as in Dubna, the Saturne group discovered the nuclear Δ excitation in the (^{3}He, t) charge exchange reaction — an effect which gives every indication of being of nuclear (rather than purely quasifree) origin and thus suggests a collective mechanism at work. A similar result was obtained at Saclay in 1986 in a study of charge exchange reactions on heavy relativistic ions (Section 4.3). Work on the collective mechanism for the (^{3}He, t) reaction was continued at Saturne in 1992 in a specially designed exclusive experiment (Section 4.5.3).

4.2 (p, n) charge exchange reactions

In this section we wish to do justice to some early investigators who had 'all but' discovered the collective Δ excitation mechanism long before it was demonstrated so convincingly in Refs [136, 137]. Back in 1977 – 1979, (p, n) charge exchange studies [150 – 152] produced results which, later work [153 – 155] showed, were typical of the collective mechanism.

For example, a study [150] on the ^{7}Li(p, n) and ^{6}Li(p, n) reactions on 800 MeV protons revealed broad (300 MeV) maxima in neutron spectra at $p_n = 1060$ MeV/c. Although there is every indication (the position in the spectrum, the direction of the shift, the width) that these maxima are due to the collective mechanism, they were associated with the formation of pions on target nuclei.

Similar broad maxima were found in a subsequent study [15] by the same group on a number of medium weight and heavy nuclei (Al, Ti, Cu, W, Pb, and U). They were again attributed to quasifree pion production in reactions of protons with nucleons inside the nucleus.

A similar conclusion was reached in Ref. [152] where the neutron spectrum showed a broad maximum 300 MeV away from the quasielastic peak. In this case the maximum was explained in terms of the formation of neutrons in an inelastic reaction with pion production.

It is only in a study [156] of neutron spectra in the elementary reaction $\mathrm{pp} \to \mathrm{n p}\pi^+$, which again reported a wide (300 MeV/c) maximum at $E_{\mathrm{p}} = 805$ MeV for $p_{\mathrm{n}} = 1025$ MeV, that one finds a vague mention of the Δ resonance, albeit in the sense of its contributing, in some phenomenological way, to the total cross section for pion production.

Nevertheless, the broad maxima observed in the above studies possess all the characteristic features of the collective mechanism of nuclear Δ excitation. Therefore some authors (see, e.g., Refs [157 – 160]) quote these works as pioneering ones, without being too much embarrassed by the interpretations we mentioned. We share the view that these works contributed significantly in this area. For example, based on the data from Ref. [152] and from the later work of the same authors [161 – 163], the A dependence of the total charge exchange cross section in the Δ peak maximum and the A and N dependences of the Δ peak shape were analysed [3, 164, 165].

The A dependence analysis assumed one-step (p, n) charge exchange with Δ excitation in the nucleus, and included the absorption of the projectile proton and of the detected neutron by the target. The general behaviour of the (p, n) charge exchange [and (^{3}He, t)] cross sections indicates the peripheral character of the process. The analysis of the shape of Δ peak showed its width to spread with A, which can be qualitatively explained by the mesonless de-excitation of the Δ. Of other Gatchina results [152, 161–163], the absence of the Δ peak shift on the deuteron should be noted.

Later (exclusive) work on the Δ excitation of nuclei under protons will be discussed in Sections 4.6.1 and 4.6.2.

4.3 Nuclear Δ excitation by heavy relativistic ions

The excitation of the nuclear Δ by heavy relativistic ions was first discovered at the Saturne Laboratory in 1986 [157] using the magnetic spectrometer SPES-4 described above (see Section 4.1.2). Ion charge identification was done using two independent ΔE signals from 1 cm thick scintillators. A resolution of $\Delta Z/Z = 0.035$ was secured. Mass identification was carried out by 17 m base flight time measurement with 300 ps resolution. This resolution permitted them, for example, to distinguish ^{19}F and ^{20}F with an accuracy of better than 1%.

The work involved the study of two mirror charge exchange reactions, $^{27}Al(^{20}Ne, ^{20}Na)$ and $^{27}Al(^{20}Ne, ^{20}F)$, under a 950 MeV/nucleon ^{20}Ne beam. The spectra displayed two peaks as functions of the reaction energy Q. The narrow maximum at $Q = -30$ MeV is interpreted as the excitation of particle–hole states of different multipolarity, and the broad one, at $Q = -300$ MeV, as a very strong internal excitation of a nucleon to the Δ resonance in target nuclei. This latter maximum is found to occur at the same Q and at a beam energy of 1100 MeV per nucleon.

Another reaction studied was the $^{12}C(^{14}N, ^{14}C)$ reaction under a 880 MeV/c ^{14}N beam, which exhibited a weak Δ excitation around $Q = -300$ MeV, but ^{14}O nuclei were not seen in the mirror channel above the background. Finally, the study of the $^{12}C(^{12}C, ^{12}N)$ reaction at 900 MeV/nucleon showed practically no Δ excitation.

In discussing the fact that the Δ intensities of the $^{27}Al(^{20}Ne, ^{20}Na)$ and $^{27}Al(^{20}Ne, ^{20}F)$ reactions differ almost threefold (2.7) whereas the isotopic relations oblige them to be the same, the authors point out that the cross section excess for the latter reaction can be accounted for qualitatively by the specifics of the ^{20}F and ^{20}Na level systems. The ^{20}F nucleus has a number of bound states which are excited in spin–isospin transitions. Their analogues in ^{20}Na are not bound (i.e., cannot be identified as ^{20}Na by the detector). Also, the particle emission threshold for ^{20}Na is only 2.2 MeV, to be compared with 6.6 MeV for ^{20}F. Both of these facts favour the formation of ^{20}F in a bound state. In a similar way, assuming the absence (or weakness) of spin–isospin transitions that lead to bound nuclei in the final state, the features of other reactions can be explained.

Work on charge exchange reactions under heavy relativistic ions is very interesting for several reasons. First, one can study spin–isospin modes in two mirror reactions with the same projectile, thus eliminating projectile structure effects when comparing reactions. Second, measurements for different projectiles on different targets yield a great deal of information about A dependences. Finally, considering the strong absorption of heavy ions in the target and in the projectile one would expect these reactions to be highly peripheral, so there is hope that density effects can be studied by making comparisons with light-ion reactions.

However, turning to the main theme of our review, one has to admit that the primary question we are concerned with, that of the Δ excitation mechanism, was not given a direct answer in Ref. [157]. This is probably due to the fact the Δ maximum detected in the study occurs at a value of energy transfer ($\omega_{\mathrm{nucl}} = 300$ MeV) which does not allow any confidence as to the presence or absence of the Δ shift, the more so because no proton-target reference data are used.

In a somewhat indirect way, however, the participation of the collective mechanism in Δ excitation is suggested by the Dubna and Saturne studies on $p(^3He, t)\Delta^{++}$, which yield $\omega_p \sim 325$ MeV, 25 MeV more than $\omega_{\mathrm{nucl}} = 300$ MeV of the work under discussion. The 25 MeV difference can be interpreted as a shift of the nuclear Δ maximum toward lower excitation energies.

4.4 $(\pi^{\pm}, \pi^0)$ charge exchange reaction

The theoretical interpretation of the Δ maximum shift in charge exchange $(^3He, t)$ and (p, n) reactions usually assumes one-pion exchange to be involved in the reaction mechanism (see Sections 5.2 and 5.3). It is therefore of considerable interest to investigate Δ excitation reactions in which π exchange is either impossible or hindered. Among these are $(\pi^{\pm}, \pi^0)$ charge exchange reactions, in which π exchange is forbidden by the G parity conservation law. These reactions are also important because they have no Δ excitation in the projectile particle and because results for projectiles with different charges may be compared. It is also expected that the zero spin of the π meson will facilitate the theoretical interpretation of the experimental results.

The first work on the (π^-, π^0) charge exchange was carried out at LAMPF (Los Alamos) in 1987 on the 475 MeV π^- beam [158]. However, because the energy is close to the threshold value, the maximum caused by the Δ-decay π^0 mesons was difficult to discriminate against the background of the π^0 mesons from the 'direct' charge exchange of the beam π^- mesons. More definitive, if somewhat unexpected results, were obtained at the Dubna JINR synchrophasotron in 1990 [166, 167]. In that work the $(\pi^{\pm}, \pi^0)$ charge exchange reaction was studied on the H, C, and Al nuclei at the incident pion momentum of 620–1200 MeV/c using the pion channel of the INR KASPIi facility.

Fig. 13a presents the schematics of the experimental setup [159]. Mesons were identified from two Cherenkov-detected π^0-decay γ quanta. The π^0 meson energy was determined from the γ quantum energy and scattering angle.

Fig. 13b represents the experimental (solid line) and computed (dashed line) spectra of the π^0 mesons from the $\pi^+ p \to \pi^0 \Delta^{++}$ reaction. The parameters of the maximum are: $\bar{E} = (861 \pm 19)$ MeV, $\sigma = (107 \pm 22)$ MeV. In Fig. 13c, the histogram of the experimental spectrum of π^0 from the reaction $^{12}C(\pi^-, \pi^0)$ and its Gaussian approximation are given. The parameters of the maximum are: $\bar{E} = (936 \pm 7)$ MeV, $\sigma = (158 \pm 6)$ MeV. The spectrum of the π^0 mesons from $^{12}C(\pi^+, \pi^0)$ is similar and has $\bar{E} = (940 \pm 8)$ MeV, $\sigma = (130 \pm 8)$ MeV. A point which attracts attention is the large shift of the nuclear Δ peak to lower excitation energies relative to the proton peak. The maximum for ^{12}C reactions is much wider than for the proton.

Thus, the results obtained for $(\pi^{\pm}, \pi^0)$ charge exchange are similar to those for the $(^3He, t)$ and (p, n) charge exchange reactions, but the former seems to require a nonstandard theoretical explanation because the π exchange is forbidden and the ρ meson is a vector particle.

From the point of view of present-day theory (see Section 5.2.2) the π exchange mechanism [used to explain the Δ peak in the $(^3He, t)$ and (p, n) reactions] is determined

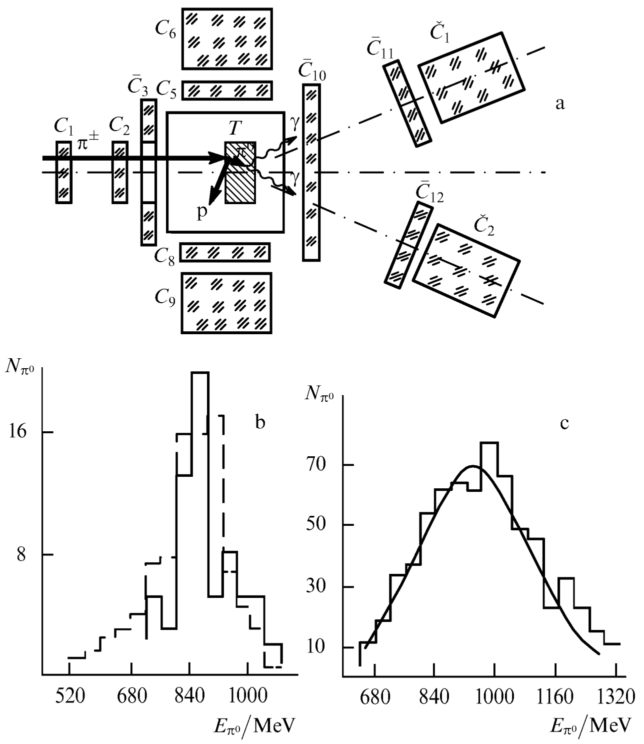

Figure 13. (a) Schematic diagram of the experimental facility for the study of the ($\pi^{\pm}$, π^0) charge exchange reaction: T — target, $\check{C}_1$ and $\check{C}_2$ — lead-glass Cherenkov counters (14 radiation lengths), $C_1 - C_3$ — beam scintillation counters, $C_5 - C_9$ — ($E - \Delta E$) counters for detecting charged particles, $C_{10} - C_{12}$ — anticoincidence scintillation counters. (b) Spectra of π^0 mesons from the p($\pi^{\pm}$, π^0) reaction. (c) Spectrum of π^0 mesons from the ^{12}C(π^-, π^0) reaction.

by the behaviour of the so-called spin-longitudinal part of the nuclear response function, which shifts the Δ peak to lower excitation energies, whereas the ρ exchange mechanism depends on the spin-transverse part, which leaves the peak unshifted. It is for this reason that the results of Refs [166, 167] appear somewhat unexpected (cf. their discussion in Section 5.3.2). They are not unique in this sense, though.

In 1989, the Saturne group investigated [168] the d, 2p(^{1}S$_0$) reaction on a beam of 1.6 GeV and 2 GeV polarised deuterons with the formation of two singlet protons, this reaction being equivalent to the (p, n) reaction, the simplest possible from the spin response analysis viewpoint. It proved possible to determine directly the longitudinal to transverse cross section ratio, and it turned out that the transverse component exceeds the longitudinal one by a factor of 1.7 for deuterons and by as much as 3 for ^{12}C. On the other hand, the behaviour of the form factor for this reaction (see Fig. 22) implies the predominance of the longitudinal component, and the Δ peak for ^{12}C was indeed found to be down by (65 ± 5) MeV (Fig. 14). Although this contradiction may prove simple to explain (see Section 5.3.2), it is obvious that the participation of the spin-transverse component of the nuclear response function in the d, 2p(^{1}S$_0$) and ($\pi^{\pm}, \pi^0$) reactions remains an intriguing and highly topical problem, and so further research into both reactions is needed. In particular, ($\pi^{\pm}, \pi^0$) charge exchange measurements on old (to ensure continuity) and new nuclei to examine the A dependence are highly desirable, as are measurements for various scattering angles

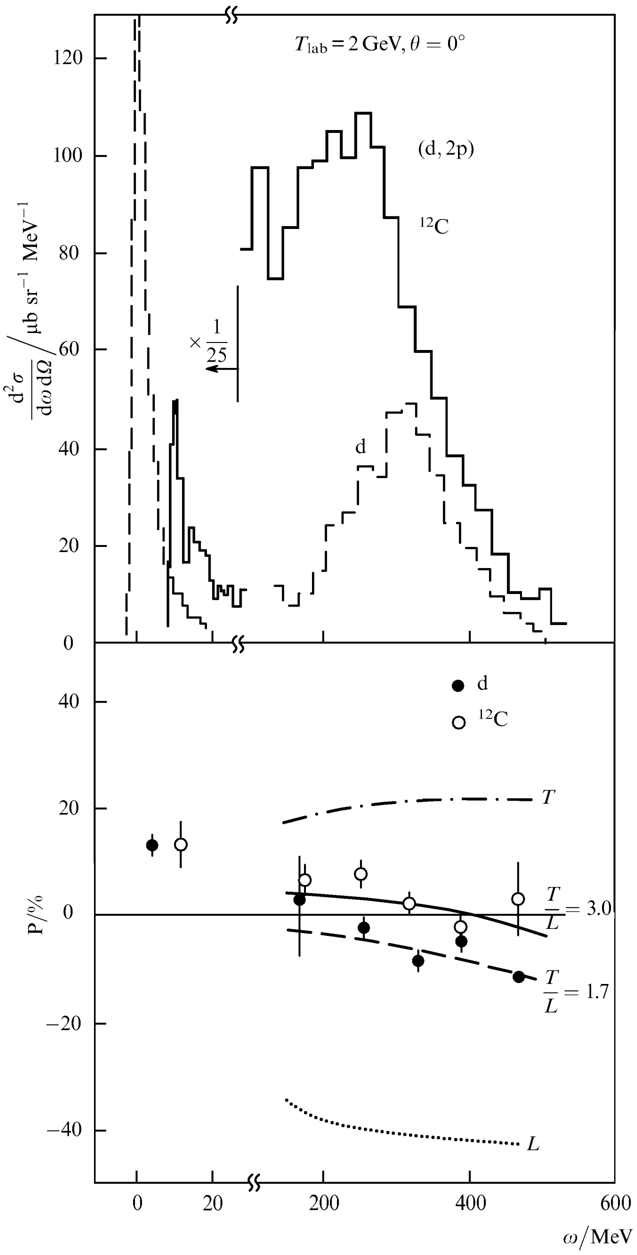

Figure 14.

and with improved accuracy. Experiments on π^0 meson Δ decay particle coincidence, which might be of help in nuclear state identification, are particularly desirable.

4.5 Exclusive experiments

The study of charge exchange reactions in inclusive experiments has led to the important discovery of the collective mechanism of Δ excitation in nuclei. It has been demonstrated in many experiments on various particles that if the energy transfer to the nucleus is on a scale of 300 MeV, and the momentum transfer is comparable to the average Fermi momentum of the nucleons, then the charge exchange cross section displays a broad Δ maximum considerably down in energy as compared to free proton Δ excitation. These results are in contrast with the accepted view on what would be expected from the quasifree mechanism of Δ excitation in the nucleus, and prove the existence of another — collective — excitation mechanism which is predominant over the quasifree one.

Valuable though inclusive experiments are, they are clearly insufficient for studying separately various aspects of the two mechanisms, such as their relative contributions to the excitation and de-excitation of the nuclear Δ isobar, the properties of the Δ excitation on the proton and neutron targets, the role of the Δ excitation in the projectile and in the target, the role of the pionic mode in the Δ excitation process, etc. To answer these and many other questions, exclusive experiments (Sections 4.5.1 – 4.5.5) and theoretical studies (Section 5) are needed.

4.5.1 Quasifree Δ isobar formation in the (p, p′) reaction. A direct experimental check on the properties of the quasifree nuclear Δ isobar excitation was made in a study [169] of the inelastic scattering of protons on d, C, and Al nuclei at $p_{\mathrm{p}} = 3.88$ GeV/c. In this work the quasifree mechanism was very convincingly separated and thoroughly studied, and we therefore discuss it in some detail here. The reaction under study was

$$\mathrm{p} + {''}\mathrm{n}{''} \to \mathrm{p}' + \Delta^0 , \quad \Delta^0 \to \mathrm{p}'' + \pi^- , \tag{17}$$

where ″n″ is the intranuclear neutron, p′ is the scattered proton, p″ the Δ^0 decay proton. The special feature of the work is the exclusive arrangement of the experiment, in which apart from p′ the products of Δ^0 decay (and they alone) were detected. The work was performed on unseparated p and π beams taken out from the inner target of the 12 GeV proton synchrotron at the Japanese National Laboratory for High Energy Physics (KEK). The FANSY facility [170] consisting of a beam, central, and frontal part (Fig. 15) was used.

The beam momentum $p = 3.88$ GeV/c and the quantity $\sigma_{\mathrm{p}}/\mathrm{p} = 1.4\%$ were obtained from flight-time measurements. To detect the inelastically scattered proton p′, the frontal spectrometer was used which detected the p′ protons in the angle range $1 - 5.5°$ with a momentum resolution of better than 1%. Flight time proton identification was used. Δ^0 isobar decay products were detected in the central part of the facility.

The reliable separation of quasifree Δ formation events was ensured by satisfying the following requirements: the frontal spectrometer detects only one proton; the central, one proton and one pion; other charged particles are absent. The selected events were cut off by the invariant mass of the $\mathrm{p}\pi^-$ pair ($M^* < 1400$ MeV) and processed by the kinematic criterion by calculating the mass of the target nucleon [″n″ in Eqn (17)] from the four-momenta of the incident proton p, scattered proton p′, and decay products π^- and p″,

$$m^{*2}_{''\mathrm{n}''} = (E_{\mathrm{p}} - E_{\mathrm{p}'} - E_{\pi^-} - E_{\mathrm{p}''})^2 - (\boldsymbol{p}_{\mathrm{p}} - \boldsymbol{p}_{\mathrm{p}'} - \boldsymbol{p}_{\pi^-} - \boldsymbol{p}_{\mathrm{p}''})^2 . \tag{18}$$

The maximum of the distribution obtained coincides with the square of the nucleon mass, i.e., the events in its neighbourhood correspond to quasifree production of the Δ. The removal of nonquasifree events was achieved by cutting off the wings of the p′ distribution. The small background which remained was accounted for by comparison with the momentum distribution obtained for $\mathrm{p}\pi^+$ pairs (unable to form Δ^{++} isobars in this particular experimental setup).

The selected 'true' quasifree events were compared with calculations taking into account the binding energy of the nucleon, the Fermi distribution, Δ width, incident momentum scatter, and the momentum resolution of the spectrometer. The results of the comparison are presented in Fig. 16a, which shows that the computed curves approximate the experi- mental points quite closely. It is seen that the Δ resonance maxima on both complex nuclei (C and Al) are shifted toward lower momenta of the scattered proton p′ (i.e., to higher energy transfers Q) compared to the position of the maximum for a simple nucleus (d). Thus it seems

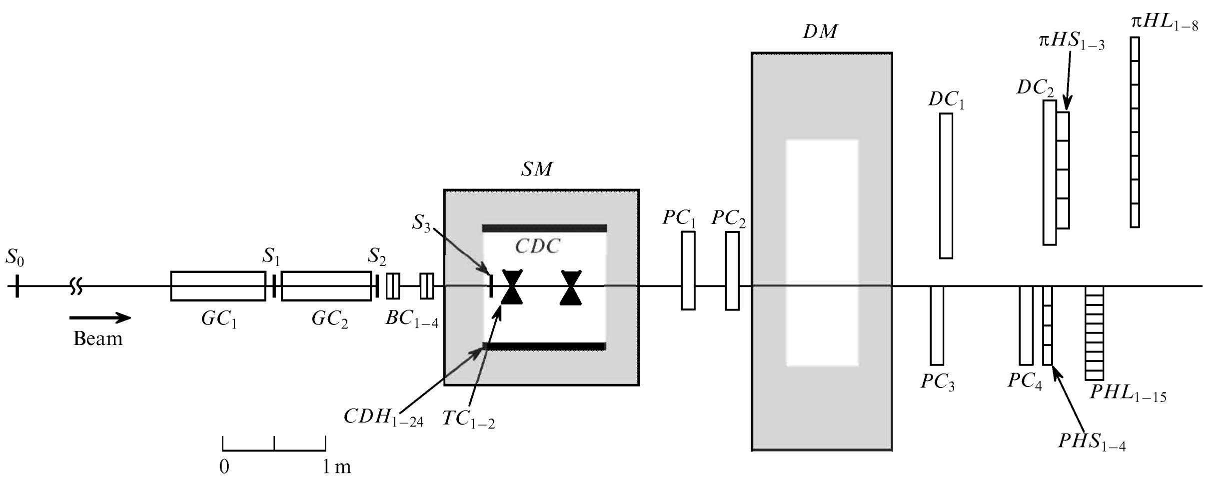

Figure 15. Schematic diagram of the FANSY facility. Beam part: $S0$–$S3$ — flat scintillation counters for separating the primary beam and measuring the time of flight; $GC_{1,2}$ — gas Cherenkov counters for separating protons and π mesons and cutting off muons and electrons; $BC_{1\text{–}4}$ and $TC_{1,2}$ — multiwire proportional chambers for determining the trajectory and profile of the beam. Central part: SM_{CDC} — solenoidal magnet ($B = 0.3$ T); CDC — cylindrical drift chamber with the target inside: $CDH_{1\text{–}24}$ — cylindrical hodoscope consisting of 24 scintillation counters, for obtaining a trigger signal and identifying particles from their time of flight (in addition to identification from $\mathrm{d}E/\mathrm{d}x$ in the chamber). Frontal part: DM — wide-aperture dipole magnet ($B_0 = 1.2$ T); $PC_{1\text{–}4}$ — multiwire proportional chambers; $DC_{1,2}$ — flat drift chambers; $\pi HS_{1\text{–}3}$, $\pi HL_{1\text{–}8}$, $PHS_{1\text{–}4}$, $PHL_{1\text{–}15}$ — scintillation hodoscopes for obtaining trigger signals and measuring time of flight.

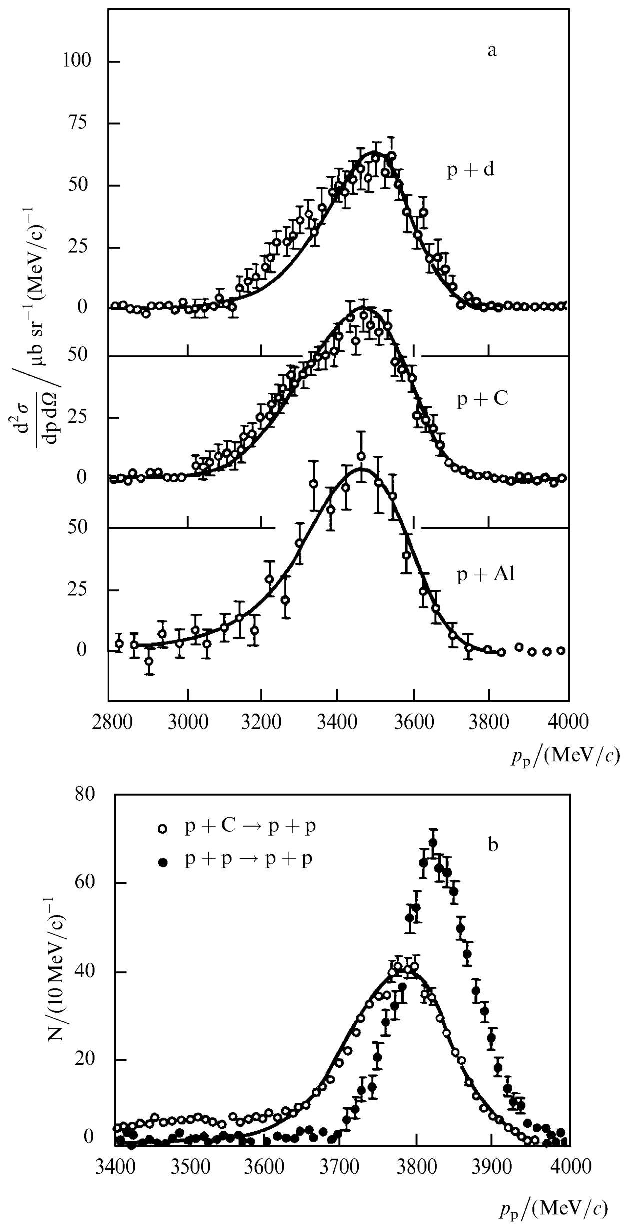

Figure 16.

proved (both by calculation and experimentally) that the unusual nuclear Δ excitation involving (in inclusive processes) a downshift of the Δ maximum cannot be accounted for by the quasifree production of the isobar on one of the nucleons bound in the nucleus.

In concluding this section we present the results of what we consider to be the most convincing experimental study of the quasifree mechanism, one which involves the comparison of the two simplest processes possible, the scattering of a proton on a free proton and on a quasifree proton. Such a comparison was carried out in the same Ref. [169] in an experimental arrangement designed to detect only two protons, the fast forward scattered one, and a relatively slow oblique one.

Data on elastic pp scattering on the free proton were obtained from the CH_2 target by subtracting the carbon target contribution; data on quasifree pp scattering, by analysing pp scattering on a proton bound in a carbon nucleus. The results of the comparison are given in Fig. 16b, which shows that the elastic quasifree peak in the spectrum of forward scattered protons is markedly lower and wider and occurs at lower momenta as compared with the elastic pp peak for the free proton. The magnitude of the shift corresponds to the energy of the removal of a nucleon from the carbon nucleus (25 MeV), and the shape of the quasifree peak is approximated well by the Gaussian curve

$$N(\mathrm{p}) = N_0 \exp\left(-\frac{p^2}{2\sigma_F^2}\right) \qquad (19)$$

of width $\sigma_F \simeq 120$ MeV/c. Note, finally, that on the qualitative level, the shift results simply from the requirement to account for the nucleon binding energy in the quasifree process.

By comparing the results of the inclusive experiments with the material of the present section, one arrives at the firm conclusion that to explain the Δ excitation in charge exchange reactions requires that, apart from the quasifree mechanism an additional — and, for these particular reactions, maybe even dominant — mechanism of collective interactions should be introduced.

Further information concerning the relative roles of and the competition between the two mechanisms may hopefully be obtained from the analysis of exclusive experiments on the decay of the nuclear Δ from the (p, n) and (^{3}He, t) charge exchange reactions.

4.5.2 Comparison of the π^+p and 2p de-excitation channels for the nuclear Δ produced in the (p, n) charge exchange reaction

Ref. [160] of 1991 presented the results of the first Δ region experiments on (p, n) reactions on neutrons in coincidence with 2p and π^+p from the de-excitation of the Δ from ^{12}C(p, n). The experiments were conducted at KEK (Japan) on the beam of 1.5 MeV/c protons from the 12 GeV proton synchrotron. To detect coincident particles, a 12 m base 50 scintillator flight-time neutron spectrometer, and the wide-angle spectrometer FANSY described in Section 4.5.1 [170], were used. The targets employed were carbon and polyethylene. Depending on the combination of the particles detected in FANSY, the detected events were classified into 6 types: no particles, only π^+, only p, p and π^+, 2p, and others†. By summing all the six, a control inclusive cross section was obtained.

The most interesting events to consider are π^+, p + π^+ and 2p, whose cross sections as a function of neutron momentum are given in Fig. 17. It is seen that the Δ maximum in the spectrum for the (p + π^+) events is shifted to much lower neutron momenta relative to the other two (identical in position) events. When recalculated to the excitation energy ω, it is found that the (π^+ + p) peak has even somewhat higher ω than in the free proton reaction, whereas the other two peaks are shifted strongly in the opposite direction. It is remarkable, however, that the invariant mass for the pπ^+ events with carbon proves to be lower than in the hydrogen case, whereas the width is larger.

A preliminary analysis of this apparent disagreement between the positions, in the neutron spectrum, of the

†Single π^+ events occur in the decay (Δ → Nπ^+) with a subsequent loss of a nucleon due to acceptance, threshold, or absorption of the nucleon by an unfilled nuclear orbit, etc.

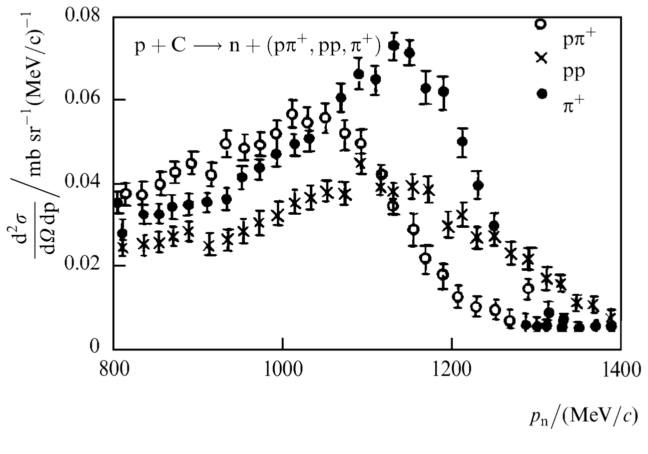

Figure 17.

$(\pi^+ + p)$ events on the one hand and of the 2p and π^+ events on the other shows that the position of the 2p and π^+ peaks in the neutron spectrum is similar to the position of the peak for the inclusive cross section, and that the $(p + \pi^+)$ peak is shifted from this latter by 100 MeV to lower momenta. Thus, it is the p and π^+events which contribute most to the peak shift seen in the inclusive spectrum. It is suggested that the anomaly in the $(p + \pi^+)$ peak position in the neutron spectrum may be due to the effect of scattering of the outgoing p and π^+ (see the next section for more on this).

A supplementary rapidity analysis [171] of the cross section for π events suggests that these form in the decay of Δ produced in collisions with individual nucleons and that the excitation of the projectile is not strong enough to produce the shift observed.

4.5.3 Study of the decay of the nuclear Δ isobar from the reaction (^{3}He, t) on ^{1}H, ^{2}H and ^{12}C

An exclusive experiment on the decay of the Δ isobar produced in the reaction $(^3\mathrm{He}, t)$ was conducted at the Saclay Laboratoire Saturne using the beam of ^{3}He of intensity 10^6 s^{-1} of energy 2 GeV [172]. The 4π-DIOGENE detector (Fig. 18) with an added triton-detection arm [173] was employed. The detector (4π-*D* in Fig. 18a) is of cylindrical shape and consists of 10 trapezoidal drift chambers placed in a 1 T longitudinal solenoidal magnetic field. The targets used were liquid hydrogen (1.3 g cm^{-2}), liquid deuterium (3.1 g cm^{-2}), and carbon (0.36 g cm^{-2}).

The detecting and momentum-analysing arm for the resultant tritons consists of a dipole magnet *DM* 1.33 m long ($B = 1.9$ T) and two sets of drift chambers *Ch*1 and *Ch*2, with hodoscopes *H*1 and *H*2, allowing energy and angle measurements in the range 1.4–2.0 GeV and $0 - 4^\circ$. To reduce the multiple scattering of the tritons, two helium bags were used. Noninteracting He nuclei were deflected in the dipole magnet and directed to a beam absorber along the vacuum tube.

The identification of charged particles (π, p, t, and impurity d) and the determination of their momenta were achieved by reconstructing their tracks making use of the momentum amplitude analysis in the drift chambers. The pions and protons of the Δ decay were identified in the polar angle range 20–132° and for $E_\pi \geqslant 15$ MeV, $E_p \geqslant 35$ MeV. The momentum resolution was typically

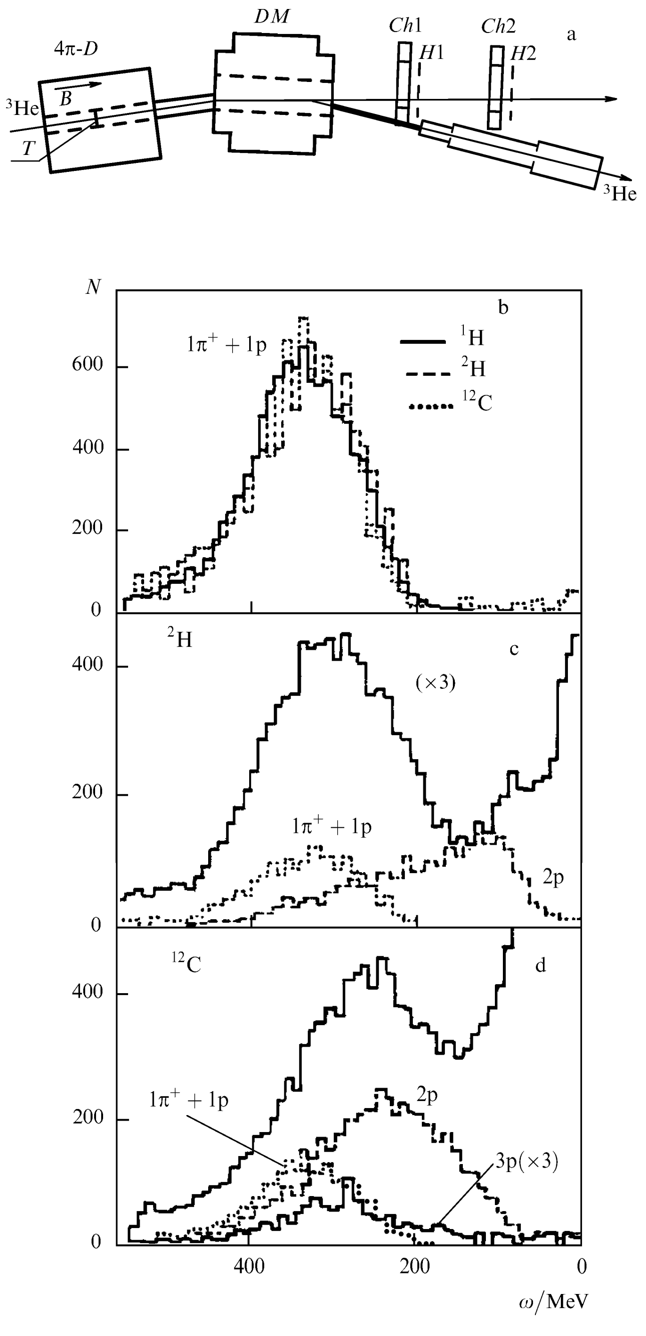

Figure 18.

18% for p and 10% for π. For the two reactions

$$p(^3\mathrm{He}, t)\Delta^{++}, \quad \Delta^{++} \to p + \pi^+ , \tag{20}$$

$$d(^3\mathrm{He}, t)\Delta^{++}(n), \quad \Delta^{++} + (n) \to p + p , \tag{21}$$

where (n) is the neutron-spectator, full kinematics can be constructed, with adequacy being ensured by the small value of the missing mass for the events involved. For the carbon target, in addition to the $p\pi^+$ and 2p events, 3p events were also detected.

The calibration of triton energy in hydrogen events (20) was made using the energy balance of the reaction. For ^{2}H and ^{12}C, the position of the peak at low excitation energy (well known from older experiments) was used. The detector efficiency was determined by a cascade calculation. The acceptance-based cutoff was found to underestimate 2p events by a factor of 1.5, and the $1\text{p} + 1\pi^+$ and 3p events, by a factor of 1.5 and almost 15, respectively.

The basic results of Ref. [172] are presented in Fig. 18b, which shows (in arbitrary units) the energy transfer spectra for π^+p (^{1}H,^{2}H and ^{12}C targets), 2p (^{2}H and ^{12}C targets) and 3p events (^{12}C target) and also the 0.3 scaled inclusive spectrum for all the events (^{2}H and ^{12}C targets) as a function of the energy transfer $\omega = E(^3\text{He}) - E(\text{t})$. It is seen that the π^+p spectra are similar for all the targets, i.e., the Fermi motion broadening is small. A feature of the 2p spectrum is the lack of the Δ peak for ^{2}H, and a marked Δ peak for ^{12}C strongly downshifted (by 100 MeV) from its position for the π^+p events. The lack of the Δ peak for ^{2}H is interpreted as being due the low density of nucleons in the deuteron nucleus [the Δ isobar produced on the deuteron proton is very unlikely to interact with a neutron-spectator of (21)].

An estimate of the missing mass and of energy balance for 2p events on ^{12}C shows that they do not involve 3 or 4 nucleon processes and hence may be interpreted as the coupling of Δh and 2p−2h states. The relative shift of the Δ peak for states with different de-excitation modes (π^+p and 2p) is explained by the strong ($\sim p_\pi^3$) threshold effect for the Δ decay pions, due to $l_\pi = 1$. The 2p channel does not have such a threshold effect, i.e., it is sensitive to the energy downshifted Δ-hole states. One can say pictorially that the (π^+p) channel of the Δ decay is available only because of the right-hand high-energy portion of the Δ maximum, whereas the 2p channel is also possible for lower energy transfers (the left-hand side of the maximum).

Recall from Section 4.5.2 that the similar behaviour of π^+p events in the (p, n) charge exchange reaction can be accounted for by p and π^+ scattering. One more explanation of this anomaly exists. It is assumed in Ref. [2] that π^+p events occur in the Δ decay of an isobar produced in the quasifree [collective] mechanism. The same view is taken in Ref. [174]. Based on the results of Ref. [172] discussed above, and developing further the view proposed there, it is pointed out that the missing mass for π^+p events is less than a few MeV, that is, the ($\Delta^{++} \to \text{p} + \pi^+$) channel does indeed select the quasifree process, in which Δ^{++} is excited with the same energy and width as for the free nucleon. In any case, it is clear that this question needs further investigation in 'still more exclusive' experiments using 'still more ideal' detectors.

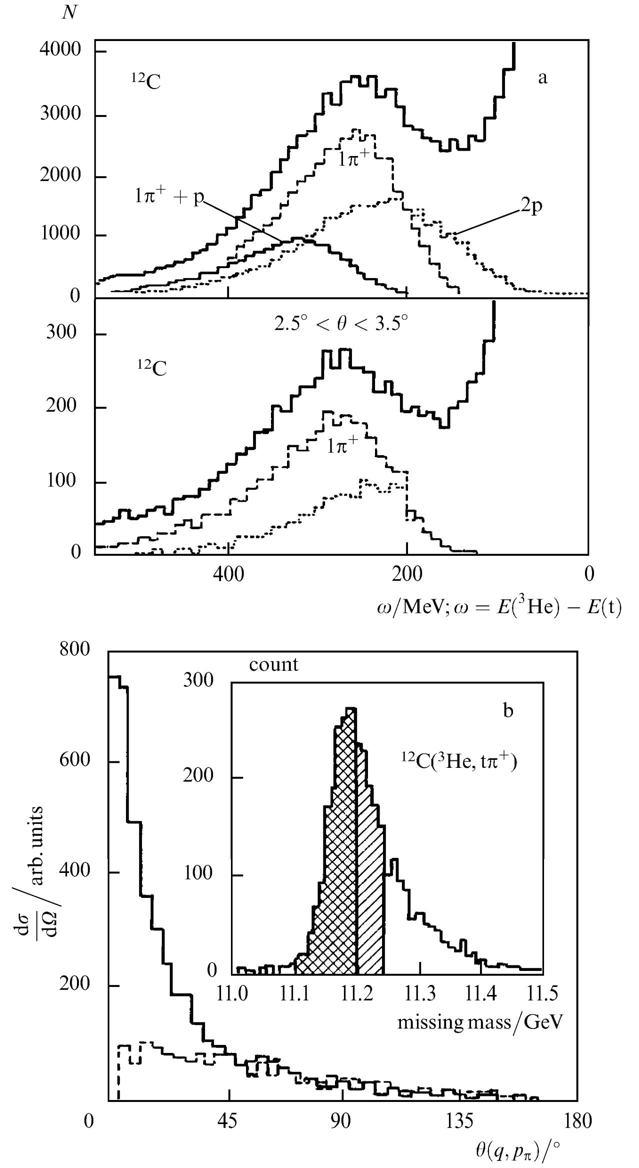

Figure 19.

4.5.4 Coherent pions from the (^{3}He, tπ^+) and (t, ^{3}He π^-) reactions

The tendency toward increasingly exclusive experiments was continued in a study on the reaction ^{12}C(^{3}He, tπ^+) at 2 GeV [175] (see also Ref. [174]), in which apart from reaction products, the energy state of the final nucleus was monitored.

The work was carried out in the Laboratoire Saturne using the DIOGENE detector described in the preceding section. Fig. 19a shows the spectrum of energy transfer, $\omega = E(^3\text{He}) - E(\text{t})$, for various decay channels. The upper portion of the figure has been discussed in part in Ref. [172] (Section 4.5.3). The high yield and the backward shift of the Δ peak for 2p events are due to the medium effects on the energy and width of the Δh states. The absence of Δ peak shift for π^+p events is accounted for by their formation in the low-density surface layer of the nucleus. These conclusions are supported by cascade calculations and by the agreement with the (p, n) decay data [160]. Refs [174] and [175] deal primarily with $1\pi^+$ events, which had not been discussed earlier in any detail. These are assumed to arise from (π^+ + N) events, in which the nucleon is not detected (either because of being a neutron or due to acceptance or threshold restrictions on the proton).

The lower portion of Fig. 19a presents events for small triton scattering angles ($2.5° < \theta_t < 3.5°$), including the 0.35 scaled inclusive events (solid line), all $1\pi^+$ events (dashed line), and $1\pi^+$ events corresponding to the formation of ground state final nuclei (dotted line with a maximum at $\omega = 250$ MeV). For the latter type of event, the insert in Fig. 19b shows the 10 MeV partitioned spectrum of the missing mass of the reaction under study. The spectrum is seen to be well concentrated near the mass of the ^{12}C nucleus ground state (11.75 GeV), and it is this fact which permits a reliable selection of events that correspond to the formation of a final nucleus in the ground and weakly excited states (left part of the maximum, with missing mass less than 11.2 GeV). The events corresponding to the final nucleus excitation energy of 25−50 MeV were separated by

1.200 – 1.250 GeV 'gates' (dashed region in the right portion of the maximum).

For both types of events (at an energy transfer of $\sim$250 MeV) the angular correlations of the momentum transfer $\boldsymbol{q}$ and the momentum of the outgoing pion $\boldsymbol{p}_\pi$ were examined, the spectra of which are shown in the bulk of Fig. 19b. It was found that for events with the final nucleus in the ground state the $\boldsymbol{q}$ and $\boldsymbol{p}_\pi$ angular correlation spectrum is sharply peaked at low relative angles (solid histogram), whereas for excited nuclei it is more uniform. This result, together with the large cross section (larger by far than suggested by the phase space) and the very low kinetic energy of the recoiling nuclei ($\sim$ 1 MeV) prompted the authors' claim to be the first to observe the formation of coherent pions outside the mass surface — a manifestation of a rather unusual process in which the reaction $(^3\mathrm{He},\mathrm{t})$ produces virtual pions that scatter from target nuclei elastically prior to becoming real. The real pion has practically the same energy as the virtual one.

The computed correlation spectrum for cascade, i.e., incoherent, pions has no sharp peak at low relative angles between $\boldsymbol{q}$ and $\boldsymbol{p}_\pi$ and shows a weak energy excitation dependence. The authors note an excellent agreement of the experimental angular distributions with theoretical calculations ([176]; see also [Ref. 177]) which show that the formation of coherent pions in the $(^3\mathrm{He},\mathrm{t}\pi^+)$ reaction is in fact the only evidence for the existence of a nuclear pionic mode (see Section 5.3).

At the Twelfth International Seminar on the Problems of High Energy Physics in September 1994, coherent pions from the excitation of resonances other than Δ in target nuclei were reported [239]. The work was performed with the LHE JINR tritium beam using the streamer-chamber GIBS spectrometer. The facility allowed detection and measurement of all charged particles in geometry close to 4π [240]. The momentum spectrum of π^- pions from the reaction $\mathrm{t} + \mathrm{C(Mg)} \to {}^3\mathrm{He} + \pi^- + \ldots$ for 9 GeV/c projectile momentum was measured.

Comparison with calculations [176, 241] and with the authors' own estimates [239] showed that, apart from the coherent π^- mesons from the Δ^-, with their narrow maximum at $p_{\pi^-} = 230-280$ MeV, the experimental spectrum also contains 30 – 50% π^- mesons with a maximum at $p_{\pi^-} = 400$ MeV/c. These take away much of the longitudinal momentum at a low momentum of the recoiling nucleus and so also behave like coherent pions.

Besides target nuclei, coherent pions may also appear in projectile nuclei during the excitation of the Δ isobar or heavier resonances in them. In such processes, however, the maximum of the pion spectrum must lie at $p_{\pi^-} \leqslant 150$ MeV/c. The authors of Ref. [239] therefore argue that the maximum at $p_{\pi^-} = 400$ MeV/c in the pion spectrum proves the formation of coherent pions in the excitation of the N(1440) and (or) N(1520) resonances in target nuclei.

4.5.5 Separation of the DEP mechanism of Δ excitation

In this section we give an account of a study [178] which is devoted to nucleon compressibility and so, on the face of it, has nothing to do with the subject matter of this review. However, the approach taken in Ref. [178] was to examine the isoscalar monopole excitation of the $\mathrm{P}_{11}(1440)$ resonance in the $\mathrm{p}(\alpha,\alpha')$ reaction, i.e., the radial mode of nucleon excitation. Experimentally, this process takes place against a very strong background from the Δ of the projectile nucleus and so is of direct interest to us here.

The study was carried out at Saturne with a beam of α particles of momentum 7 GeV/c ($E_\alpha = 4.2$ GeV) irradiating a liquid hydrogen target 4 cm thick. The momentum of the scattered α particles was analysed using the magnetic SPES-IV spectrometer described above and two drift chambers 1 m apart. The interaction vertex in the target was calculated from the intersection points of the particle trajectory with six layers of chambers. Reliable identification of the scattered α particles was secured by the time-of-flight method and by the use of plastic scintillators in ΔE measurements.

The missing energy ($\omega = E_\mathrm{i} - E_\mathrm{f}$) spectrum was measured for four scattering angles: 0.8°, 2.0°, 3.2°, and 4.1°. The results for $\theta = 0.8°$ are shown in the upper portion of Fig. 20a. The spectrum exhibits a strong rise in yield above the production threshold for Δ related π mesons, and shows a highly pronounced structure above 400 MeV, indicative of the strong excitation of the $\mathrm{P}_{11}(1440)$ resonance. The main

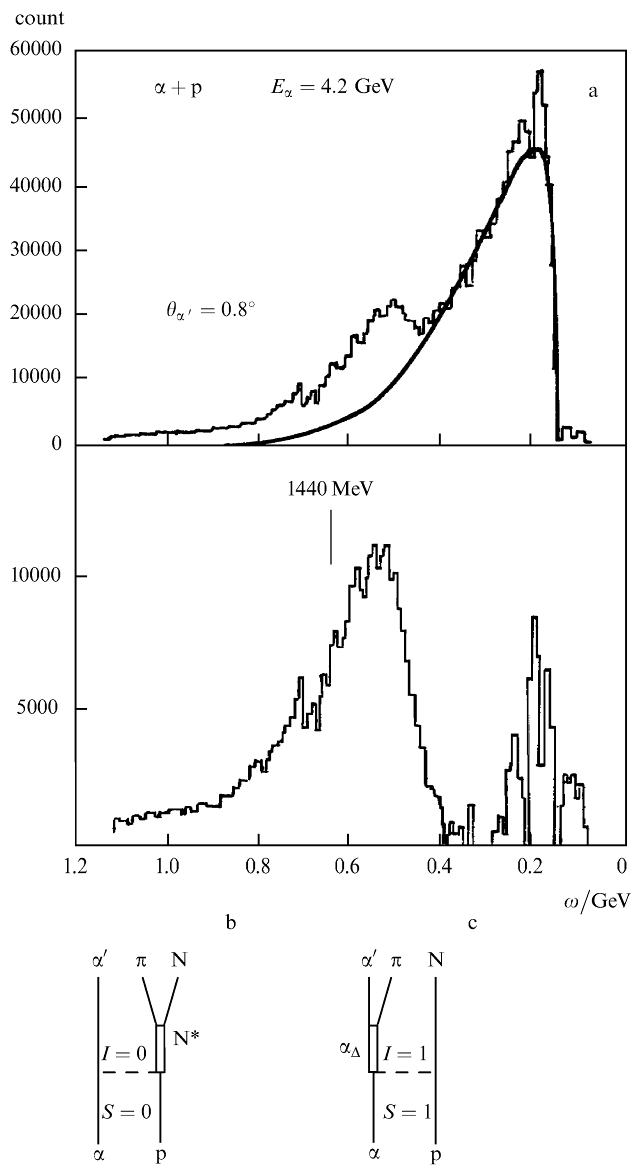

Figure 20.

diagrams for this processes are shown in Figs 20b and 20c. Fig. 20b corresponds to the excitation of the $P_{11}(1440)$ resonance; Fig. 20c, to the Δ isobar excitation. It is seen from the figures that the Δ excitation is possible only in a projectile nucleus (i.e., in the DEP mechanism), since the excitation on the proton target (DET mechanism)† is forbidden by the isospin conservation law (N^* cannot be replaced by Δ in Fig. 20b).

By subtracting from the experimental spectrum the result calculated for the diagram of Fig. 20c (solid line in the upper portion of Fig. 20a) the authors arrive at the $P_{11}(1440)$ resonance excitation spectrum they are interested in (lower portion of Fig. 20a). We are concerned here with the inverse problem, to separate from the experimental spectrum the part corresponding to the Δ excitation of the α projectile. If not altogether correct, the following approach seems to be fairly reasonable. As follows from the authors' supplementary analysis including the ^{4}He form factor and making use of other $P_{11}(1440)$ resonance data, the lower part of Fig. 20a is in general a good description of the excitation spectrum of this resonance. Thus in a sense the computed curve in the upper portion of Fig. 20a is further experimental evidence for the DEP mechanism acting in the α projectile.

An analogous conclusion can be drawn about the angular distributions, which must be similar for both cases since both diagrams of Figs 20b and 20c correspond to the monopole excitation with $L = 0$ (but with different spin–isospin structures). This conclusion is borne out by experiment.

Our procedure of transforming a computed result into experimental one has gained some acceptance. For example, in Ref. [179], which provides theoretical probabilities for the DET and DEP mechanisms in various reactions on nucleons, the above results on the energy spectrum and the angular distribution of the Δ excitation of the ^{4}He projectile nucleus are considered as a good experimental check on the calculations performed (see Section 5.3.2).

5. Attempts at theoretical interpretation

As already stated in the Introduction, the theoretical interpretation of the Δ excitation in nuclei is still uncertain, which is not surprising considering that the Δ is a hadron and that a qualitative theory of the strong interaction is still lacking‡. Yet phenomenological attempts to explain the major qualitative features of the Δ isobar have been undertaken for long, based on the properties of the free Δ as a spin–isospin excitation of the nucleon, and with the recognition of the special role of the pion in this elementary excitation (the Δ isobar is a pion–nucleon resonance). This strong coupling between the nucleon, pion and Δ isobar allows a natural extrapolation into the nucleus, which contains interacting nucleons and pions and is therefore expected to exhibit Δ excitations (nuclear Δ isobar). The nuclear Δ isobar is currently a widely held idea substantiated by a whole series of experimental facts which we have described in the previous sections. At this point, only two processes, pion–nucleus scattering and photoabsorption, will be touched on.

†DEP is for Δ excitation in the projectile; DET, in the target.

‡It will be recalled that QCD is quantitative only in the asymptotic freedom region.

The basic characteristics of Δ region pion–nucleus scattering are determined by the small mean free path of the pion in nuclear matter (~1 fm). The πN interaction takes place at the surface of the nucleus. The total and differential cross sections are determined by the scattering at the black disk with a radius equal to the nuclear interaction radius.

In fact, experiments show (see, e.g., Refs [180, 181]) that

$$\sigma_{\mathrm{tot}} \simeq 2\pi R^2 \sim A^{2/3} , \tag{22}$$

and that $\mathrm{d}\sigma/\mathrm{d}\Omega(\Theta)$ in the neighbourhood of the cross section peak shows a diffraction pattern with deep Fraunhofer located minima. The cross section versus energy curve has a characteristic Δ maximum for $A < 50$ nuclei, which, as A increases, shifts by $\delta E \approx -15A^{1/3}$ MeV with respect to the Δ peak of the free Δ. The width of the nuclear Δ peak exceeds that of the free isobar Δ peak and increases with A, and its height is also greater than for the free Δ. Analysis of the experiments described in the preceding section shows that the properties of the Δ excitation in hadron reactions are determined by the competition of the quasifree and collective mechanism, of which the latter is prevailing one.

Equally compelling evidence for the existence of the nuclear Δ isobar comes from electromagnetic processes. The $\sigma_{\gamma A}$ total cross section has a Δ maximum at $E_\gamma \approx 300$ MeV all the way up to the heaviest nuclei. The nucleus is transparent for photons of intermediate energy as primary particles, and the cross section scales with A. The cross section per nucleon is approximately constant for all nuclei $\sigma_{\gamma A}/A \simeq$ const but is somewhat less than $\sigma_{\gamma\mathrm{H}}$, and the Δ peak is practically unshifted from its free Δ position while being markedly broadened [1]. Again the implication may be that the nuclear Δ excitation involves both mechanisms, but this time with about equal weight.

In the preceding sections both mechanisms have been described very much phenomenologically, based on what one sees in experiment, and invoking some quite simple ideas. In the present section we shall try to employ the Δ-hole model in order to give a semipopular account of these mechanisms from the theoretical and computational viewpoints and also to clear up why their effect on the nuclear Δ isobar is different in hadron and electromagnetic processes. Other (relativistic and chiral) theoretical concepts will not be considered.

5.1 Quasifree mechanism of nuclear Δ excitation

It has been believed for quite some time (and indeed by some quite recent workers [171, 182]) that the most natural formation mechanism for the nuclear Δ is its quasifree production on one of the bound nucleons in the target nucleus or (and) — a recent idea (see Section 5.3.2) — in the projectile nucleus. Experiments do not substantiate this view. Nor do calculations.

A detailed discussion of the simplest possible mechanism for the quasifree production of the Δ isobar in nuclei has been given, for example, for the $^{12}\mathrm{C}(^3\mathrm{He},\mathrm{t})$ reaction [139, 153, 155, 184]. The argument used in these studies is schematically as follows. Consider, to be specific, one of the protons in ^{12}C, with Fermi momentum $\boldsymbol{p}_{\mathrm{N}}$, and suppose the quasifree production mechanism excites a Δ^{++} isobar on this proton (Fig. 21a). Then the parameters of the nuclear Δ maximum are determined by the convolution of the differential cross section $\mathrm{d}\sigma(\mathrm{p})/\mathrm{d}Q\,\mathrm{d}\Omega(\mathrm{t},\omega')$ for $\mathrm{p}(^3\mathrm{He},\mathrm{t})\Delta^{++}$

with the momentum distribution function $\rho(\boldsymbol{p}_{\mathrm{N}})$ for nucleons in the carbon nucleus,

$$\frac{\mathrm{d}\sigma^{(\mathrm{C})}}{p\,\mathrm{d}Q\,\mathrm{d}\Omega} \simeq \int \frac{\mathrm{d}\boldsymbol{p}_{\mathrm{N}}\,\rho(\boldsymbol{p}_{\mathrm{N}})\,I(\boldsymbol{p}_{\mathrm{N}})\,\mathrm{d}\sigma^{(\mathrm{p})}}{p\,\mathrm{d}Q\,\mathrm{d}\Omega}\left[\mathrm{t}(Q)\omega'(Q,\ \boldsymbol{p}_N)\right], \quad (23)$$

where $I(\boldsymbol{p}_{\mathrm{N}})$ is the ratio of the initial particle fluxes for reactions on the nucleon when in rest and with momentum $\boldsymbol{p}_N$. The momentum distribution $\rho(\boldsymbol{p}_{\mathrm{N}})$ was taken from the harmonic oscillator model. The cross section for $\mathrm{p}(^3\mathrm{He},\mathrm{t})\Delta^{++}$ was approximated by the Jackson corrected [185] Breit–Wigner function and by available tabulated data. The nucleon energy E_{N} was evaluated by

$$E_{\mathrm{N}} = M_A - M_{A-1} - T_{A-1} = m_{\mathrm{N}} - \varepsilon_{\mathrm{N}} - \frac{p_{\mathrm{N}}^2}{2(M_A - m_{\mathrm{N}} + \varepsilon_{\mathrm{N}})}. \quad (24)$$

The energy of removal of a nucleon from the carbon, $\varepsilon = m_{\mathrm{N}} + M_{A-1} - M_A$, was taken to be $\varepsilon = 25$ MeV. The quantity ω' was calculated by

$$\omega'^2 = (Q + E_{\mathrm{N}})^2 - (\boldsymbol{p}_0 - \boldsymbol{p}_{\mathrm{t}} + \boldsymbol{p}_{\mathrm{N}})^2. \quad (25)$$

The calculation of Eqn (23) was made for $p_{^3\mathrm{He}} = 4.40$, 6.81, and 10.79 GeV/c. As an example, the result for $p_{^3\mathrm{He}} = 10.79$ GeV/c [155] is shown as the dashed line in Fig. 21b. The result was normalised to the theoretical value $R_{\mathrm{th}} = 0.8$, which was also obtained from the quasifree production model (see Section 4.1.1). The figure clearly shows that the quasifree production peak is markedly shifted to higher excitation energies with respect to experiment and that the role of this Δ excitation mechanism is relatively small.

Thus, the mechanism of quasifree excitation of the Δ isobar in nuclei fails both qualitatively (the Δ peak shifts in the opposite direction) and quantitatively (small size of the effect) as an explanation of experimental facts observed in inclusive reactions.

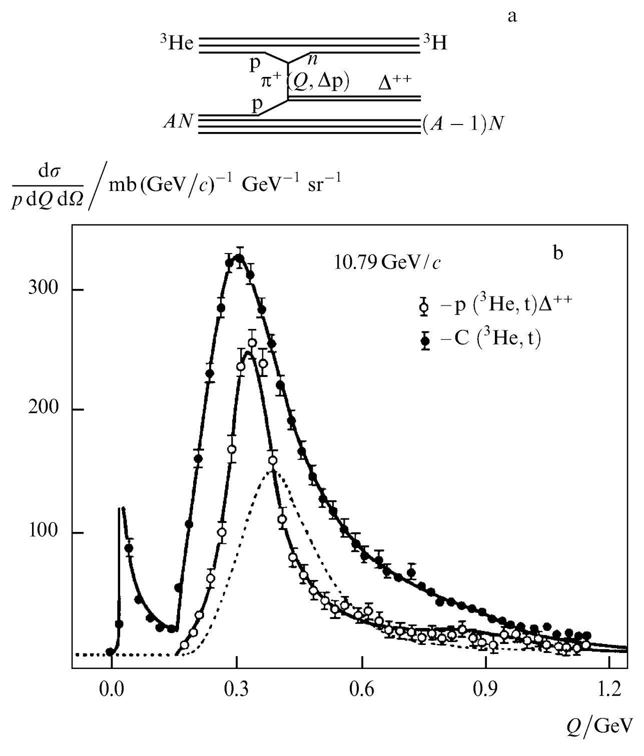

Figure 21.

Still, the above calculations do not rule out completely the participation of the quasifree mechanism in nuclear Δ excitation. Recall that in a special experimental setup (see Section 4.5.1) the quasifree mechanism does manifest itself in all its detail. In the inclusive arrangement, however, its influence is obscured by stronger — collective — mechanisms acting to shift the Δ peak in the opposite direction.

5.2 Collective mechanisms for nuclear Δ excitation

Of the collective nuclear Δ excitation mechanisms now in currency, the two most popular ones are the collective Δ-hole (Δ-h) excitations within the potential Δ-h model, and the collective spin–isospin nuclear excitations of what might be called the 'pion-like wave' type.

Common to both concepts is the notion of the Δ isobar as a nuclear constituent which interacts with the nucleons and pions, and in doing so acquires some specifically nuclear features which set it apart from the free Δ resonance.

The nuclear Δ isobar idea requires a number of new concepts for its theoretical treatment, such as the Δ isobar Hamiltonian, H_Δ, the binding energy of the Δ isobar, ε_Δ, the polarisation operator, $\prod_\Delta$, Δ propagator, $\pi\mathrm{N}\Delta$ and $\gamma\mathrm{N}\Delta$ vertices, etc. Moreover, it should be remembered that the properties of the nuclear Δ isobar may depend on such factors as the competition between the collective and quasifree formation mechanisms, the Pauli principle, Fermi motion, short-distance correlation, projectile and ejectile form factors, the mesonless de-excitation channel $\mathrm{N}\Delta \to 2\mathrm{N}$, background effects, etc.

As a means for obtaining information, pion scattering, hadron and nucleus charge exchange, photoabsorption, and nuclear electroexcitation in the Δ region are employed. The information itself comes about in the form of the reaction cross section as a function of momentum (or energy) transfer, four-momentum, mass number, and the proton to nucleon number ratio. The parameters of the theory are extracted from the earlier data on pion–nucleus total and differential scattering cross sections, on pion absorption, pion production in NN reactions, and properties of π mesoatoms. Basically, the information on nuclear Δ excitation obtained in inclusive experiments describes how the parameters of the nuclear Δ maximum (height, width, position) depart from their free Δ values. A qualitative explanation of these results can be obtained within the Δ-hole model.

5.2.1 Δ-hole model. The basic ingredients of the Δ-hole (Δ-h) model are the formation of the Δ isobar in the nuclear medium, its subsequent propagation, and ($\Delta \to \pi\mathrm{N}$) decay (or the mesonless $\mathrm{N}\Delta \to 2\mathrm{N}$ de-excitation). In this model the Δ isobar is treated (see, e.g., Ref. [73]) as a nuclear quasiparticle (baryon) comprising the nucleus together with nucleons; and the nucleus itself is a multiparticle system of nucleons and Δ isobars interacting with both one another and pions.

In the pion–nucleus interaction at intermediate energies the Δ isobar production is the predominant process and contributes most to the total cross section. It is therefore for this interaction that the Δ-h model was originally developed. The basic concepts of the model, however, hold for the nuclear Δ from other processes as well.

We will follow Ref. [73] in describing the essential features of the Δ-h model. As a first approximation to the picture of interacting nucleons, pions, and Δ isobars, the independent-particle potential model, or one-particle model, was chosen. Recall that a self-consistent potential (real in one-particle models, and complex in the optical one) with a single particle moving in its field obviates multi-particle interaction difficulties†.

By analogy with the one-particle nuclear shell model, in which a nucleon in the nucleus is described by the Hamiltonian

$$H_{\rm N}^{(0)} = M_{\rm N} + T_{\rm N} + V_{\rm N} \,, \tag{26}$$

where $M_{\rm N}$ is the nucleon mass, $T_{\rm N}$ the nucleon kinetic theory, and $V_{\rm N}$ the one-particle potential, the nuclear Δ isobar is described by the Hamiltonian

$$H_\Delta^{(0)} = M_\Delta + T_\Delta + V_\Delta \,, \tag{27}$$

in which M_Δ, T_Δ and V_Δ have a similar meaning for the Δ.

The spectrum of the Hamiltonian $H_\Delta^{(0)}$ is determined from the condition

$$H_\Delta^{(0)}|\Delta_\delta\rangle = E_\delta|\Delta_\delta\rangle = (M_\Delta + \varepsilon_\delta)|\Delta_\delta\rangle \,, \tag{28}$$

where δ is the set of quantum numbers for the one-particle states $|\Delta_\delta\rangle$ of the isobar, and ε_δ is its binding energy.

The excited nucleus is described in the Δ-h model by the state

$$|(\Delta\text{-h})_{\delta\nu}\rangle = |(\Delta_\delta N_\nu^{-1})\rangle \,, \tag{29}$$

in which N_ν^{-1} describes a hole in the nucleon state $|N_\nu\rangle$, and Δ_δ, a Δ isobar in the state $|\Delta_\delta\rangle$. The energy of Δ-hole excitations is

$$E_\delta - E_\nu = M_\Delta - M_{\rm N} + \varepsilon_\delta - \varepsilon_\nu \approx M_\Delta - M_{\rm N} \approx 300\,{\rm MeV}. \tag{30}$$

The next approximation is to include the interaction of the Δ-h states with the pion field. To this end the coupling Hamiltonians $H_{\pi{\rm NN}}$, $H_{\pi{\rm N}\Delta}$ and the free pion Hamiltonian H_π are introduced. The Hamiltonian for one (ith) baryon is then

$$H_i = H_{\rm N}^{(0)} + H_\Delta^{(0)} + H_\pi + H_{\pi{\rm NN}} + H_{\pi{\rm N}\Delta} \,, \tag{31}$$

and the total Hamiltonian of the nucleus is the sum of Eqn (31) over all A baryons,

$$H_{\rm nucl} = \sum_{i=1}^{A} H_i \,. \tag{32}$$

The inclusion in $H_{\rm nucl}$ of the term $H_{\pi{\rm N}\Delta}$ enables the Δ-h model to account for the $\Delta \to \pi{\rm N}$ decays (whose width Γ_Δ differs from the free $\Gamma_\Delta^{z,{\rm N}}$ decay Δ because of the phase volume change) and for one-pion exchange (Δ-h) production. The width Γ_Δ of the $\Delta \to \pi{\rm N}$ decay may be incorporated into the one-particle potential (27) as an additional imaginary term

$$H_\Delta^{(0)} = M_\Delta + T_\Delta + V_\Delta - \frac{\rm i}{2\Gamma_\Delta(E)} \,. \tag{33}$$

By way of systematically improving the Δ-h model one includes kinematic effects (recoil, binding), the Pauli principle (narrowing), and the coupling to reaction channels (broadening).

†The other problem, the validity of the potential concept in this energy region, clearly remains, thus rendering the description approximate. One further difficulty in treating the Δ excitation as a collective state is due to the short lifetime of the Δ; this difficulty is also neglected (see Section 5.2.3).

In a general form, the propagation of the Δ isobar in the nuclear medium can be described in terms of an effective, complex optical Δ nuclear potential consisting of a central and a spin-orbital term:

$$V_\Delta(E, \boldsymbol{r}) = V_0(E)\,\frac{\rho(\boldsymbol{r})}{\rho(0)} + 2\boldsymbol{l}_\Delta \boldsymbol{s}_\Delta V_{LS}(r) \,. \tag{34}$$

The potential parameters are chosen by fitting data to the elastic scattering and absorption of pions by nuclei [186, 187].

Without here going into the analysis of the mathematical formalism of the Δ-hole interaction, and omitting specific expressions for the Δ nuclear potential, the form factors of the incident and final particles, the response function, Δ propagator, etc., it is worthwhile to pause briefly to discuss certain general principles of the theoretical interpretation of the observed nuclear Δ features in various interactions.

5.2.2 On the role of the nuclear response spin structure

In the nuclear Δ excitation process the primary particle transfers isospin, momentum (four-momentum) and spin (moment) to the nucleus. The nature of the interaction depends on the preferential mutual orientation of the momentum transfer $\boldsymbol{q}$ and the moment $\boldsymbol{\sigma}$, which may be either longitudinal $(\boldsymbol{q}\cdot\boldsymbol{\sigma})\tau_a$ or transverse $(\boldsymbol{q}\times\boldsymbol{\sigma})\,\tau_a$ (τ_a is the isospin operator). The longitudinal operator accounts for the excitation of the states with pion quantum numbers, whereas the transverse accounts for magnetic and isovector excitations (for example, ρ meson exchange in the nuclear interaction and photon exchange in the electromagnetic). Under certain conditions (by choosing the primary particle type or by varying the angle keeping the four-momentum fixed), a preferential response to either the longitudinal or transverse part of the interaction may be obtained, which facilitates the theoretical interpretation of the results. We now consider several types of interaction adopting the simplest interpretation possible in each particular case, namely, one-meson (π or ρ) exchange for the hadron–nucleus interaction and one-photon exchange for the electromagnetic one.

The pion–nucleus interaction involved in the one-pion exchange mechanism is related to the longitudinal character of the spin response function $\boldsymbol{q}\cdot\boldsymbol{\sigma}$. According to the Δ-hole model, the interaction in this case scales with $kq\cos\Theta$ and is attractive (Δ peak shifting down in energy). If the ground state nucleus has its spin and isospin zero, $J = I = 0$, then the pion field excites in it states with $I = 1$ and with anomalous values of spin and parity J^π: $0^-, 1^+, 2^-$, etc. The attraction is strongest for partial waves with $l < 3$, for which a shift and broadening of the Δ maximum — that is, a change in the mass (decrease) and in the width (spreading) of the free Δ — takes place. A similar shift for small l is also expected (and indeed is observed) in the total pion–nucleus interaction cross section, this latter being related to the forward scattering amplitude via the optical theorem. Note that it was in measuring the total cross section for the pion–nucleus interaction where the anomaly of the nuclear Δ excitation was observed first [188, 189].

In the case of the electromagnetic nuclear Δ excitation the picture is different, since the spin part of the photo-absorption response (real photons) is transverse $(\boldsymbol{q}\times\boldsymbol{\sigma})$, whereas for inelastic electron scattering (virtual photons) it is of mixed nature.

According to the Δ-h model, for the $(\boldsymbol{q} \times \boldsymbol{\sigma})$ response the interaction scales with $kq \sin\Theta$ and does not shift the Δ peak, which is consistent with the photoabsorption data (see Section 3.5.3). The only changes the peak parameters undergo relative to the free Δ case are broadening and reduction in height (per nucleon). The cross section per nucleon remains practically constant over a wide range of mass numbers, $9 \leqslant A \leqslant 235$.

For inelastic electron scattering a more complex picture obtains. In the first Born approximation, the differential cross section for ee′ scattering may be decomposed into contributions from longitudinally and transversely polarised photons, and the Δ region is dominated by the latter. Comparison with experiment does indeed yield a photoabsorption-like (no-shift no-broadening) picture at low $[\sim 0.1\ (\mathrm{GeV}/c)^2]$ four-momentum transfers, but displays an increase in the Δ isobar invariant mass as four-momentum grows (see Section 3.5.2). This dependence is beyond the simplest Δ-h model and will be discussed in the next section.

An even more complex structure is found in baryon charge exchange processes. In the wave impulse approximation the cross section may be written in the form

$$\frac{\mathrm{d}\sigma}{\mathrm{d}t} = N\left[F_{\mathrm{T}}^2(t)\,\frac{\mathrm{d}\sigma_{\mathrm{T}}}{\mathrm{d}t}\,(t)R_{\mathrm{T}} + F_{\mathrm{L}}^2(t)\,\frac{\mathrm{d}\sigma_L}{\mathrm{d}t}\,(t)R_{\mathrm{L}}\right], \tag{35}$$

where N is the absorption factor, and $F^2(t)$, $\mathrm{d}\sigma(t)/\mathrm{d}t$ and R are the transverse (T) and longitudinal (L) form factors, elementary cross sections, and response functions, respectively. In this approximation the transverse and longitudinal parts of the response separate, and one of them may be enhanced by appropriately choosing the projectile and ejectile particles [$F_{\mathrm{T}}^2(t)$ and $F_{\mathrm{L}}^2(t)$ may differ widely].

As an example, Fig. 22 taken from Ref. [2] shows the course of $F_{\mathrm{L}}^2(t)$ (solid lines) and $F_{\mathrm{T}}^2(t)$ (dashed lines) for the $(^3\mathrm{He},\mathrm{t})$, $\mathrm{d},2\mathrm{p}(^1\mathrm{S}_0)$ and some other reactions. The reaction $(^3\mathrm{He},\mathrm{t})$ is seen to be quite suitable for the study of the spin-longitudinal response. $F_{\mathrm{L}}^2(t)$ does not become very steep, thus securing a large cross section for Δ excitation. The longitudinal to transverse form factor ratio is

$$(F_{\mathrm{L}}/F_{\mathrm{T}})^2 = \exp(-0.31t)\,, \tag{36}$$

which, for $-t = 3.5$, is close to 3. This allows the possibility of making one of the terms in Eqn (35) predominant, which is important for the theoretical analysis of cross section behaviour. Comparison of the form factors for $\mathrm{d},2\mathrm{p}(^1\mathrm{S}_0)$ also suggests that the longitudinal component dominates over the transverse one (see the discussion of this reaction in Section 4.4).

The general conclusion that can be drawn from the nuclear response analysis for various charge exchange reactions (light and heavy ions, nucleons) is that in all cases, whatever the projectile, the Δ excitation of the nucleus shows characteristic features (energy downshift and Δ peak broadening) suggesting the collective character of the Δ excitation of the target nucleus. In the one-pion exchange mechanism these features are determined by the spin-longitudinal component of the nuclear response function.

As already stated, these features cannot be accounted for by considering quasifree Δ production on one of the nucleons (see Fig. 1u) and taking into account the Fermi motion and binding energy effects, because in this case a shift of the Δ maximum upwards in energy must result.

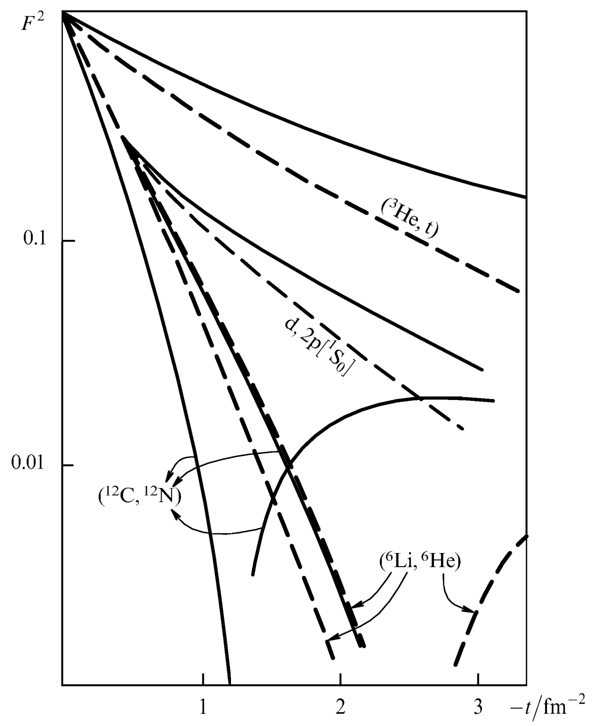

Figure 22.

Another quasifree idea, Δ excitation in the projectile [171] (see Fig. 1v) is also discarded [3] as an explanation of the Δ peak downshift, because this mechanism must be target independent, and in particular suggests a Δ shift on the deuteron — which is not observed [151, 152, 161–163, 168, 172] (see, however, Section 5.3.2 for more on this).

This is substantiated by an isospin weight calculation for p, n charge exchange on the nucleus [3] which gives a fraction of about 1/3 for projectile Δ production (for a proton target, even 1/10). This is not inconsistent with experiments on the electromagnetic nuclear Δ. There, due to the spin-transverse predominance, the Δ peak shift is not seen, but Δ excitation is again collective (more precisely, is not purely quasifree, as seen from the lack of an upward energy shift) and cannot be ascribed to the projectile since the photon is a structureless particle.

Standing somewhat apart are pion charge exchange data, which also display a Δ maximum downshift [166, 167] even though the response function should apparently be transverse here (because the π exchange is G parity prohibited, it is most natural to expect the ρ exchange diagram to be dominant). This is one of the challenges one faces in interpreting nuclear Δ excitation in the way described. A possible way out is a hypothesis [190] that the Δ peak shift has nothing to do with the specifics of the reaction mechanism but rather depends on the properties of the Δ isobar in nuclei. It is argued that all the experimental data can be explained by introducing a binding of the order of 20–70 MeV for the Δ in nuclei. [Other attempts at the theoretical description of the $(\pi^{\pm}, \pi^0)$ reactions will be described in Section 5.3.2].

5.2.3 Collective Δ isobar excitations of pion wave type

The collective mechanism of the excitation of the nuclear Δ as a superposition of Δ-h states has a difficulty of principle, due to the very short lifetime of the isobar. In fact, it is argued [74] that the Δ isobar that forms in the nucleus has just enough time to get to the neighbouring nucleon before decaying and hence cannot in principle feel the entire nuclear potential (dependent on the size and shape of the nucleus) as a collective state would. It is therefore believed that the collective excitation can hardly be a superposition of pure Δ-h states. However, the collective Δ state of the nucleus can be constructed as a superposition of Δ-h and pion degrees of freedom. Put simply, the mechanism is as follows.

Suppose that the Δ isobar formed in the nucleus decays by the pion channel ($\Delta \to \mathrm{N} + \pi$). Because this is a two-particle large-width ($\sim$ 100 MeV) channel, the decay pion retains the resonant energy, i.e., can form a further Δ with another nucleon. In the pion decay of this new Δ the process may repeat itself, etc., leading to a collective Δ excitation of the type of superposed Δ-h and pion degrees of freedom (pion-like wave, see Figs 1n to 1o)†. Clearly the difficulty due to the short lifetime of the Δ resonance is eliminated, and the collective excitation may in principle spread over the whole of the nucleus.

The mathematical description of a pion excitation propagation in Ref. [74] relies on two well known methods, one of which treats pion scattering in terms of a pion refraction coefficient in the nuclear matter [195] and the other employs the properties of the pion propagator in the nucleus [196], both approaches being developed further in Ref. [74]. In particular, although the pion propagator for low excitation energies had been studied extensively in connection with pion condensation (see Section 2) and with precritical phenomena [20–22, 25, 194, 197], in the region of the Δ isobar relativistic calculations were needed. They had been performed, in collaboration with the author of Ref. [74], in an earlier work [193].

The results of Ref. [74] were used by its author to calculate (^{3}He, t) charge exchange cross sections on Δ excited nuclei. In the high transfer limit $qR \gg 1$, the cross section is shown to be expressible in terms of the imaginary part of the pion propagator taken on the nuclear surface. The approximation employed describes well the data on the tritium spectrum for relatively low ^{3}He energies. It is pointed out that the approach taken in the work had also been developed in Refs [198, 199] in which, however, only a nonrelativistic response function had been used.

Apart from the works mentioned, Ref. [201] addressed the idea of a collective pion-like wave in the nuclear medium. To interpret the Δ shift, a simple two-level infinite-matter zero-Δ-width model was considered. In this model, the Δ-h states and pions in the medium are treated as a system of two levels in the ω, q plane, which in the absence of interaction cross at some q (Fig. 23a taken from Ref. [202]). Switching on the (πNΔ) interaction leads to a strong mixing of the two states in this region and results in the exchange of their structure. The pionic branch (π-b) shifts to lower energies, and the Δ branch, to higher. The Δ-h force is thus distributed between the two modes. It is argued that the pionic mode accounts for a sizeable part (25–30 MeV) of the Δ peak downshift for (^{3}He, t) at 2 GeV. A more realistic two-level model will be described in Section 5.3.2.

†Prior to Ref. [74] the pion-like excitation of the nuclear medium had been discussed in Refs [191 – 193], in which the Δ maximum shift in (^{3}He, t) was explained qualitatively as a manifestation of the collective concentration of force along a pion line in the medium (Migdal pionic branch [194]).

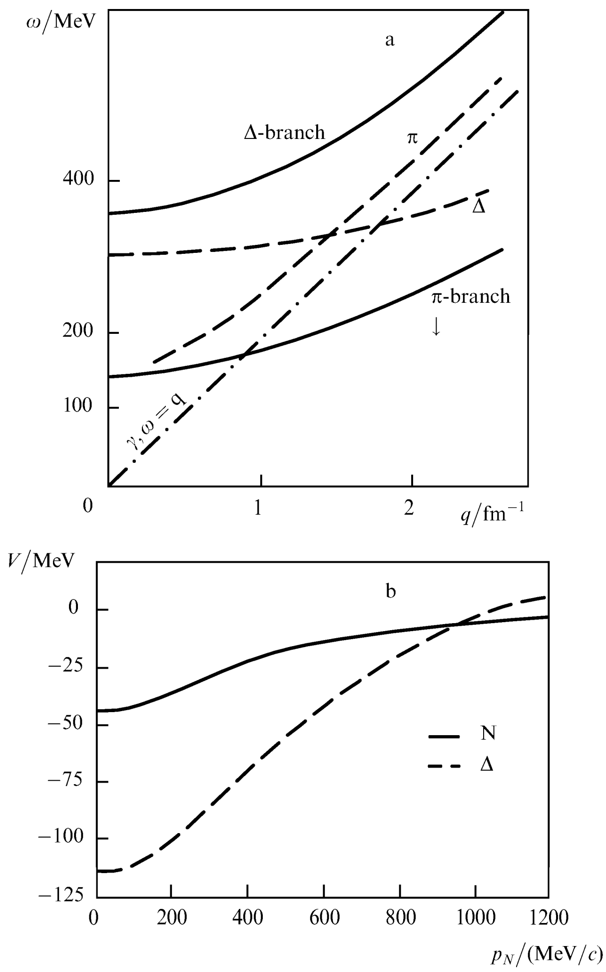

Figure 23.

5.2.4 Momentum dependent Δ nuclear potential. (πNΔ) versus (πNN) coupling

In Section 3.5.2 we discussed the shift of the Δ peak with increasing Q^2 in electronuclear reactions [126], an effect which is hard to explain in terms of the well accepted electromagnetic nuclear Δ concept. A nonstandard explanation was undertaken in Ref. [129] by introducing a momentum-dependent Δ nuclear potential. This is an extension of the earlier proposal [203] that the shift of the quasielastic peak in electron–nuclear scattering is due to the fact that the target-bound and recoiling nucleons feel an effective potential which depends on the momentum.

The initial data used in Ref. [129] were the statistically most accurate ^{3}He, C and Fe measurements of Refs [121–125]. In order to correct for Δ peak shifts due to other electron scattering mechanisms contributing to the cross section in the Δ region, the cross section model of Ref. [204] was adopted. The model implies that the low-energy tail of the cross section for heavier than Δ_{1232} nucleon resonances may shift the invariant mass of the peak to higher Δ, whereas the high-energy tail of the quasideuteron absorption, to lower. It was found that the Δ peak position correction is $+10$ MeV for $Q^2 = 0.1\ (\mathrm{GeV}/c)^2$ and -15 MeV for $Q^2 = 0.5\ (\mathrm{GeV}/c)^2$ (for the average values of Q^2 the two corrections compensate each other). The corrections reduce to 35 MeV the experimental [126] Δ peak shift. The 'remainder' is attributed to the influence of the momentum-dependent Δ nuclear potential

$$V_{\Delta}(p_{\rm f}) = \omega + V_{\rm N}(p_{\rm i}) - (p_{\rm f}^2 + W_{\Delta}^2)^{1/2} + \left(\frac{k_{\rm F}^2}{2} + M^2\right)^{1/2}, \quad (37)$$

where ω is the energy loss, $p_{\rm i}$ and $p_{\rm f}$ are the initial and final nucleon momenta, respectively, $V_{\rm N}(p_{\rm i})$ is the nucleon potential for the initial momentum, $k_{\rm F}$ the Fermi momentum, and M the nucleon mass.

The nucleon and Δ potentials are parameterised by the depth V_0, momentum p_0, and constant V_1:

$$V(p) = -\frac{V_0}{1 + p^2/p_0^2} + V_1 \ . \quad (38)$$

The values of V_0, p_0 and V_1 were obtained from a least-squares spline fit. For the nucleon–carbon potential they were found to be $V_0^{\rm N} = (46 \pm 6)$ MeV, $p_0^{\rm N} = (430 \pm 100)$ MeV, and (tentatively) $V_1 = (38 \pm 3)$ MeV; for the Δ–carbon, $V_0^{\Delta} = (153 \pm 22)$ MeV, $p_0^{\Delta} = (628 \pm 88)$ MeV and $V_1^{\Delta} = (38 \pm 3)$ MeV. The imaginary part of the potential is estimated to be 70 MeV (from Δ peak broadening due to the NΔ → NN contribution).

Fig. 23b presents the dependence of the nucleon–nuclear and Δ–nuclear potentials on nucleon momenta in the range 400–1000 MeV/c. It is seen that the Δ potential at $q < 950$ MeV is deeper than the nucleon one. The authors of Ref. [129] believe that this may be due to the (πNΔ) coupling being stronger than (πNN) [205]. They also do not attach too much significance to the fact that $V_1^{\Delta} > 0$ (which would imply that the Δ–nuclear potential is repelling at higher momenta) because this value is obtained under the assumption $V_1^{\rm N} = 0$. To check the validity of the value $V_1^{\Delta} > 0$ requires further data for $Q^2 > 0.5$ (GeV/c)^2 and a knowledge of mechanisms of various peak-shifting reactions.

5.3 Some specific theoretical approaches

5.3.1 Δ-hole model including (Δ-h) correlations in the longitudinal channel

The predicting ability of modern theoretical models of the nuclear Δ will be demonstrated by first giving a detailed description of one of them and then comparing it briefly with other, both earlier and later models. The reference model is taken from Ref. [206] which proposes a specific approach to the nuclear Δ excitation in the (p, n) and (^{3}He, t) charge exchange reactions. This 1990 paper is in a sense a borderline between purely inclusive and increasingly exclusive models. In fact it summarises all the previous results obtained in the theory of nuclear Δ excitation as is clearly evident from its frequent quotation in subsequent work.

The model of Ref. [206] goes as follows. The Δ isobar is produced in a one-step direct charge exchange process

$$A + a \rightarrow (B + \Delta) + b \ , \quad (39)$$

which is treated within the framework of the Distorted Wave Impulse Approximation (DWIA). $A(B)$ and $a(b)$ denote the target (final nucleus) and incident (outgoing) particle, respectively. For $a = {}^3$He, the form factor is considered.

The interaction of the resultant Δ with the final nucleus B (hole) is described in terms of a one-particle complex potential and (Δ–N^{-1}) residual interaction. The latter is calculated within the Tamm–Dancoff approximation in the coupled channel formalism.

The inclusive cross section for the process is written in the form

$$\frac{{\rm d}^2\sigma}{{\rm d}E_b\,{\rm d}\Omega_b} = \frac{E_a E_b E_A E_{B+\Delta}}{2\pi h^2 c^2 W} \times \frac{k_b}{k_a} \times {\rm Im}(-\langle\rho \mid G \mid \rho\rangle) \ , \quad (40)$$

where E_i is the total energy of the particles ($i = a$, b, A and $B + \Delta$), k_a (k_b) is the wave number of $a(b)$, W the total energy of all particles in the centre of momentum system, $\mid\rho\rangle$ is the doorway state excited by the reaction, and G is the Green's function that describes the motion of the ($A + \Delta$) system. In constructing the input state

$$\mid\rho\rangle = \langle\chi_b^{(-)}\varphi_b \mid t_{\rm NN,N\Delta} \mid \chi_a^{(+)}\varphi_a\varphi_A\rangle \quad (41)$$

one uses the internal wave functions φ_a and φ_b of the particles a and b, the target wave function φ_A (assuming $J_A^{\pi} = 0^+$), projectile distorted wave functions $\chi_a^{(+)}$ and $\chi_b^{(-)}$ in the incident and exit channels, and the effective $t_{\rm NN,N\Delta}$ transition operator NN → NΔ.

The expression for the Green's function is taken in the form

$$G = \left(E + \frac{i\Gamma_{\Delta}}{2} - H_B - T_{\Delta} - U_{\Delta} - V_{\rm N\Delta,N\Delta}\right)^{-1} \ , \quad (42)$$

where E is the excitation energy of the ($B + \Delta$) system, Γ_{Δ} is the energy dependent free decay width of Δ, T_{Δ} is the kinetic energy operator, U_{Δ} the Δ–nuclear potential, H_B the Hamiltonian of nucleus B, and $V_{\rm N\Delta,N\Delta}$ is the residual interaction describing the (Δ–N^{-1}) correlations. The Δ–nuclear potential U_{Δ} is taken to be a complex Woods–Saxon potential with parameters from Refs. [186, 187, 207], the width Γ_{Δ} is taken from Ref. [199]. $V_{\rm N\Delta,N\Delta}$ is assumed to consist of π and ρ exchange potentials with an added short-range interaction. In the momentum representation $V_{\rm N\Delta,N\Delta}$ can be written as a sum of the longitudinal (LO) and transverse (TR) components, whose contribution is assumed to be equilibrium:

$$V_{\rm N\Delta,N\Delta} = \left[V^L_{\rm N\Delta,N\Delta}(\boldsymbol{S}_1\cdot\hat{\boldsymbol{q}})(\boldsymbol{S}_2^+\cdot\hat{\boldsymbol{q}}) + V^T_{\rm N\Delta,N\Delta}(\boldsymbol{S}_1\times\hat{\boldsymbol{q}})\cdot(\boldsymbol{S}_2^+\times\hat{\boldsymbol{q}})\right]\boldsymbol{T}_1\cdot\boldsymbol{T}_2^+ \ . \quad (43)$$

Here

$$V^{\rm L}_{\rm N\Delta,N\Delta} = 4\pi hc\left(f_{\pi}^2(t)\,\frac{v_{\pi}}{m_{\pi}^2} + f_{\pi}^2(t)\,\frac{g'_{\Delta\Delta}}{m_{\pi}^2} - 2f_{\rho}^2(t)\,\frac{v_{\rho}}{3m_{\rho}^2}\right) \ , \quad (44)$$

$$V^{\rm T}_{\rm N\Delta,N\Delta} = 4\pi hc\left(f_{\pi}^2(t)\,\frac{g'_{\Delta\Delta}}{m_{\pi}^2} + f_{\rho}^2(t)\,\frac{v_{\rho}}{3m_{\rho}^2}\right) \ , \quad (45)$$

where $f(t = \omega^2 - q^2) = f_{i\rm N\Delta}(\Lambda_i^2 - m_i^2)/(\Lambda_i^2 - t)$ are the meson–baryon vertex factors ($i = \pi, \rho$), $v_i = q^2/(t - m_i^2)$, $g'_{\Delta\Delta} \sim 0.3$ is the Landau–Migdal parameter† (in units of $J_{\pi\rm NN} = 4\pi hc f_{\pi\rm NN} f_{\pi\rm NN}/m_{\pi}^2 \approx 1600$ MeV fm^3), $f_{\pi\rm N\Delta}^2 = 0.324$, $f_{\rho\rm N\Delta}^2 = 16.63$, $m_{\pi} = 0.14$ GeV, $m_{\rho} = 0.77$ GeV, $\Lambda_{\pi} = 0.78$ GeV, $\Lambda_{\rho} = 2$ GeV.

The $t_{\rm NN,N\Delta}$ transition operator in Eq. (41) is taken in the form

$$t_{\rm NN,N\Delta} = g'_{\rm N\Delta}J_{\pi\rm N\Delta}\left(\frac{\Lambda_{\pi}'^2 - m_{\pi}^2}{\Lambda_{\pi}'^2 - t}\right)^2\left[(\boldsymbol{\sigma}_1\cdot\hat{\boldsymbol{q}})(\boldsymbol{S}_2^+\cdot\hat{\boldsymbol{q}}) + (\boldsymbol{\sigma}_1\times\hat{\boldsymbol{q}})\cdot(\boldsymbol{S}_2^+\times\hat{\boldsymbol{q}})\right]\tau_1\boldsymbol{T}_2^+ \quad (46)$$

†This value of the (short-flight repulsion) parameter g' preserves the required attraction strength.

with $J_{\pi N\Delta} = 4\pi\hbar c f_{\pi NN} f_{\pi N\Delta}/m^2 = 800$ MeV fm^3, $g'_{N\Delta} = 0.335$, $\Lambda'_\pi = 650$ MeV.

In calculating the ^{12}C(p, n) and ^{12}C(^{3}He, t) reactions, a shell-model configuration for the ground state wave function of ^{12}C was employed. The Δ-h model included all S-hole and P-hole states and all the Δ orbitals with $l_\Delta \leqslant 8$ (up to 24 states in total). Calculations with and without Δ-h correlations were made.

When comparing with the experimental data [151, 208, 209], the authors of Ref. [206] point out that the $t_{NN,N\Delta}$ interaction of the form (46) is adequate to give both the shape and magnitude of the cross section for the p(p, n)Δ^{++} and p(^{3}He, t)Δ^+ reactions (better than the OPE interaction does) and in particular does not require the excitation of the target nucleus Δ to be considered.

In comparing the ^{12}C(p, n) calculations with experiment, authors first pointed out that much of the observed shift of the Δ peak relative to its proton position (40 of 70 MeV) is attributable to trivial factors (kinematics, broadening). As to the remaining 30 MeV, a calculation with and without Δ-h correlations (solid and dashed lines in Fig. 24a, respectively) showed precisely this latter effect to be the contributor. Here the energy dependence of π exchange plays the dominant role. It was shown that in the longitudinal (LO) channel a backshift occurs for all multipoles and is a maximum for the lowest one (Fig. 24b). All the multipoles up to 9^+ were included. The transverse (TR) channel, while showing no appreciable shift, contributes to the height of the Δ peak more than the LO channel does.

By comparing with experiment, similar LO and TR results were obtained from calculations for the ^{12}C(^{3}He, t) reaction which, as in the p(^{3}He, t) case, also included the form factor of the incident ^{3}He. For this reaction, a direct comparison of form-factor and point-particle results was made (solid and 0.34 scaled dashed lines, respectively), to show that the inclusion of the form factor leads to just a trivial energy downshift (Fig. 24c).

For the ^{12}C(^{3}He, t) reactions, PWIA (plane wave impulse approximation) calculations were also performed (0.25 scaled dashed line in Fig. 24d), which showed that the relevant theoretical cross sections differ only in magnitude from (but are identical in shape to) their DWIA counterparts (solid curve). The implication is that scattering at intermediate incident energy leads primarily to a pure absorption of the flux.

The authors of Ref. [206] conclude by emphasising that the Δ peak shift in the (p, n) and (^{3}He, t) reactions is caused in their approach by strongly attractive, very-short-range correlations in the longitudinal spin–isospin LO channel, and that this attraction is due to the energy-dependent π exchange interaction. Some disagreement with experiment in the low energy region is accounted for by the neglect of NN^{-1} excitations and by the possible failure of the equal weight assump-tion for the LO and TR channels in Eqn (43) for $V_{N\Delta,N\Delta}$.

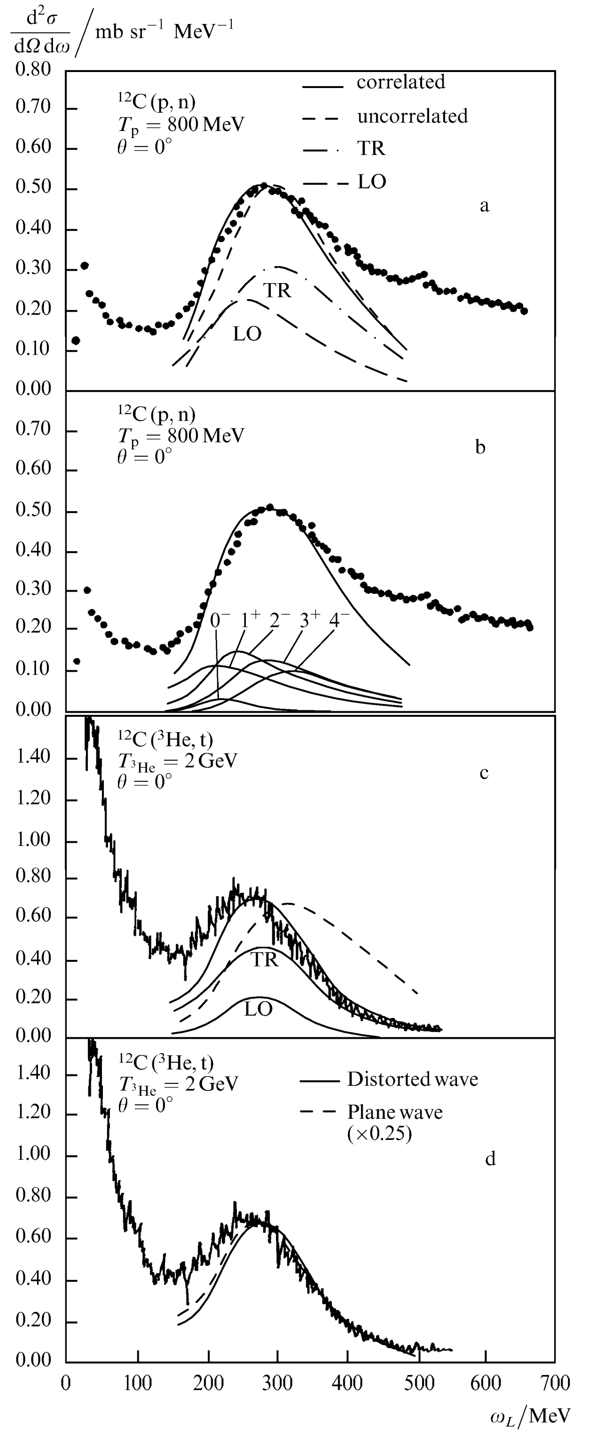

Figure 24.

isobar in an optical potential, one-meson (π, ρ) exchange mechanism, short-range correlation corrections]. Let us discuss briefly some points of difference between those studies and Ref. [206].

5.3.2 Other approaches

Although it is uncharacteristic of a data-oriented review, the reason why we have discussed Ref. [206] in such detail is that, as we see it, it draws a bottom line under a large series of theoretical studies of the latter half of the 1980s, which had also described inclusive experiments and involved the same or similar concepts [one-step primary Δ-h excitation, fast particle scattering, the motion of the Δ isobar in an optical potential, one-meson (π, ρ) exchange mechanism, short-range correlation corrections]. Let us discuss briefly some points of difference between those studies and Ref. [206].

In one of the early studies (Ref. [199], 1985) the Δ peak shift was explained in terms of the pure OPE mechanism with the excitation of one longitudinal (LO) channel. Such a model does account for the peak shift but greatly underestimates the peak height (giving less than the approach (46) of Ref. [206]). Also, the model cannot account for the data for ^{3}He energies of 4 and 11 GeV [138], which the $t_{NN,N\Delta}$ interaction of the form (46) can.

In 1985–1989 work on the $(NN \to N\Delta)$ transition [210–212], as well as the π exchange, the ρ exchange was considered. $(^3He, t)$ was assumed to be a one-step reaction, and in describing the motion of ^3He and t the DWIA method was used. If somewhat ahead of the story, note that in their later work the authors of those studies found the ρ exchange dispensable [213, 214].

Standing somewhat apart is Ref. [215], according to which the response function is dominated not by Δ but by collective pion excitations of the nuclear matter. We have described this mechanism in much detail when discussing Ref. [74] (see Section 5.2.4). As a small addendum, note that in analysing the response of the nucleus on spin–isospin excitation in the Δ region, the short-range repulsion [216, 217] was taken into account. To calculate the scattering, the Glauber–Sitenko model was used.

The reader will remember that the collective pion-like excitation idea was also considered in Ref. [201] in 1989 (see Section 5.2.3).

In Ref. [171], 1989, the $(NN \to N\Delta)$ transition is described by means of the OPE potential taking into account the excitation of the projectile nucleus ^3He and the contribution from the πN amplitude S wave. Fig. 25 presents the results for the $p(^3He, t)p\pi^+$ reaction. The dotted curve shows the calculation for the DET mechanism alone; the solid curve includes the DEP mechanism and the S wave contribution. The experimental points are taken from Ref. [149].

Ref. [171] highlights the difference between the $p(^3He, t)p\pi^+$ and $n(^3He, t)\pi N$ results which manifests itself as different Δ peak shapes. The Δ maximum shape calculation for the reaction on the neutron (with DEP, DET, and S wave mechanisms) is shown in Fig. 25 by a dashed curve. Because of the large difference in the proton and neutron results, it is argued that one cannot compare experimental data on the $(^3He, t)$ reaction on the proton and the nucleus.

It is also argued that DEP is adequate to explain the experimentally observed [218] features of the Δ excitation in the deuteron (cf. Section 5.2.2); the behaviour of the Δ excitation in heavier nuclei is not considered, however. Later (in 1992), the high-energy extrapolation of the (near-threshold) results of Ref. [171] was questioned on the grounds that the DEP contribution disappears as the initial energy increases [165, 219].

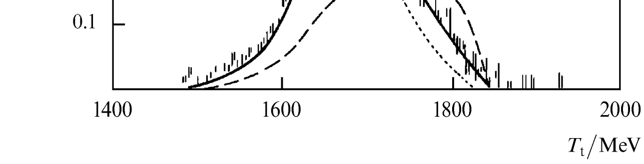

Figure 25.

We may summarise the discussion of the theoretical studies of the late 1980s by saying that they do indeed have much in common and provide a satisfactory qualitative description of exclusive experiments (Δ peak shift in the right direction) — but are not sufficient as far as quantitative description is concerned.

Now let us step over the self-imposed limit of the year 1990, Ref. [206], to consider a few later theoretical studies which show the same tendency to exclusiveness characteristic of modern experimental work.

Delorme and Guichon [220]†, developing their earlier proposed simple two-level Δ excitation model (Ref. [201], see Section 5.2.3) show that much of the backward Δ shift in $(^3He, t)$ may be attributed to a previously undetected pion mode. Refs [200] and [220] develop a more realistic two-level model, one which in place of infinite nuclear matter considers specific (^{12}C and ^{208}Pb) nuclei, takes into account that $\Gamma_\Delta \neq 0$, and includes both types of Δ de-excitation and peak broadening.

The analysis was carried out within the random phase approximation (RPA)‡ framework and adopting the local density approximation for the lowest-order polarisation (Δ-h) propagator $\prod_0(\boldsymbol{q}, \boldsymbol{q}', \omega)$, where $\boldsymbol{q}$ and $\boldsymbol{q}'$ are the ingoing and outgoing momenta, and ω is the energy. The essential features of the old model remained in the new one, however: The Δ excitation strength also recedes from the pion line and the pure Δ-h region, shifting up and down as shown in Fig. 23a. The details of the shift depend on the values of the $\pi N\Delta$ coupling constant and the Migdal parameter g' (Fig. 23a is for $g' = 0.5$).

Realistic calculations give two maxima for the longitudinal part of the nuclear response function $\boldsymbol{\sigma} \cdot \boldsymbol{q}$ in the ω, q plane, between which there is a valley located near the free pion line $\omega^2 = p^2 + m^2$. This result is confirmed by the fact that the total pion–nucleus cross section is predicted reasonably well both in the sense of its scaling with $A^{2/3}$, and in that the Δ shift scales with $A^{1/3}$. The two maxima correspond to the ordinary Δ-h excitations and the pionic branch. Estimates show that the downward shift due to the pionic mode is 25 MeV for ^{12}C and 30 MeV for ^{208}Pb. It is emphasised that the spin-transverse $\boldsymbol{\sigma} \times \boldsymbol{q}$ contribution to the pion channel is not large because of the small coupling between them [222, 223]. In two-level language, this is interpreted as implying no intersection between the Δ-h and the ρ lines. It is noted that so far the charge exchange reactions $(^3He, t)$, even though peripheral, suit best for studying the pion mode§.

Apart from charge exchange, Refs [200, 220] also employ data on the electromagnetic nuclear excitation. Photon absorption is depicted in the ω, q plane by the line $\omega = q$ (real photons), and to the inelastic electron scattering (virtual photons) there corresponds the region $Q^2 = q^2 - \omega^2 > 0$ below the line. In either case the spin-transverse $\boldsymbol{\sigma} \times \boldsymbol{q}$ part of the nuclear response

†More detailed, if preliminary calculations are given in Ref. [200].

‡This approximation is used in theoretical response function calculations, that is, in determining the parameters (mode, energy) of nuclear excitations due to spin–isospin operators [221]. Formally, RPA is equivalent to the theory of finite Fermi systems.

§While absorbed less than ^3He, real pions probe a region in between the maxima which is away from the π branch. A pion response from the entire nuclear interior might be obtained from inelastic neutrino scattering, but this is not yet practical [202].

function†, with practically no coupling to the pion channel, is analysed. In the ω, q plane the transverse part of the response function has one maximum. The results of the analysis agree with experiment.

Ref. [183] of 1992 notes the experimental dependence of the peak shift on the type of isobar de-excitation channel involved, an observation noticed in the exclusive Δ decay study [160, 172] we described earlier (see Sections 4.5.2 and 4.5.3). Recall that, from Refs [160, 172], the $N\Delta \to NN$ channel shows a strong backward shift, whereas in the $\Delta \to N\pi$ channel it is absent. As opposed to Refs [160, 172], Ref. [183] attributes this to a two-step Δ excitation ($NN \to N\Delta$, $N\Delta \to NN$).

The same work proposes an experimental method for separating information on DET and DEP Δ excitation in the projectile and in the target (see Figs 1u, 1v, 1w). To this end one examines simultaneously the reactions (^{3}He, t) and (^{3}He,^{3}He), which should differ considerably in the neighbourhood of $T_{^3\mathrm{He}} = 2$ GeV studied in Ref. [172] because the latter reaction becomes DEP dominated at this energy. The role of the DEP mechanism depends on the energy of ^{3}He. For $T_{^3\mathrm{He}} = 10$ GeV the mechanism is still important for (^{3}He,^{3}He) but is negligible for (^{3}He, t). In addition to the results of Ref. [171], it is noted [183] that on the proton target the DEP mechanism is not strong but acts to improve agreement with experiment at high energies; on the neutron it is more pronounced, especially at high energies. The study of the relative role of DET and DEP on nucleons was continued in Ref. [179], in which the weights of both mechanisms are compared for the (^{3}He, t), (^{3}He,^{3}He) and (^{4}He,^{4}He) reactions based on the isotopic relations. The results are tabulated in Table 3.

Table 3.

Reaction	DET	DEP	Reaction	DET	DEP
p(^{3}He, t)	2	2/9	n(^{3}He, t)	2/3	2/3
p(^{3}He,^{3}He)	6/9	134/9	n(^{3}He,^{3}He)	6/9	86/9
p(^{4}He,^{4}He)	0	64/3	n(^{4}He,^{4}He)	0	64/3

It is seen from the table that in the N(^{4}He,^{4}He) reactions only the DEP mechanism of Δ excitation is possible (because of the breakdown of isospin conservation for DET); N(^{3}He,^{3}He) reactions must be dominated by DEP, p(^{3}He, t) by DET, and for n(^{3}He, t) the two mechanisms are weighted equally. Based on their previous work [171, 183], the authors of Ref. [179] predict a marked difference in shape for the outgoing energy distribution for the DEP and DET mechanisms. Their spectrum for the DEP mechanism was confirmed experimentally in the Saturne work on the p(^{4}He,^{4}He) reaction [178]. Also, in Ref. [179] the cross section for p(^{4}He,^{4}He) was calculated and found to agree qualitatively with the measurements [178] of both the energy and angular distributions (see Section 4.6.5).

Refs [176] and [177] analysed the exclusive experimental studies on ^{12}C(p, nπ^+) [175] and ^{12}C(^{3}He, tπ^+)^{12}C$_{\mathrm{g.s}}$ [174] mentioned in Section 4.6.4, which display coherent 250 MeV pions with an angular distribution strongly peaked forward with respect to the momentum transfer $\boldsymbol{q}$ (see Figs 19a and 19b).

The analysis showed that these results are due to the spin structure of excitation $\boldsymbol{S}^+\cdot\boldsymbol{q}$ and de-excitation $\boldsymbol{S}\cdot\boldsymbol{q}$ operators which are involved in the spin-longitudinal (LO) channel and lead to a $k_\pi q\cos\theta_\pi$ angular distribution. The angular distribution corresponding to the spin-transverse (TR) channel is proportional to $k_\pi q\sin\theta_\pi$. The computed energy and angular distribution of the coherent pions from ^{12}C(^{3}He, tπ^+)^{12}C$_{\mathrm{g.s}}$ compare well with the experimental data of Ref. [175].

The discovery of coherent pions in the ^{12}C(^{3}He, tπ^+)^{12}C$_{\mathrm{g.s}}$ reaction with a ground-state-conserved target nucleus is believed to indicate the existence of a pionic mode in the nucleus. The coherent pions, initially outside the mass surface (because they are virtual) undergo multiple scattering within nuclei and so become real mass-surface pions. Curiously, the recoil kinetic energy of a finite nucleus is low (< 1 MeV), $T_\pi = T_{^3\mathrm{He}} - T_{\mathrm{t}}$, $M_{^3\mathrm{He}} \approx M_{\mathrm{t}}$, but the virtual to real conversion is still possible if the momentum required for the pion to move onto the mass surface will be received by the nucleus as a whole.

In concluding this section we mention attempts [224, 225] at a theoretical description of ($\pi^\pm, \pi^0$) charge exchange experiments [166, 167]. Recall that the Δ peak downshift found in those experiments is similar to that for reactions (^{3}He, t), even though the reaction mechanisms are different. The basic assumption of Refs [224, 225] is the predominance of the ρ meson exchange diagram ('transverse' mechanism), because the π exchange ('longitudinal' mechanism) is forbidden by the G-parity conservation law. The approach adopted is an RPA, infinite nuclear medium, circular approximation analysis (Fig. 1x), in which the spin-transverse response is proportional to the imaginary part of the propagator $\prod^0$ [the sum of (N-h) and (Δ-h) free propagators]. Apart from the ρ meson exchange, the short-range repulsion is included ($g' \simeq 0.6-0.7$). The calculation shifts the Δ peak to higher excitation energies, which is in contradiction with the ($\pi^\pm, \pi^0$) charge exchange data similar to those for (^{3}He, t). It is suggested that this similarity in spite of the different reaction mechanisms ['longitudinal' for (^{3}He, t) and 'transverse' for ($\pi^\pm, \pi^0$)] may be due to the strong change in the properties of the Δ isobar itself as compared to the free state (for the proton target, including the ρ meson exchange provides agreement with experiment).

Recall that the transverse response difficulty in the ($\pi^\pm, \pi^0$) charge exchange reaction was also encountered in a study of the reaction d, 2p(^{1}S$_0$) on a polarised deuteron beam [168] (see Section 4.4). In that work the behaviour of the form factors (see Fig. 22) and Δ peak angular distributions implies the predominance of the longitudinal component, whereas tensor analysis of the spin observables emphasises the transverse component. Experiment shows a strong downward energy shift of the Δ peak, thus favouring the longitudinal component (see Fig. 14).

In Ref. [2], which analyses the data of Ref. [168], it is this last result which is given credence, on the grounds that the spin observables may be highly distorted in the [d, 2p(^{1}S$_0$)] reaction.

Whatever the validity of this conclusion, both the charge exchange reaction ($\pi^\pm, \pi^0$) and the reaction d, 2p(^{1}S$_0$) clearly call for further investigation, both wider in scope

†The transverse part was shown to be predominant in inelastic electron scattering experiments with longitudinal–transverse separation.

and improved in precision. In particular, Refs [224] and [225] discuss pion charge exchange mechanisms which form intermediate pion–nucleon resonances in the S channel and proceed via the excitation of the Δ resonance through the exchange by a ρ meson in the t channel. A significantly reduced contribution from diagrams with intermediate-state nucleon and Δ isobar is shown. As a result of this reduction, the cross section turns out to be sensitive to contributions from the higher resonances $N^*(1440, 1/2^+)$, $N^*(1520, 3/2^-)$, and $\Delta(1620, 1/2^-)$. The amplitude of the process is strongly dependent on the relative signs and magnitudes of the resonance coupling constants, which are scarcely known from the experimental data available.

5.4 Exotic Δ states in the nucleus

In the combined 1982 INR-JINR effort, collisions of 350 MeV Dubna phasotron protons with copper nuclei were employed to investigate the spectrum of 90° pions in the 30–110 MeV energy range [226]. The spectrum was found to be anomalous in that it increased toward lower energies. The subsequent study of this effect at the Saturne synchrotron with the Ga target [227] showed this increase to be limited to pion energy of about 60 MeV, and later work [228] showed the anomaly to be about 5 MeV in width. Finally, based on a supplementary Dubna study on varying-angle low-energy pion production [229] the anomaly was interpreted [230, 190] as a narrow resonance at a nuclear excitation energy of 350 MeV.

The unusually narrow width of a resonance state at a very high excitation needs a nonstandard explanation. At present we are aware of two hypotheses that explain the anomaly, namely the formation of 2Δ states and of Δ balls in the nucleus.

5.4.1 2Δ states

According to the former hypothesis [230, 190], the unusually small resonance width at very high excitation is accounted for by the formation, in the nucleus, of a resonance state with two Δ isobars decaying by the scheme $\Delta \to N + \pi$. All the major features of the anomalous resonance are then explained by assuming that the binding energy of the Δ inside the nuclear matter is 125 MeV (i.e., 2 to 3 times greater than usually assumed).

In fact, the position of the resonance is determined by the minimum energy for the excitation of two Δ isobars in the nucleus: $E_{\min} = 2(M_\Delta - M_N - \varepsilon_\Delta) = 350$ MeV, and the maximum kinetic energy of the Δ decay pions is $T_{2\pi}^{\max} = E_{\min} - 2m_\pi = 70$ MeV. To the small pion energy there corresponds a small phase space, i.e., a small resonance width.

To check the hypothesis experimentally, measurements capable of detecting both Δ decay pions are required.

5.4.2 Δ balls

The second hypothesis [231] suggests the formation of a localised state, a so-called Δ ball, in the nucleus. It is known that the $(\Delta-N)$ interaction is attractive in character and stronger than the NN interaction. Consequently, in the vicinity of the nuclear Δ the nucleon density exceeds its equilibrium value, and the field on the Δ is larger than it is away from this region. If the excess field is large enough to produce discrete levels in the interaction potential well, the Δ isobar can localise on one of the levels to form a Δ ball. The effective mass of the Δ ball is $M_B \simeq 10 M_N$. This is the excess mass of the ball matter plus the associated mass of the nuclear liquid which participates in the collective motion as the ball moves. As long as the Δ isobar remains within the ball, the ball nuclear matter is compressed. After the decay of the Δ the ball starts to expand and the compression energy is transferred to all the nuclear particles.

The decaying Δ isobar emits a pion, whose energy, by the Pauli principle, cannot be large because the decay nucleon cannot occupy states with low $(p < p_F)$ momentum. Estimates put the energy at 70–80 MeV, which is close to the experimental value. The low pion energy again implies a narrow resonance.

The experimental verification of the second hypothesis rests on the proof that in the decay of a narrow resonance only one pion is emitted. Particular attention is paid to the fact that some of the pions may have a negative charge (because of the charge exchange of the Δ^+ isobar to Δ^0 for in-medium neutrons). Finally, the authors of Ref. [231] indicate that resonant γ quanta from the $\Delta \to N + \gamma$ decay may be observed.

5.5 Collective excitation of other baryon resonances in nuclei

As already mentioned in Sections 3.1.1 and 5.2, a collective Δ excitation in a nucleus may arise if the Δ resonance is wide and decays by the two-particle pion scheme. These conditions prove to have greater generality. If the S channel of an elementary two-particle interaction has a wide resonance with a predominantly two-particle decay channel, it was shown back in 1975 [232] that in the nuclear matter excitation spectrum a collective branch is bound to appear.

This possibility was analysed in Ref. [3], so often quoted here, by considering a group of nine strange Λ and Σ resonances, 25–400 MeV in width and having a fairly high (20–60%) probability of decaying via the two-particle channel $N\bar{K}$. An example is the $\Lambda(1820)$ resonance, whose width is 70–90 MeV and whose $N\bar{K}$ channel decay probability is 55%–65%.

It is suggested that the collective effects involved in the excitation of strange resonances in nuclei may be detected by the shift and broadening of the relevant peaks in the total cross sections of ~ 1 GeV/c K^- mesons on nuclei with respect to the analogous peaks for K^- mesons on deuterons. A comparison of currently available data [233–237] suggests that while the collective excitation of strange baryons in nuclei is still a moot question, further work along these lines is important.

Note also that nuclear photoabsorption experiments have not exhibited any analogues of resonances heavier than Δ, even though such resonances are well known for free nucleons (see Section 3).

6. Conclusion

The existence of the Δ isobar in the nucleus has received solid experimental support in recent years. It has been observed in practically all the investigated nuclei, whether excited in hadron (nucleus, nucleon, pion) charge exchange reactions or in electromagnetic processes.

The former invariably display strong Δ excitation of nuclei on an energy transfer scale of 300 MeV and for momentum transfers comparable to the average Fermi momentum of nucleons in the nucleus. It is primarily nuclear Δ excitation which determines the cross section for hadron charge exchange processes in the Δ region. Quasielastic charge exchange with the excitation of ordinary nuclear levels contributes relatively little, and as the initial energy decreases, increasingly so.

At the dawn of nuclear Δ studies it was believed that the excitation of the Δ proceeds via quasifree formation on one of the nucleons of the nucleus. Calculations and specially performed experiments have shown that, compared to the free Δ, such a mechanism should broaden the Δ peak, shift it to higher excitation energies, and reduce the height.

There is, however, much evidence from inclusive experiments on hadron charge exchange in nuclei that even if the quasifree mechanism does operate in the nucleus, its expected features do not manifest themselves but, instead, the Δ peak shifts to lower energies and increases in height. This suggests something other than a quasifree — collective — Δ excitation mechanism, not related to the spin–isospin excitation of one of the nucleons but representing the response of the nucleus as a whole. The two possibilities usually considered are collective (Δ-h) excitations, with their subsequent correlations, and the collective spin–isospin excitation in the form of a wave propagating through the nuclear medium as a superposition of Δ-hole and pion degrees of freedom (pion-like branch).

It is the separation and subsequent study of each of the mechanisms mentioned which is the primary objective of the experimental work on the hadron processes of nuclear Δ excitation. It seems safe to say that both objectives have been fairly successfully achieved: not only are the quasifree and collective mechanisms experimentally separated and examined, but it has also proved possible to separate the pion-like branch in the latter mechanism. Specifically, it is worthwhile to mention the experimental separation of the DET and DEP mechanisms, the study of the pionic mode of nuclear Δ excitation, and the investigation of various channels of Δ de-excitation.

Unlike hadron processes, neither of the two varieties of the electromagnetic nuclear Δ excitation that have been investigated (photoabsorption and inelastic electron scattering) exhibits a detectable Δ peak shift for $Q^2 \simeq 0.1\ (\mathrm{GeV}/c)^2$, even though the specially designed experiments on the partial photoproduction of hadrons on nuclei suggest that this process also — like hadron interactions — involves a quasifree mechanism producing an upward energy shift. The lack of a Δ shift is presumably due to a collective Δ-hole mechanism competing with the quasifree one.

The unshifted peak is undoubtedly the most intriguing result, one which is common to both varieties of the electromagnetic nuclear Δ excitation, and requires a nonstandard approach for its explanation. A posteriori, the lack of a Δ peak in electromagnetic processes may be attributed to the fact that they have no contribution from a pion-like wave-type mechanism, which produces an additional downward energy shift in hadron processes.

The following results are also of interest:

1. The mass number independence of the Δ region photoabsorption cross section per nucleon (universal curve), and no signs of other — higher-energy — resonances like those familiar for nucleons [133].

2. Enhancement of the invariant mass W of the nuclear Δ peak as a function of the Q^2 transfer in inelastic electron scattering.

Most workers take the Δ-hole (Δ-h) model as a basis for explaining the experimental data. The model assumes that the Δ isobar is another nuclear constituent — together with the nucleons — and that it interacts with both the latter and pions. Accordingly, the model involves the total Hamiltonian of the nucleus, which includes the nucleon, Δ isobar, and free pion Hamiltonians, and also the Hamiltonians for the πNN and πNΔ coupling.

The excitation of the nucleus is interpreted in the Δ-h model as the appearance of a hole in one of nucleonic states and of a Δ isobar on one of the Δ orbitals of the nucleus. The energy of the Δ-h excitation is of the order of 300 MeV. The in-medium propagation of the Δ is described by an effective, complex optical potential using a residual interaction in the form of short mean-free-path (Δ-h) correlations [206].

Affecting the response function of the nucleus are the parameters of the primary and final particles, the particle form factors, the energy, momentum, spin, and isospin transfers, the exchange mechanism type involved (for example, one-meson for certain hadron processes, and one-photon for electromagnetic ones), the preferential mutual orientation of the momentum transfer $\boldsymbol{q}$ and the moment $\boldsymbol{\sigma}$, which determines the nature of the interaction (attraction or weak repulsion), etc. The difficulty with this approach is the ambiguity as to how to choose model parameters.

Theoretical calculations within the Δ-h model explain nuclear Δ excitation quite well qualitatively, but as yet cannot pretend to a quantitative status. Nor can other theoretical concepts, though.

We may summarise this review by saying that while much has been done in the study of the problem discussed, many questions remain concerning both the experimental results themselves and — especially — their interpretation. To answer them, new and higher-quality data and new theoretical approaches are required.

The general direction to be taken in future experimental research is, as we see it, toward more exclusiveness, wider range of four-momentum transfer, higher statistical accuracy, and more reliable removal of background reactions. The objects to be studied are nuclei with different A and N/Z, and the projectiles to be used are hadrons (nucleons, nuclei, and pions), photons, and electrons.

The following are some of the specific experiments to be carried out in the near future:

1. Exclusive experiments on nuclear Δ excitation by monochromatic γ quanta, with detection of Δ decay (de-excitation) products and determination of the excitation energy of the final nucleus. High-energy electron accelerators [88, 87] with universal charged-particle and γ detectors might be employed (see, e.g., Refs [30, 238]).

2. Investigation of nuclear Δ excitation in electroproduction processes at large and various Q^2, to check the observed [129] dependence of the invariant mass of the Δ isobar, W, on Q^2.

3. New, more accurate measurements of the photoabsorption of monochromatic γ quanta by nuclei in the Δ region, in order to determine reliably the position and height of the Δ peak, and in particular to establish the presence, or otherwise, of a Δ shift in this process.

4. Measurement of the photoabsorption of monoenergetic γ quanta in the region of heavier than Δ baryon resonances, to examine the mass dependence of the excitation intensity of the resonances, and in particular to study the D_{13} resonance reduction effect [133, 132, 135].

5. Investigation of the $W(Q^2)$ dependence in hadron processes, with detection of all shift-imitating background reactions, and of various Δ de-excitation channels.

To obtain a more accurate theoretical picture, the following experiments may prove particularly helpful:

6. Further exclusive experiments on hadron charge exchange processes, to find out more about the dependence of the nuclear Δ peak position on the Δ de-excitation channel type [160, 172].

7. Further study of the $(^3\mathrm{He}, \mathrm{t}\pi^+)$ reaction, with the final nucleus excitation energy fixed, to develop a better understanding of the scattering of virtual pions with their transformation into real ones [174, 175]; and of how this process relates to the existence of the nuclear pion mode.

8. Further work on the $(\mathrm{t}, ^3\mathrm{He}\,\pi^-)$ reaction (the subject pioneered in Refs [239, 240]), in order to study the excitation of resonances heavier that Δ_{1232} in nuclei.

9. Precision study of the $(\pi^{\pm}, \pi^0)$ charge exchange reaction, first investigated in Refs [166, 167], to learn more about the nuclear excitation mechanism involved.

10. Polarised proton beam measurement of the polarisation characteristics of the (p, n) charge exchange reaction, to elucidate the mechanism of the reaction $^{12}\mathrm{C}[\mathrm{d}, 2\mathrm{p}(^1\mathrm{S}_0)]$ studied in Ref. [168].

11. Continuation of the experiments [157] on nuclear Δ excitation by heavy relativistic ions, to investigate the A dependence, the density effect, and the mirror charge exchange reactions.

12. More studies on the comparative role of the DEP and DET mechanisms in the $(^3\mathrm{He}, \mathrm{t})$, $(^3\mathrm{He}, ^3\mathrm{He})$ and $(^4\mathrm{He}, ^4\mathrm{He})$ reactions on protons and neutrons [183, 178, 239, 240].

Finally, the following experiments might be of help in elucidating the exotic nature of nuclear $(\mathrm{t}, ^3\mathrm{He})$ processes:

13. Search for 2Δ states by detecting two pions from the decay of two Δ isobars as proposed in Ref. [230].

14. Search for Δ balls by detecting 80–90 MeV π mesons from the decay of narrow resonances at $E = 350$ MeV and by observing resonant γ quanta from $\Delta \to \mathrm{N} + \gamma$ [231].

15. Exploration of the possibility of collective excitation of strange baryon resonances by observing the shift and broadening of the relevant peaks in the total cross sections for K^- meson scattering from nuclei [232, 3].

In conclusion, all experimental facts and all known theoretical approaches have proved to accommodate themselves quite well in a single framework developed here for the purpose, without the authors being confronted with an awkward choice of either stretching or lopping them off Procrustean style. As time goes on, however, it cannot be ruled out that 'the victim' will grow further, but it is our feeling that the growth will be widthwise rather than lengthwise, and so our scheme will in general remain true. If not, it is the 'bed' which will have to be adjusted — something the mythical robber would not consider.

Acknowledgements. The authors are pleased to express their sincere gratitude to Yu V Gaponov, F A Gareev, A B Kurepin, Yu A Ratis, E A Strokovskii, N S Topil'skaya and V N Tikhonov for many fruitful discussions.

References

1. Ahrens J *Nucl. Phys. A* **446** (2) 229 (1985)
2. Gaarde C *Annu. Rev. Nucl. Part. Sci.* **41** 187 (1991)
3. Strokovskii E A, Gareev F A, Ratis Yu L *Fiz. Elem. Chastits At. Yadra* **24** 603 (1993) [*Phys. Part. Nuclei* **24** 255 (1993)]
4. Bohr N *Collected Scientific Works* Vol. 2 (Ed. G R Nielsen) (Amsterdam: North-Holland, 1972)
5. Migdal A B *J. Phys. (Moscow)* **8** 331 (1944)
6. Belyaev S T, Zelevinskii V G *Usp. Fiz. Nauk* **147** 210 (1985) [*Sov. Phys.-Usp.* **28** 854 (1985)]
7. Bohr O, Mottelson B, Pines D *Phys. Rev.* **110** 936 (1958)
8. Belyaev S T *K. Dan. Vidensk. Selsk. Mat.-Fys. Medd.* **31** (11) 1959
9. Solov'ev V G *Vliyanie Parnykh Korrelyatsii Sverkhprovodyashchego Tipa na Svoistva Atomnykh Yader* (Effect of Superconduction Pair Correlations on the Properties of Atomic Nuclei) (Moscow: Gosatomizdat, 1977)
10. Glauber R J *Lectures in Theoretical Physics* **1** 315 (1959)
11. Franco V, Glauber R J *Phys. Rev.* **142** 1195 (1966)
12. Glauber R J, in *Proc. of the 2nd Int. Conf. on High Energy Physics and Nuclear Structure in Rehovoth 1967* (Amsterdam: North-Holland, 1967) p. 254
13. Landau L D *Zh. Eksp. Teor. Fiz.* **30** 1058 (1956); **32** 59 (1957) [*Sov. Phys.-JETP* **3** 920 (1956); **5** 101 (1957)]
14. Galitskii V M, Migdal A B *Zh. Eksp. Teor. Fiz.* **34** 139 (1958) [*Sov. Phys.-JETP* **7** 96 (1958)]
15. Migdal A B *Teoriya Konechnykh Fermi-Sistem i Svoistva Atomnykh Yader* (Theory of Finite Fermi Systems and the Properties of Atomic Nuclei) (Moscow: Nauka, 1965)
16. Gaponov Yu V, Lyutostanskii Yu S *Pis'ma Zh. Eksp. Teor. Fiz.* **15** 173 (1972); **18** 130 (1973) [*JETP Lett.* **15** 120 (1972); **18** 75 (1973)]
17. Gaponov Yu V, Lyutostanskii Yu S *Yad. Fiz.* **19** 62 (1974) [*Sov. J. Nucl. Phys.* **19** 33 (1974)]
18. Gaponov Yu V, Lyutostanskii Yu S *Fiz. Elem. Chastits At. Yadra* **12** 1324 (1981) [*Sov. J. Part. Nuclei* **12** 528 (1981)]
19. Yukawa H *Proc. Phys.-Math. Soc. Jpn.* **17** 48 (1935)
20. Migdal A B *Fermiony i Bozony v Sil'nykh Polyakh* (Fermions and Bosons in Strong Fields) (Moscow: Nauka, 1978)
21. Migdal A B *Zh. Eksp. Teor. Fiz.* **61** 2209 (1971); **63** 1993 (1972) [*Sov. Phys.-JETP* **27** 1184 (1972); **36** 1052 (1973)]
22. Migdal A B *Nucl. Phys. A* **210** 421 (1973)
23. Mukhin K N, Patarakin O O *Usp. Fiz. Nauk* **133** 377 (1981) [*Sov. Phys.-Usp.* **24** 161 (1981)]
24. Bel'kov A A , Bunyatov S A, Mukhin K N, Patarakin O O *Pion–Pionnoe Vzaimodeistvie* (The Pion–Pion Interaction) (Moscow: Energoatomizdat, 1985)
25. Borzov I N et al. *Fiz. Elem. Chastits At. Yadra* **12** 848 (1981) [*Sov. J. Part. Nuclei* **12** 338 (1981)]
26. Cohen J, Eisenberg J M *Nucl. Phys. A* **395** 389 (1983)
27. Krasnov V A et al., in *Programma Eksperimental'nykh Issledovanii na Mezonnoi Fabrike IYaI AN SSSR. Trudy 3 Vsesoyuznogo Seminara, April 1983* (Programme of Experimental Studies at USSR Acad. Sci. INR Meson Facility, Proceedings of the Third All-Union Seminar, Zvenigorod, 23-27 April 1983) (Moscow, 1984) p. 194
28. Bayukov Yu D, Efremenko Yu V et al., Preprint ITEP 4-91 (1991)
29. Kurepin A B et al. Preprint INR Acad. Sci. USSR P-0484 (Moscow, 1986)
30. Patarakin O O et al. Preprint INR Acad. Sci. SSSR 769/92 (1992)
31. Skyrme T H R *Proc. R. Soc. London, Ser. A* **260** 127 (1961)
32. Skyrme T H R *Nucl. Phys.* **31** 556 (1962)
33. Skyrme T H R *Proc. R. Soc. London, Ser. A* **226** 521 (1954); **230** 277 (1955)
34. Donoghue J F et al. *Phys. Rev. Lett.* **53** 747 (1984)
35. Nikolaev V A *Fiz. Elem. Chastits At. Yadra* **20** 401 (1989) [*Sov. J. Part. Nuclei* **20** 173 (1989)]
36. Makhan'kov V G, Rybakov Yu P, Sanyuk V I *Usp. Fiz. Nauk* **162** 1 (1992) [*Sov. Phys.-Usp.* **35** 55 (1992)]
37. Hofstadter R *Annu. Rev. Nucl. Sci.* **7** 231 (1957)

38. Feynman R P *Photon–Hadron Interactions* (New York: Benjamin, 1972)
39. Gell-Mann M *Phys. Lett.* **8** 214 (1964)
40. Zweig G *CERN Report* 81821/TH401 (1964)
41. Abe F et al. *Phys. Rev. Lett.* **72** (13) 1977 (1994)
42. Abachi S et al. *Phys. Rev. Lett.* **72** (14) 2138 (1994)
43. Struminskii B V Preprint JINR P-1939 (Dubna, 1965)
44. Bogolyubov N N, Struminskii B V, Tavkhelidze A N Preprint JINR D-1968 (Dubna, 1965)
45. Bogolyubov N N et al. Preprint JINR D-2075 (Dubna, 1965)
46. Han M Y, Nambu Y *Phys. Rev. B* **139** 1006 (1965)
47. Miyamoto Y *Prog. Theor. Phys. Suppl.* (Extra issue number) **187–192** (1965)
48. Gross D, Wilczek F *Phys. Rev. Lett.* **30** 1343 (1973)
49. Politzer H D *Phys. Rev. Lett.* **3** 1346 (1973)
50. Fritzsch H, Gell-Mann M, Lentwyler H *Phys. Lett. B* **47** 365 (1973)
51. Bander M *Phys. Rep.* **75** 205 (1981)
52. Bogolyubov N N et al. Preprint JINR P-2141 (Dubna, 1965)
53. Chodos A et al. *Phys. Rev. D* **9** 3471 (1974)
54. Bogolyubov P N *Fiz. Elem. Chastits At. Yadra* **3** 144 (1972) [*Sov. J. Part. Nuclei* **3** 71 (1972)]
55. Bogolyubov P N, Dorokhov A E *Fiz. Elem. Chastits At. Yadra* **18** 917 (1987) [*Sov. J. Part. Nuclei* **18** 391 (1987)]
56. Pho M, Goldhaber A S, Brown G E *Phys. Rev. Lett.* **51** 747 (1983)
57. Goldstone J, Jaffe A *Phys. Rev. Lett.* **51** 1518 (1983)
58. Wilson K G *Phys. Rev. D* **10** 2445 (1974)
59. Makeenko Yu M *Usp. Fiz. Nauk* **143** 161 (1984) [*Sov. Phys.-Usp.* **27** 401 (1984)]
60. Arbuzov B A *Fiz. Elem. Chastits At. Yadra* **19** 6 (1988) [*Sov. J. Part. Nuclei* **19** 1 (1988)]
61. Logunov A A, Soloviev L D, Tavkhelidze A N *Phys. Lett. B* **24** 181 (1967)
62. Scifman M A, Vainstein A I, Zakharov V I *Nucl. Phys. B* **147** 385 (1979)
63. Efimov G V, Ivanov M A *Fiz. Elem. Chastits At. Yadra* **20** 1129 (1989) [*Sov. J. Part. Nuclei* ***20*** 479 (1989)]
64. Okun' L B *Fizika Elementarnykh Chastits* (Physics of Elementary Particles) (Moscow: Nauka, 1988)
65. Okun' L B *Leptony i Kvarki* (Leptons and Quarks) (Moscow: Nauka, 1990)
66. Gaponov Yu V, in *Materialy XVIII Zimnei Shkoly LIYaF* (Leningrad, 1983) (Proceedings of the Eighteenth Winter School of the Leningrad Institute of Nuclear Physics) p. 43
67. Gareev F A et al. *Fiz. Elem. Chastits At. Yadra* **19** 864 (1988) [*Sov. J. Part. Nuclei* **19** 373 (1988)]
68. Aubert J J et al. *Phys. Lett. B* **123** 275 (1983)
69. Bodek A et al., Preprint SLAC-PUB-3041 (1983)
70. Titov A I *Yad. Fiz.* **40** 76 (1984) [*Sov. J. Nucl. Phys.* **40** 50 (1984)]
71. Baldin A M *Fiz. Elem. Chastits At. Yadra* **8** 429 (1977) [*Sov. J. Part. Nuclei* **8** 175 (1977)]
72. Brown G E et al. *Nucl. Phys. A* **505** 823 (1989)
73. Ericson T, Weise W *Pions and Nuclei* (Oxford: Clarendon Press, 1988)
74. Dmitriev V F *Yad. Fiz.* **46** 770 (1987) [*Sov. J. Nucl. Phys.* **46** 435 (1987)]
75. Levinger J S *Phys. Rev.* **84** 43 (1951)
76. Levinger J S *Bull. Am. Phys. Soc.* **26** 13 (1951)
77. Levinger J S *Phys. Rev.* **97** 970 (1955)
78. Levinger J S *Phys. Lett. B* **82** 181 (1979)
79. Austern N *Phys. Rev.* **100** 1522 (1955)
80. Feld B *Nuovo Cimento, Suppl.* **2** 145 (1955)
81. Nedorezov V G, Ranyuk Yu N *Fotodelenie Yader za Gigantskim Rezonansom* (Nuclear Photofission beyond the Giant Resonance) (Kiev: Naukova Dumka, 1989)
82. *Rep. NPL Univ. Illinois*, N19 (USA, 1980)
83. Crawford G I, in *Proceedings of the 2nd Workshop on Perspectives in Nuclear Physics at Intermediate Energies, Triest, 1985* (Singapore: World Scientific, 1985) p. 182
84. Argan P et al., Rap. Saclay DPh N2162 (Saclay, 1984)
85. Arends J et al. *Phys. Lett. B* **98** (6) 423 (1981)
86. Antony I et al. *Nucl. Instrum. Methods Phys. Res. A, Accel. Spectrum. Detect. Assoc. Equip.* **301** 230 (1991)
87. 'Research Program at CEBAF', in *Report of 1987 Summer Study Group* (Newport News, 1987)
88. Belyaev S T et al. Preprint INE 5046/2 (Moscow, 1990)
89. Belyaev S T et al. Preprint INE 5726/2 (Moscow, 1994)
90. Artyunyan F R, Tumanyan V A *Zh. Eksp. Teor. Fiz.* **44** 2100 (1963) [*Sov. Phys.-JETP* **17** 1412 (1963)]
91. Kazakov A A et al. Preprint INR Acad. Sci. USSR P-0329 (1984)
92. Aleksandrov B M et al. *Kratkie Soobshcheniya po Fizike* (6) 53 (1989) [*Sov. Phys.-Lebedev Inst. Rep.* (6) 68 (1989)]
93. Schaerf C, in *Proc. 6 Sem. Electr. Int. of Nuclei, Moscow, 1984* (INR 1986) p. 243
94. Torn C K et al., Preprint BNL 42935 (Brookhaven, 1989)
95. Bocquet J P et al., in *Particles and Nuclei, 13 Int. Conf. (Perugia, Italy, June 1993)*; *Book of Abstracts* **2** 835 (1993)
96. Lepretre A et al. *Nucl. Phys. A* **367** (2) 237 (1981)
97. Chollet C et al. *Phys. Lett. B* **127** (5) 331 (1983)
98. Audit G et al., in *Abstract on the Conf. on Nucl. Phys. with Electromagnetic Probes, Paris, 1985* (CEN Saclay, 1985) p. 196
99. Veyssiere A et al. *Nucl. Phys. A* **199** (1) 45 (1973)
100. Ahrens J et al. *Phys. Lett. B* **146** (5) 303 (1984)
101. Ries H et al. *Phys. Lett. B* **139** (4) 254 (1984)
102. Ahrens J et al. *Nucl. Phys. A* **251** (3) 479 (1975)
103. Gurevich G M et al. *Nucl. Phys. A* **273** (2) 326 (1976)
104. Vlasenko V G et al. *Yad. Fiz.* **23** 504 (1976) [*Sov. J. Nucl. Phys.* **23** 265 (1976)]
105. Lebedev A I et al. *Voprosy Atomnoi Nauki i Tekhniki, Ser. Fiz.* **1** 33 (1978) [*Problems of Atomic Science and Technology*]
106. Baldwin G C, Klaiber G S *Phys. Rev.* **71** 3 (1947)
107. Ishkhanov B S et al. *Usp. Fiz. Nauk* **160** 57 (1990) [*Sov. Phys.-Usp.* **33** 204 (1990)]
108. Barton M Q, Smith J H *Phys. Rev.* **95** 573 (1954)
109. Barton M Q, Smith J H *Phys. Rev.* **110** 1143 (1958)
110. Stein P C et al. *Phys. Rev.* **119** 348 (1960)
111. Garvey J et al. *Nucl. Phys.* **70** 241 (1965)
112. Smith I L et al. *Nucl. Phys. B* **1** 483 (1967)
113. Arends J et al. *Z. Phys. A* **298** 103 (1980)
114. Arends J et al. *Z. Phys. A* **305** 205 (1982)
115. Homma S et al. *Phys. Rev. Lett.* **45** 706 (1980)
116. Homma S et al. *Phys. Rev. C* **27** 31 (1983)
117. Kanazawa M et al. *Phys. Rev. C* **35** (5) 1828 (1987)
118. Baba K et al. *Nucl. Phys. A* **415** 462 (1984)
119. Arends J et al. *Nucl. Phys. A* **526** 479 (1991)
120. Arends J et al. *Nucl. Instr. Meth.* **201** 361 (1982)
121. O'Connell J S et al. *Phys. Rev. Lett.* **53** 1627 (1984)
122. O'Connell J S et al. *Phys. Rev. C* **35** 1063 (1987)
123. Baran D T et al. *Phys. Rev. Lett.* **61** 400 (1988)
124. Barreau P et al. *Nucl. Phys. A* **402** 515 (1983)
125. Maziani Z E et al. *Phys. Rev. Lett.* **54** 1233 (1985)
126. Sealock R M et al. *Phys. Rev. Lett.* **62** (12) 1350 (1989)
127. Anderson R et al. *Nucl. Instrum. Methods* **66** 328 (1968)
128. Simon E G et al. *Nucl. Phys. A* **233** 381 (1980)
129. O'Connell J S, Sealock R M *Phys. Rev. C* **42** (6) 2290 (1990)
130. Ahrens J, Ferreira L S, Weise W *Nucl. Phys. A* **485** 621 (1988)
131. Frois B, in *Proc. Int. Conf. of Nucl. Phys.* Vol. 2 (Florence, 29 Aug.–3 Sept. 1983) p. 221
132. Frommhold Th et al., in *Particles and Nuclei, 13 Int. Conf., Perugia, Italy, June 1993*; *Book of Abstracts* **1** 425 (1993)
133. Frommhold Th et al. *Phys. Lett. B* **295** 28 (1992)
134. Bianchi N et al. *Phys. Lett. B* **299** 219 (1993)
135. Anhinolfi M et al., in *Proc. of Int. Nucl. Phys. Conf., Wiesbaden, 1992* Contribution 2.3.12.
136. Vorob'ev G G et al. *Programma Eksperimental'nykh Issledovanii na Mezonnoi Fabrike IYaI AN SSSR. Trudy 3 Vsesoyuznogo Seminara 23 - 27 April 1983, Zvenigorod* (Programme of Experimental Studies at USSR Acad. Sci. INR Meson Facility, Proceedings of the Third All-Union Seminar, Zvenigorod, 23-27 April 1983) (Moscow, 1984) p. 313
137. Ellegaard C et al. *Phys. Rev. Lett.* **50** 1745 (1983)
138. Ableev V G et al. *Pis'ma Zh. Eksp. Teor. Fiz.* **40** 35 (1984) [*JETP Lett.* **40** 763 (1984)]

139. Ableev V G et al. *Yad. Fiz.* **46** 549 (1987) [*Sov. J. Nucl. Phys.* **46** 300 (1987)]
140. Ableev V G et al. *Yad. Fiz.* **48** 27 (1988) [*Sov. J. Nucl. Phys.* **48** 17 (1988)]
141. Ableev V G et al. *Prib. Tekh. Eksp.* **1** 33 (1983) [*Instrum. Exp. Tech.* **26** (1) 31 (1983)]
142. Ableev V G, Strokovskii E A *Doklad na 27 Vesennei Shkole TsIYaI po Yadernoi Fizike, April 1989* (Proceedings of the GDR Acad. of Sci. CINR Twenty-Seventh Spring School, Rossendorf, April 1989)
143. Ableev V G, Candidate's Dissertation, JINR, 1989
144. Strokovskii E A, Doctor's Dissertation, JINR, 1991
145. Glauber R J *Lectures Theor. Phys.* (New York: Wiley-International 1959); *Science* **1** 315 (1959)
146. Sitenko A G *Ukr. Fiz. Zh. (Ukrainian SSR)* **4** 152 (1959) [*Ukr. Phys. J.*]
147. Grorud E et al. *Nucl. Instrum. Methods* **188** 549 (1981)
148. Contardo D et al. *Phys. Lett. B* **168** (4) 331 (1986)
149. Ellegaard C et al. *Phys. Lett. B* **154** 110 (1985)
150. Riley P J et al. *Phys. Lett. B* **68** 217 (1977)
151. Bonner B E et al. *Phys. Rev. C* **18** 1418 (1978)
152. Baturin V N et al. *Pis'ma Zh. Eksp. Teor. Fiz.* **30** 86 (1979) [*JETP Lett.* **30** 78 (1979)]
153. Eliseev S M et al., in *Tr. 8 Mezhd. Seminara po Problemam Fiziki Vysokikh Energii, OIYaI, D2-86-668* (Proceedings of the Eighth International Seminar on Problems in High Energy Physics, JINR) (Dubna, 1986) p. 308
154. Ableev V G et al., JINR E1-87-797 (Dubna, 1987)
155. Ableev V G et al., in *Tr. 9 Mezhd. Seminara po Problemam Fiziki Vysokikh Energii, OIYaI, D1-2-88-652* (Proceedings of the Ninth International Seminar on Problems in High Energy Physics, JINR) (Dubna, 1989)
156. Glass G et al. *Phys. Rev. D* **15** 36 (1977)
157. Bachelier D et al. *Phys. Lett. B* **172** 23 (1986)
158. Clausen B L et al. *Phys. Rev. C* **35** 1028 (1987)
159. Abramov V V et al., in *Programma Eksperimental'nykh Issledovanii na Mezonnoi Fabrike IYaI AN SSSR. Trudy 4 Vsecoyuznogo Seminara* (Programme of Experimental Studies at USSR Acad. Sci. INR Meson Facility, Proceedings of the Fourth All-Union Seminar) (Moscow: JINR, 1986) p.235
160. Chiba J et al. *Phys. Rev. Lett.* **67** (15) 1982 (1991)
161. Baturin V N et al. *Yad. Fiz.* **31** 396 (1980) [*Sov. J. Nucl. Phys.* **31** 207 (1980)]
162. Baturin V N et al. Preprint LNPHI-483 (Gatchina, 1979)
163. Baturin V N et al. Preprint LNPHI-1322 (Gatchina, 1987)
164. Gareev F A et al., in *Proc. of the 6th Int. Conf. on Nuclear Reaction Mechanisms, Villa Monastero, Varenna, Italy, Milano, June 1991* p. 622
165. Gareev F A et al., JINR, E2-92-7 (Dubna, 1992)
166. Golubeva M B et al. *Pis'ma Zh. Eksp. Teor. Fiz.* **51** 298 (1990) [*JETP Lett.* **51** 338 (1990)]
167. Berlev A I et al. *Izv. Akad. Nauk SSSR Ser. Fiz.* **54** 76 (1990) [*Bull. Acad. Sci. USSR Phys. Ser.* **54** 79 (1990)]
168. Ellegaard C et al. *Phys. Lett. B* **231** 365 (1989)
169. Nagae T et al. *Phys. Lett. B* **191** 31 (1987)
170. Ishimaru K et al. *Nucl. Instrum. Methods Phys. Res. A, Accel. Spectrum. Detect. Assoc. Equip.* **237** 559 (1985)
171. Oset E, Chiino E, Toki H *Phys. Lett. B* **224** 249 (1989)
172. Hennino T et al. *Phys. Lett. B* **283** 42 (1992)
173. Alard J P et al. *Nucl. Instrum. Methods Phys. Res. A, Accel. Spectrum. Detect. Assoc. Equip.* **261** 379 (1987)
174. Rousteau S et al., in *Particles and Nuclei, 13th Int. Conf., Perugia, Italy, June 1993; Book of Abstracts* **2** 500 (1993)
175. Hennino T et al. *Phys. Lett. B* **303** 236 (1993)
176. Oltmanns P et al. *Phys. Lett. B* **299** 194 (1993)
177. Osterfeld F et al., in *Particles and Nuclei, 13th Int. Conf., Perugia, Italy, June 1993*; *Book of Abstracts* **2** 498 (1993)
178. Morsch H P et al. *Phys. Rev. Lett.* **69** (9) 1336 (1992)
179. Fernandez de Cordoba P et al., in *Particles and Nuclei, 13th Int. Conf., Perugia, Italy, June 1993*; *Book of Abstracts* **2** 502 (1993)
180. Carrol A S et al. *Phys. Rev.* **14** 635 (1974)
181. Zeidman B et al. *Phys. Rev. Lett.* **40** 1316 (1978)
182. Faldt G, Lazard C, Lombard R *Phys. Rev. C* **36** 1037 (1987)
183. Fernandez de Cordoba P, Oset E *Nucl. Phys. A* **544** 793 (1992)
184. Ableev V G et al. *Phys. Lett. B* **264** 264 (1991)
185. Jackson J D *Nuovo Cimento* **34** 1644 (1964)
186. Hirata M et al. *Ann. Phys. (USA)* **120** 205 (1979)
187. Horikawa J, Thies M, Lenz F *Nucl. Phys. A* **345** 386 (1980)
188. Binon F et al. *Nucl. Phys. B* **17** 168 (1970); **33** 421 (1971); **40** 608 (1972)
189. Wilkin C et al. *Nucl. Phys. B* **62** 61 (1973)
190. Kurepin A B *Nucl. Phys. A* **519** 395 (1990)
191. Dmitriev V F, Suzuki T, in *Nuklon – Nuklonnye i Adron – Yadernye Vzaimodeistviya pri Promezhutochnykh Energiyakh. Tr. Simpoziuma, 23-25 Aprelya 1984* (Proceedings on Nucleon – Nucleon and Hadron – Nucleus Interactions at Intermediate Energies) (Leningrad, 1984) p.301
192. Chanfray G, Ericson M *Phys. Lett. B* **141** 163 (1984)
193. Dmitriev V F, Suzuki T *Nucl. Phys. A* **438** 697 (1985)
194. Migdal A B *Rev. Mod. Phys.* **50** 107 (1978)
195. Ericson T E O, Hufner S *Phys. Rev. B* **33** 601 (1970)
196. Dover C B, Lemmer R H *Phys. Rev. C* **7** 2312 (1973)
197. Alberico W M, Ericson M, Molinari A *Phys. Lett. B* **92** 153 (1980)
198. Esbensen H, Toki H, Bertsch G F *Phys. Rev. C* **31** 1816 (1985)
199. Esbensen H, Lee T-S H *Phys. Rev. C* **32** 1966 (1985)
200. Delorme J, Guishon P A M, in *10th Biennalle de Phys. Nucl.* (Aussois, March 6 – 10, 1989); Rap. Saclay DPh – N2574 (Saclay, 1989) p. C. 4.1.
201. Guishon P A M, Delorme J, in *Proc. 5-e JourneÒes d'Etudes Saturne* (Pirac, 1989) p. 53
202. Ericson M *Nucl. Phys. A* **518** 116 (1990)
203. O'Connell J S, Schroder B *Phys. Rev. C* **38** 2447 (1988)
204. Lightbody W, O'Connell J S *Comput. Phys.* **2** (3) 57 (1988)
205. Brown G E et al. *Phys. Lett. B* **118** 39 (1988)
206. Udagawa T, Hong S-W, Osterfeld F *Phys. Lett B* **245** 1 (1990)
207. Hirata M et al. *Phys. Lett. B* **70** 281 (1977)
208. Cassapakis C G et al. *Phys. Lett. B* **63** 35 (1976)
209. Lind D A *Can. J. Phys.* **65** 637 (1987)
210. Jain B K *Phys. Rev. C* **32** 1253 (1985)
211. Santra A B, Jain B K *J. Phys. G* **13** 745 (1987)
212. Jain B K, Santra A B *Nucl. Phys. A* **500** 681 (1989)
213. Jain B K, in *Proc. of the Int. Workshop 'Pion in Nuclei', Peniscola, Spain, June 1991* (Singapore: World Scientific, 1992) p. 406
214. Jain B K, Santra A B, in *Proc. of the Int. Workshop 'Pion in Nuclei', Peniscola, Spain, June 1991* (Singapore: World Scientific, 1992) p. 423
215. Gaarde C, Dmitriev V F, Sushov O P *Nucl. Phys. A* **459** 503 (1986)
216. Dmitriev V F Preprint INP Siberian Branch Acad. Sci. 86-118 (Novosibirsk, 1986)
217. Dmitriev V F Preprint INP Siberian Branch Acad. Sci. 89-14 (Novosibirsk, 1989)
218. Gaarde C *Nucl. Phys. A* **478** 475c (1988)
219. Gareev F A et al. Preprint JINR, E2-92-6 (Dubna, 1992)
220. Delorme J, Guichon P A M *Phys. Lett. B* **263** 157 (1991)
221. Bohr A, Mottelson B *Nuclear Structure* Vol. 2 *Nuclear Deformations* (New York: Benjamin, 1974)
222. Oset E, Weise W *Phys. Lett B* **77** 159 (1978)
223. Oset E, Toki H, Weise W *Phys. Rep.* **83** 281 (1982)
224. Topil'skaya N S *Candidate's Dissertation* (Moscow, 1994)
225. Kurepin A B et al. *Tezisy Dokladov 42 Soveshchaniya 'Yadernaya Spektroskopiya i Struktura Atomnogo Yadra', 21-24 Apr. 1992* (Abstracts of XLII Seminar 'Nuclear Spectroscopy and the Structure of the Atomic Nucleus') (Alma-Ata, 1992) p. 355
226. Krasnov V A et al. *Phys. Lett. B* **108** 11 (1982)
227. Julien J et al. *Phys. Lett. B* **142** 340 (1984)
228. Sanovillet G et al. Note CEA-N-2483 (Saclay, 1986)
229. Akimov Yu K et al. *JINR Rapid Comm.* **3** 11 (1989)
230. Kurepin A B, Oganesyan K O *Pis'ma Zh. Eksp. Teor. Fiz.* **49** 603 (1989) [*JETP Lett.* **49** 693 (1989)]
231. Khodel' V A *Yad. Fiz.* **52** 1355 (1990) [*Sov. J. Nucl. Phys.* **52** 858 (1990)]
232. Lenz F *Ann. Phys.* **95** 348 (1975)

233. Bugg D V et al. *Phys. Rev.* **168** 1466 (1968)
234. Abrams R J et al. *Phys. Rev. D* **4** 3235 (1971)
235. Afanas'ev V N et al. *Yad. Fiz.* **47** 1656 (1988) [*Sov. J. Nucl. Phys.* **47** 1049 (1988)
236. Bowen T et al. *Phys. Rev. D* **2** 2599 (1970)
237. Cool R L et al. *Phys. Rev. D* **1** 1887 (1970)
238. Mukhin K N, Patarakin O O Preprint. Kurchatov Inst. 5276/2 (1990)
239. Avramenko S A et al. *Doklad na XII Mezhdunarodnom Seminare po Problemam Fiziki Vysokikh Energii 'Relyativistskaya Yadernaya Fizika i Kvantovaya Khromodinamika'* (Proceedings of the Twelfth International Seminar on Problems in High Energy Physics 'Relativistic Nuclear Physics and Quantum Chromodynamics') (Dubna, 1994) Abstracts, p.22
240. Avramenko S A et al. *Pis'ma Zh. Eksp. Teor. Fiz.* **55** 676 (1992) [*JETP Lett.* **55** 707 (1992)]
241. Fernandez de Cordoba P et al. *Phys. Lett. B* **319** 416 (1993)
242. Avramenko S A et al. *JINR Rapid Comm.* **6** (63) 5 (1993); Avramenko S A et al. *JINR Comm.* E1-94-311 (JINR, Dubna, 1994)
243. Oset E et al., in *Delta Excitation in Nuclei* (Singapore: World Scientific, 1994) p. 159
244. Hersman F W, in *Proc. of the Int. Conf. 'Pions and Nucleons at Intermediate Energies', Dubna, Russia, May 1994* (Singapore: World Scientific, 1994) p. 205
245. Strokovsky E A et al. *Doklad na XII Mezhdunarodnom Seminare po Problemam Fiziki Vysokikh Energii 'Relyativistskaya Yadernaya Fizika i Kvantovaya Khromodinamika'* (Proceedings of the Twelfth International Seminar on Problems in High Energy Physics 'Relativistic Nuclear Physics and Quantum Chromodynamics') (Dubna, 1994) Abstracts, p. 75